UC/CLC Campus Earthquake Program

Initial Source and Site Characterization Studies for the U.C. Santa Barbara Campus

Archuleta, R., Nicholson, C., Steidl, J., Gurrola, L.,
Alex, C., Cochran, E., Ely, G., and Tyler, T.

Institute for Crustal Studies

University of California, Santa Barbara

December, 1997

UCRL-ID-129196

PREFACE

This report was prepared under the UC/CLC Campus Earthquake Project. This project was initiated as part of the Campus-Laboratory Collaboration (CLC) Program created by the University of California - Office of the President (UCOP).

The UC/CLC Campus Earthquake Project, which started in March 1996, currently is a partnership between four campuses of the University of California – Los Angeles, Riverside, San Diego, and Santa Barbara – and the Lawrence Livermore National Laboratory (LLNL). It is designed to estimate the effects of large earthquakes on those campuses. On each campus, a critical site has been selected by the campus administration to demonstrate the methods and procedures used by the CLC project. The sites selected are: the new Academic Health Center at UC Los Angeles, the Rivera Library at UC Riverside, the Thornton Hospital at UC San Diego, and the Engineering 1 building at UC Santa Barbara.

In the first phase, March 1996 to February 1999, the project will focus on the estimation of strong ground motions at each target site. The estimates are obtained by using an integrated geological, seismological, and geotechnical approach that brings together the unique capabilities of the Campus and Laboratory collaborators. In addition to its application of state-of-the-art scientific and engineering methods, the project is designed to include a large student participation for pedagogical purposes. Many of the site-specific results are also applicable to the risk evaluation of other sites on each campus. In the second phase, March 1999 to February 2002, the project is planning to perform the structural dynamic response analyses of the target structures to the estimated ground motions determined in the first phase, and to extend the integrated studies of strong ground motion effects to other UC campuses which are potentially at risk from large earthquakes.

This report describes the initial seismic source and site characterization studies performed for the UC Santa Barbara campus, where a new seismic station with both borehole and surface instruments has been installed. The Principal Investigator at Santa Barbara is Professor Ralph Archuleta.

This UC/CLC project is funded from several additional sources, which leverage the core support provided by the Office of the President. They are: the University Relations Program at LLNL, directed by Dr. Claire Max, and the offices of the appropriate Vice-Chancellors on the various campuses. At UC Santa Barbara, the Vice-Chancellor for Administrative Services is Dr. David Sheldon, the Executive Vice-Chancellor is Dr. Donald Crawford, and the Vice-Chancellor for Research is Dr. France Cordova.

The Director of the UC/CLC Campus Earthquake project is Dr. Francois Heuze from LLNL.

EXECUTIVE SUMMARY

The University of California Campus-Laboratory Collaboration (CLC) project is an integrated 3-year effort involving Lawrence Livermore National Laboratory (LLNL) and four UC campuses—Los Angeles (UCLA), Riverside (UCR), Santa Barbara (UCSB), and San Diego (UCSD)—plus additional collaborators at San Diego State University (SDSU), at Los Alamos National Laboratory and in industry. The primary purpose of the project is to estimate potential ground motions from large earthquakes and to predict site-specific ground-motions for one critical structure on each campus. This project thus combines the disciplines of geology, seismology, geodesy, soil dynamics, and earthquake engineering into a fully integrated approach. Once completed, the CLC project will provide a template to evaluate other buildings at each of the four UC campuses, as well as provide a methodology for evaluating seismic hazards at other critical sites in California, including other UC locations at risk from large earthquakes. Another important objective of the CLC project is the education of students and other professionals in the application of this integrated, multi-disciplinary, state-of-the-art approach to the assessment of earthquake hazard. For each campus targeted by the CLC project, the seismic hazard study will consist of four phases: **Phase I** – Initial Source and Site Characterization, **Phase II** – Drilling, Logging, Seismic Monitoring, and Laboratory Dynamic Soil Testing, **Phase III** – Modeling of Predicted Site-Specific Earthquake Ground Motions, and **Phase IV** – Calculations of 3D Building Response. This report covers **Phase I** for the UCSB campus and includes results up through March 1997.

The UCSB campus is located within one of the more seismically active regions of California and can thus expect to experience moderate to large, and perhaps even great, earthquakes within the lifetime of many existing and proposed university buildings. The UCSB **Phase I** study largely consists of two parts: a regional study that defines the tectonic province, the style of deformation, and the location, geometry, and slip rate of active faults that may act as possible sources for large earthquakes, and a local study that is focused more on site characterization and campus-specific conditions that may affect the propagation of seismic waves and the expected ground motions at the CLC-designated UCSB campus building. The UCSB building targeted for specific study is the 5-story Engineering I tower. The location of the borehole seismic monitoring station was changed, however, from the location initially proposed because of expected interference from planned new campus construction. The borehole station was thus installed between the 6-story Broida Hall and the Geology building, not far from Engineering I. The borehole data and resulting CLC model studies will thus be applicable to all three buildings, given their proximity to each other.

Earthquake Source Characterization

This report summarizes the state of knowledge in earthquake source characterization, both regionally within southern California and locally for the UCSB campus, based on reviews of existing literature, on past seismic hazard reports, on recent and on-going investigations of the region, and on our own personal experience in the geology, seismotectonics, geophysics and seismic hazard studies of the area. Our methods are similar to those adopted by the Southern California Earthquake Center (SCEC) in which, for example, earthquake recurrence intervals are calculated by integrating seismic moment rates estimated

from geological data for specific faults, geodetic measurements of regional strain rates, and regional seismicity data. This unique integrated approach—that combines geology, seismology and geodesy to evaluate possible earthquake source regions, recurrence rates, and seismic hazard—was pioneered by UC research people, first locally for the City of Santa Barbara (Nicholson, 1992) and subsequently for the southern California region as a whole (Ward, 1994).

The UCSB campus can expect to experience potentially damaging ground motions from regional earthquake sources, like the **San Andreas fault**, or from near-regional earthquake sources, like the **Santa Ynez fault**, the **Oak Ridge fault**, or possibly the **Santa Monica–Channel Islands thrust** system. These source regions can produce large, and potentially even great earthquakes that could generate large ground motions of long duration and relatively long period. The primary seismic hazard to UCSB, however, originates from a series of local active faults, some of which are blind and do not crop out at the surface where they are easily studied and characterized. These active local faults define, for the most part, the raised marine terrace upon which UCSB is located, and consist of: (1) the north-dipping, blind **North Channel–Red Mountain–Pitas Point fault** system that controls the steep sea cliff to the south; (2) the steeply south-dipping **More Ranch–Mission Ridge–Arroyo Parida fault** system that controls the northern campus escarpment; and (3) the secondary **Goleta Point fault** that truncates the campus bluff to the east and may act to segment the More Ranch fault. Because of its size, proximity, and inferred slip rate and because it likely extends directly beneath UCSB, the **North Channel fault** is believed to be the main controlling structure in terms of seismic hazard to the campus. This fault is easily capable of generating moderate to large earthquakes (in the magnitude M6 to M7 range) that would produce large displacement, high acceleration ground motions at UCSB. The estimated probability of exceeding such high ground accelerations (> 0.5 g) within 50 years at UCSB is typically on the order of 10% (Jackson et al., 1995; Frankel et al., 1996; Petersen et al., 1996)

Major issues concerning identification and characterization of earthquake sources in the vicinity of UCSB include the present poor understanding of the style of large-scale deformation within the western Transverse Ranges tectonic province, the difficulty in accurately characterizing the geometry, slip rate and maximum magnitude of blind or offshore faults, like the **North Channel fault**, and the reliability of commonly used 2D kinematic fold models to infer deep fault structure. Differing interpretations of the fundamental deformation style lead to significantly different characterizations of the blind faults in terms of their characteristic magnitudes, of the details of their fault and slip geometry relative to surface installations, and of their estimated rate of earthquake occurrence. All of these are important critical parameters in estimating the probabilities of potential site-specific ground motions that such source regions may produce. There is also significant uncertainty regarding how and if secondary structures or other along-strike discontinuities, like cross faults, tear faults or lateral ramps, observed near the surface may act to segment dynamic rupture of earthquakes at depth.

The major problem is that each of the different types of data used—and the methods or models used for analysis—are subject to potentially large uncertainties arising from limited temporal or spatial

sampling of events or of the long-term regional deformation, as well as from limited accuracy and resolution of critical fault parameters. Present model predictions of the seismic moment release rate by SCEC for moderate to large earthquakes in southern California are a factor of two greater than the rate observed since 1850. Estimating slip rates for the offshore faults is particularly problematical, since, except where these faults cross the northern Channel Islands, detailed paleoseismic data are typically not available. Segmenting long faults into individual rupture segments in an objective way also remains a difficult problem even where major faults are mapped in detail, and considerable debate exists as to whether any technique is useful for evaluating the characteristics of blind low-angle subsurface faults or detachments. The problems of fault segmentation and slip rate estimation are thus particularly acute for blind faults, which so far must rely on indirect interpretation and modeling of surface observations.

Local UCSB Site Characterization

This report also includes a number of site-specific studies of the UCSB campus, many of which were conducted for the very first time as a result of this CLC initiative. These multi-disciplinary studies were conducted to provide a better understanding of local source and site conditions that may affect estimates of earthquake ground motion, and include: (**a**) more detailed GIS-based mapping of active faults and folds in the Santa Barbara area, including the pattern of offshore faults in the Santa Barbara Channel; (**b**) improved estimates of campus uplift and near-campus surface fault slip rates using paleoseismological techniques; (**c**) compilation of campus borehole studies to produce subsurface structure contour maps and improved estimates of subsurface fault and fold geometry; (**d**) shallow seismic refraction profiles to estimate P- and S-wave velocities; (**e**) cone-penetration tests (CPT) to evaluate soil properties around the campus-designated critical structure; (**f**) *in situ* downhole velocity measurements; and (**g**) portable array monitoring of local seismicity to evaluate campus-wide amplitude variations to weak ground motion.

Results of these more detailed studies show that over much of the UCSB campus, approximately 5 m of unusually low-velocity, dry Quaternary terrace deposits (P-wave velocities of 350-500 m/s and S-wave velocities of 200–350 m/s) overlie low-density, low-velocity saturated Sisquoc Formation (P-wave velocities of ~1500 m/s and S-wave velocities of ~400 m/s). These low near-surface velocities and the strong impedance contrast between this cover material and deeper, higher-velocity basement rocks may cause significant local site amplification. The campus is also situated directly above a sedimentary syncline caused by folding in the hanging wall of the north-dipping oblique-reverse **North Channel fault**. This hanging-wall fold and fault geometry may produce additional site amplification due to focusing, directivity and other dynamic effects associated with reverse faults. Variations across the UCSB campus in weak ground motion have been observed already from the portable array monitoring of local earthquake activity. In subsequent CLC reports, these results will be further integrated with the uphole and downhole seismic monitoring data, and with results from dynamic tests of soil and rock samples retrieved from the deep boreholes drilled on campus, to model expected ground motions and 3D building response of the Engineering I tower caused by specific regional and local earthquake sources.

TABLE OF CONTENTS

TABLE OF FIGURES

1.0 INTRODUCTION

The University of California Campus-Laboratory Collaboration (CLC) project is an integrated three-year effort involving Lawrence Livermore National Laboratory (LLNL) and four UC campuses—Los Angeles (UCLA), Riverside (UCR), Santa Barbara (UCSB), and San Diego (UCSD)—plus additional collaborators at San Diego State University (SDSU), at Los Alamos National Laboratory and in industry. The primary purpose of the project is to estimate potential ground motions from large earthquakes and to model the building response to these predicted ground-motion estimates for one critical structure on each campus. This project thus combines the disciplines of geology, seismology, geodesy, soil dynamics, and earthquake engineering into a fully integrated approach. Once completed, the CLC project will provide a template to evaluate other buildings on each of the four UC campuses, as well as provide a methodology for evaluating seismic hazards at other critical sites in California, including other UC locations at risk from large earthquakes. Another important objective of the CLC project is the education of students and other professionals in the application of this integrated, multi-disciplinary, state-of-the-art approach to the assessment of earthquake hazard.

California is the most seismically active region of the continental United States. This earthquake activity is distributed on a system of faults that covers nearly the entire State. **Figure 1** shows the active fault map of California produced by the California Division of Mines and Geology (CDMG). Most UC campuses are located in close proximity to at least one of these known active faults. This, plus the prior earthquake history of these sites, indicates that several UC campuses—including those in southern California under study by the CLC project (UCLA, UCR, UCSB, and UCSD)—are likely to experience moderate to large earthquakes within the lifetime of many existing university buildings. Fortunately, in terms of seismic hazard assessment, an intensive research program, coordinated by the Southern California Earthquake Center (SCEC) is already underway that is focused on understanding the seismic hazards and regional tectonics of southern California. A primary effort of SCEC is the improvement of our ability to identify and characterize potential earthquake sources within this region, and to predict the ground motion and other effects from these sources. Thus, largely through the efforts of SCEC, this region has become the prototype for the development of new approaches to seismic hazard analysis that integrate data from several different earth science disciplines and engineering.

Using these new techniques, a preliminary estimate of the regional seismic hazard—typically expressed as the probability or expected frequency of exceedance for a certain level of peak ground acceleration within a certain time period—has been determined by SCEC (**Figure 2**) for southern California (Jackson et al, 1994). Revised versions of this map have been produced by the US Geological Survey (Frankel, 1996) and by CDMG (Petersen et al, 1996). These maps confirm that the seismic hazard to several UC campuses is both real and significant. The CLC project is thus in the fortunate position of being able to capitalize on this regional research effort, and on the techniques, methods and database of hazard information SCEC and others have developed, to form a more focused and coordinated seismic hazard study for each specific UC campus site.

1.1 Methods and Philosophy of the CLC Seismic Hazard Project

The basic approach of the CLC project is to combine the substantial expertise in geology, in seismology and in engineering that exists within the UC system with recent advances in earthquake hazard assessment, in seismic wave propagation, in soil dynamics, and in modeling building response to develop an improved methodology for evaluating the seismic hazard to UC campus facilities. The UC campuses currently chosen to test and apply this new methodology are UCLA, UCR, UCSB, and UCSD. The basic procedure is to first identify possible earthquake source regions and local campus site conditions that may affect estimates of earthquake ground motion. Various geological, geophysical, and geotechnical studies are conducted to characterize each campus, with specific studies focused on the location of the CLC target building. The project will then drill and log deep boreholes on each campus to provide direct *in situ* measurements of subsurface material properties, and to install uphole and downhole 3-component seismic sensors to monitor and record strong and weak ground motion. The boreholes provide access to deeper materials below the soil layer that have relatively high seismic shear-wave velocity. Comparison of the uphole and downhole recordings of earthquakes provide empirical estimates of the local site response. The data, observations, and results are combined with earthquake rupture scenarios of identified causative faults using non-linear soil models to provide site-specific estimates of strong ground motion near the target building. The predicted ground motions are then used as inputs into 3D dynamic building models to evaluate the response of the target building to large earthquakes. Thus for each campus targeted by the CLC project, the seismic hazard study will consist of four phases: **Phase I** – Initial Source and Site Characterization, **Phase II** – Drilling, Logging, Seismic Monitoring and Laboratory Dynamic Soil Testing, **Phase III** – Modeling of Predicted Site-Specific Earthquake Ground Motions, and **Phase IV** – Calculations of 3D Building Response.

This report covers **Phase I** for the UCSB campus and includes results up through March 1997. It summarizes the state of knowledge in earthquake source characterization, both regionally within southern California and locally for the UCSB campus, based on reviews of existing literature, on past seismic hazard reports, on recent and on-going investigations of the region, and on our own personal experience in the geology, seismotectonics, geophysics and seismic hazard studies of the area. This unique integrated approach—that combines geology, seismology and geodesy to evaluate possible earthquake source regions, recurrence rates, and seismic hazard—was pioneered by UC research people, first locally for the City of Santa Barbara (Nicholson, 1992) and subsequently for the southern California region (Ward, 1994).

This report also includes a number of site-specific studies of the UCSB campus, many of which were conducted for the very first time as a result of this CLC initiative. These multi-disciplinary studies were conducted to provide a better understanding of local source and site conditions that may affect estimates of earthquake ground motion, and include: (**a**) GIS-based mapping of active faults and folds in the Santa Barbara area, including the pattern of offshore faults in the Santa Barbara Channel; (**b**) improved estimates of campus uplift and near-campus surface fault slip rates using paleoseismological

techniques; (c) compilation of campus borehole foundation studies to produce near-surface structure contour maps; (d) shallow seismic refraction profiles to estimate both P- and S-wave velocities; (e) cone-penetration tests (CPT) to evaluate soil properties around the campus-designated critical structure; (f) *in situ* downhole velocity measurements; and (g) portable array monitoring of local seismicity to evaluate campus-wide amplitude variations to weak ground motion.

Fundamental issues regarding earthquake source characterization, characteristic magnitudes, fault segmentation and earthquake recurrence—especially as they relate to seismic hazards affecting the UCSB campus—are also discussed. In particular, we consider major issues revealed by the preliminary site and source characterization studies that potentially have an impact on UCSB hazard evaluation. These characteristics include subsurface structure, hanging-wall fault geometry, velocity interfaces, and unusual soil conditions that may affect the propagation, attenuation, variation and amplification of strong ground motion on campus as produced by large local and regional earthquakes.

2.0 UC SANTA BARBARA STUDY AREA

2.1 Seismic Hazard Exposure of the UCSB Campus

This CLC report focuses on the UC campus at Santa Barbara. **Figures 1, 2, and 3** show UCSB relative to the state map of active faults (CDMG, 1994), the probability of peak ground acceleration (SCEC, 1996), and the location of historical earthquakes (1932-1996) in southern California, respectively. These three figures reinforce the concept that UCSB is situated in an area of active faulting with relatively high seismic risk from earthquakes that occur both onshore and offshore of southern California. In the preliminary seismic hazard map produced by SCEC, UCSB is likely to experience levels of peak acceleration of 0.2 g or greater at least 3 or 4 times per century (**Figure 2**), and both the SCEC and CDMG hazard maps estimate that the 50-yr probability of exceeding 0.5 g to 0.6 g is nearly 10% (Jackson et al, 1994, Petersen et al, 1996).

The UCSB study area largely consists of two parts: a regional study area that defines the tectonic province, the style of deformation, and the location, geometry, and slip rate of active faults that may act as possible sources for large earthquakes, and a local study area that is focused more on site characterization and campus-specific conditions that may affect the propagation of seismic waves. The identification and characterization of earthquake sources of potential significance to UCSB typically follows increasing levels of detail for diminishing distance ranges to the campus

2.2 UCSB Campus Critical Structure Designation

To demonstrate the effectiveness and applicability of this method of seismic hazard evaluation for individual buildings at risk, one particular structure on each UC campus is chosen for more detailed site studies and to model its building response to the predicted earthquake ground motions. For UCSB, the UCSB administration chose the 5-story Engineering I tower located on the eastern edge of the campus. **Figure 4** shows a map of the UCSB campus with the location of the Engineering I building, the site of the CLC boreholes for uphole and downhole seismic monitoring, and the locations of seismic refraction

profiles conducted as part of the CLC project. The Engineering I tower was chosen because of its size and relatively high occupancy rate. In addition, the building is scheduled for extensive seismic retrofitting in the near future. The proposed building modifications will enable the CLC project to more accurately model the building response, and thus the effectiveness of the retrofitting process itself. Subsequent concerns regarding possible interference from new campus construction resulted in a change in the placement of the CLC borehole instruments from the site originally proposed. The actual location for the CLC boreholes is between the 6-story Broida Hall physics building and the 2-story Webb Hall geology building, not far from Engineering I. The borehole data and resulting CLC model studies will thus be equally applicable to all three buildings, given their close proximity to each other.

3.0 SEISMOTECTONIC SETTING OF THE UC SANTA BARBARA CAMPUS

3.1 Regional Setting

The UCSB campus is located within a complicated zone of deformation associated with the Pacific–North American plate boundary. This zone represents an unusual continental transform that has evolved into its present form over the last 20 to 30 Ma(e.g., Atwater, 1970, 1989; Nicholson et al, 1994). It currently consists of a wide belt of northwest-trending deformation extending from the Gulf of California to Cape Mendocino, and from the offshore continental shelf on the west to the eastern California shear zone on the east. Within this broad zone of deformation, relative plate motion is accommodated predominantly by right-lateral displacement on a series of major northwest-striking faults (**Figure 1**). The San Andreas fault (SAF) is the principal member of this series, accommodating up to 70% of the relative plate motion of about 50 mm/yr in central California. In southern California, this plate boundary deformation branches into a system of major sub-parallel right-lateral fault zones. The main members of this system are the north and south branches of the SAF, the San Jacinto, the Whittier-Elsinore, and the Newport-Inglewood fault zones. The remaining right slip is distributed among offshore faults, such as the San Gregorio-Hosgri and San Clemente faults to the west, and faults of the eastern California shear zone, such as those that ruptured in the 1992 Joshua Tree-Landers earthquake sequence in the Mojave desert. Additional components of plate boundary convergence are accommodated on a system of reverse and oblique-reverse faults and folds. This is particularly true in the region of the western Transverse Ranges tectonic province (**Figure 5**), where predominantly east-west-striking left-oblique and reverse faults appear to be active. However, it is the major right-lateral faults that have produced—at least so far—the great historical earthquakes in California, like the 1857 Fort Tejon and 1906 San Francisco earthquakes on the SAF.

3.2 The Western Transverse Ranges Province

UCSB sits within the western Transverse Ranges tectonic province. The western Transverse Ranges are a unique physiographic region of California characterized by a central highlands, dominated by uplift, erosion and strike-slip faulting, and flanked by active fold-and-thrust belts (Keller et al, 1987; Namson and Davis, 1988; Yeats et al, 1988). **Figure 5** shows a schematic map of many of the major

tectonic elements of the western Transverse Ranges (Sorlien, 1995). These predominantly east-west-trending structures generally cut across the major northwest-trending faults that make up the greater SAF system. Geological and geophysical evidence indicates that these structures are tectonically rotated (e.g., Kamerling and Luyendyk, 1979, 1985; Crouch and Suppe, 1993) and based on seismological and geodetic studies, these structures are continuing to rotate today (Jackson and Molnar, 1990; Feigl et al, 1993; Molnar and Gibson, 1994). Within the western Transverse Ranges, a significant part of the recent (<5 Ma) plate motion has been taken up in large-scale crustal shortening on predominantly west-striking low- to moderately-dipping reverse, oblique-reverse and thrust faults that join sub-parallel left-lateral strike-slip faults as significant earthquake sources. **Figure 6** shows one of several different model cross sections that have been proposed to explain how this component of shortening may be accommodated (Anderson, 1993; Lettis and Namson, 1993). Tectonic geomorphology suggests that much of this active folding, faulting and uplift has migrated to the edges of the fold-and-thrust belts (Keller et al, 1987; Keller et al, 1988).

Several important implications in terms of earthquake hazard assessment follow directly from this basic understanding of western Transverse Ranges development. First, because of the large-scale crustal shortening involved, the earthquake hazard within this province includes a significant contribution from active buried (or blind) low- to moderately-dipping faults (e.g., **Figure 6**) that do not crop out at the surface where they are easily identified and characterized. Several of these faults likely sole into a master detachment fault at depth that is responsible for the long-wavelength folding of the Santa Ynez Mountains. In **Figure 6**, this is referred to as the San Cayetano thrust system. Second, because of the tectonic rotations involved, faults within this province typically exhibit a significant component of oblique slip and have undergone an unusual and complicated history of deformation—evolving from oblique-normal into strike-slip, oblique-reverse or even oblique-thrust faults. This implies two things: (1) resolving only the dip-slip component of faulting may not properly estimate the hazard; and (2) folding associated with the recent uplift and crustal shortening will not necessarily correspond to simple 2D fault-related fold models (**Figure 6**) that do not take into account this rotation, strike-slip deformation, and prior fault history. Thus, the reliability and applicability of simple 2D fault-related fold models often used to infer the location, geometry and slip rate of active subsurface 3D fault structures within the western Transverse Ranges province must be seriously evaluated (Kamerling and Nicholson, 1995)—if such model results are used to control estimates of regional seismic hazard.

4.0 GEOLOGIC STUDIES RELATED TO EARTHQUAKE SOURCE CHARACTERIZATION

4.1 GIS-based Mapping and Earthquake Source Methodology

There are a number of ways to identify and characterize earthquake source regions. The most systematic and comprehensive regional study of earthquake sources in southern California has been recently completed by SCEC (Jackson et al, 1995). We utilize this SCEC database as a basis for our regional hazard analysis of UCSB because it integrates different geological and geophysical datasets

to characterize earthquake sources and to estimate earthquake recurrence rates. Within the SCEC source model, each fault judged capable of producing strong ground motions that contribute to seismic hazard is first characterized in terms of: (1) the type of source; (2) its location (distance from the study area) and orientation; (3) the frequency-magnitude distribution for the source; and (4) estimates of the uncertainties in the parameters. The SCEC source model for southern California contains 65 source zones classified by how well the average displacement per event, displacement rate, and the date of the last major earthquake along each fault segment is known. The results (and uncertainties) are then used to estimate conditional probabilities of earthquake occurrence on each fault segment and the results are summed to yield estimates of the regional seismic hazard (**Figure 2**). **Table 1** lists some of the major active fault segments within 100 km of the UCSB campus, as well as their inferred lengths, slip rates, maximum magnitudes and recurrence intervals.

To facilitate the integration of geologic and geophysical data into a comprehensive earthquake hazard analysis, we incorporate these datasets into a Geographical Information System (GIS) data archive and mapping program. Preliminary maps of the Santa Barbara and Ventura areas have been compiled using Arc-Info and Arc-View (**Figure 7**). These maps utilize a GIS database synthesized from mostly geotechnical, industrial and academic research sources. Pertinent geologic, structural, and geomorphic data are input and assigned individual layers. This enables us to produce site-specific geologic maps, like **Figure 7**, that include regional surface geology, soil type and results from recent mapping studies at UCSB of active fault and fold structures in the Santa Barbara-Goleta-Carpinteria area. A digital elevation model (DEM) with 100-m resolution forms the base map for the GIS database. This GIS capability allows the generation of 3-dimensional perspective views that relate geomorphology to active tectonic structures (**Figure 8**) and enhances our ability to identify and visualize multi-dimensional aspects of the earthquake hazard that include both source and site conditions.

4.2 Regional Earthquake Sources

The regional sources described below are typically those faults within 100 to 200 km of the study area judged to be capable of generating M≥ 7.0 earthquakes that might produce significant strong ground motions within the Santa Barbara area. In general, these faults have estimated slip rates of 3 mm/yr or greater, and hence characteristic recurrence rates on the order of hundreds rather than thousands of years. These faults are shown in **Figure 1**. Although these faults are considered the most active within the State, the specific hazard to UCSB from many of these faults is diminished by their relatively large distance from the site. These faults can, however, generate very large earthquakes that could produce significant ground motions (> 0.2 g) at UCSB having relatively long periods and long duration.

San Andreas Fault: The most significant regional earthquake source in California is the SAF. The UCSB campus lies, at its closest approach, about 60 km south of the SAF that last ruptured in the M7.9 earthquake of 1857 (**Figure 1**). The 1857 earthquake produced intensities of MM VI-VII in Santa Barbara. Estimated duration of shaking lasted in the range of 60 to 90 sec (Agnew and Sieh, 1978), indicating that large, long-duration ground motions can be expected in the Santa Barbara area from this

source. SCEC divides the 1857 stretch into 3 principal segments: Cholame (about 50 km long), Carrizo (120 km), and Mojave (130 km). The remaining 200 km of the fault to the southeast is divided into two more segments: San Bernardino (80 km) and Coachella (115 km). In southern California, the SAF exhibits slip rates that vary from about 35 mm/yr (Cholame segment) to about 25 mm/yr (Coachella segment)(Sieh et al, 1989). Based upon paleoseismic data, each segment, apart from perhaps Cholame, is inferred to rupture individually to produce its own characteristic sized earthquake. In addition, two or more contiguous segments can rupture together to produce a much larger event. For example, the 1857 earthquake (M7.9) is believed to have ruptured, from northwest to southeast, the Cholame, Carrizo and Mojave segments. All segments (with the possible exception of the Cholame segment) are estimated to be capable of producing earthquakes greater than M7.0 individually, and the characteristic earthquakes estimated for the two segments, Carrizo and Mojave, closest to the study area are M7.5 to M7.6. Preferred conditional probabilities estimated by SCEC for the Carrizo, Mojave and San Bernardino segments rupturing individually during the next 30 years are 18±9%, 26±11% and 28±13%, respectively, if interactions are not considered, and the probability that at least one characteristic earthquake will occur on the southern SAF during the next 30 years is estimated at 66%. Additional concerns from this source for UCSB arise from possible enhanced seismic radiation and/or directivity effects for a dynamic rupture that propagates to the southeast around the Big Bend region of the SAF, and the possible sympathetic triggering of a large, local earthquake within the western Transverse Ranges province as a result of a large SAF event (e.g., Molnar, 1992; 1995).

San Jacinto Fault: SCEC divides the San Jacinto fault system into 7 individual segments. The main segments (San Bernardino Valley, San Jacinto and Anza) are estimated to carry about 12 mm/yr of right-lateral relative plate motion. This system has been the source of several M>6 earthquakes during the past 100 years, but only the 1892 event near Anza may have been greater than M7. Only the northwestern end of the San Bernardino Valley segment (characteristic magnitude M6.8) is within 200 km of the study area. The San Jacinto and Anza segments lie beyond 200 km from UCSB. The Anza segment is estimated to be capable of generating magnitude 7.0-7.5 earthquakes, with an estimated repeat time of 250 (+321, -145) years. A cascade rupture of all 7 segments would produce an estimated M7.5 earthquake. Failure of the San Bernardino to Anza stretch would produce an M7.4 event.

Whittier-Elsinore Fault: The Whittier-Elsinore fault system is broken into 5 segments by SCEC. The three central segments (Glen Ivy, Temecula and Julian) have an estimated slip rate of 5 mm/yr. The Whittier segment and the northwestern end of the Glen Ivy segment are within 200 km of the study area, and have estimated individual characteristic magnitudes of M6.8-6.9. The rest of the Glen Ivy segment and the Temecula and Julian segments are within 200 to 300 km, but the largest earthquake estimated for any of these is about magnitude M7.1. The characteristic magnitude estimated for a cascade of all 5 segments is M7.4, with a recurrence rate of 25% per 1000 years.

Garlock Fault: The left-lateral strike-slip Garlock fault is about 250 km long and separates the Sierra Nevada and Basin-and-Range tectonic provinces from the Mojave desert. Following Wesnousky

(1986), SCEC divides the fault into largely two segments. The 100 and 130 km lengths for the east and west segments of the Garlock fault give estimated magnitudes of M7.3 within 200 km and M7.5 within 300 km of UCSB, respectively. McGill and Sieh (1993) deduce displacements ranging from 2 to 7 m per event, and slip rates from 1 to 11 mm/yr. SCEC adopts a preferred value of 7.5 mm/yr for both segments.

White Wolf Fault: The White Wolf fault approaches to within 90 km of the UCSB campus and was the source of the M7.7 Kern County earthquake of 1952. This is the largest earthquake in southern California since 1857, and caused damage in Santa Barbara where liquefaction effects were also reported. The White Wolf fault is a south-dipping oblique-reverse fault located at the northern boundary of the Transverse Ranges province. SCEC assigns an estimated fault rupture length of 89 km to the 1952 event; other estimates vary from about 60 km (Wesnousky, 1986) to 80 km (Ward, 1994). The 1952 earthquake only produced surface rupture along the northeastern 45 km of the fault; it did not rupture the surface along the main fault trace to the southwest. Based on these length estimates, SCEC and Wesnousky calculate characteristic magnitudes of M7.3 and M7.2, respectively. Stein and Thatcher (1981) estimate the slip rate to be in the range 3.0–9.0 mm/yr over the last 0.6 to 1.2 Ma The significance of this fault to seismic hazard within the Santa Barbara area depends mainly on the recurrence interval of the characteristic earthquake, for which estimates vary widely. Wesnousky estimates a return period of 300 years, based upon data from Stein and Thatcher (1981), but application of the integrated SCEC methodology results in much larger estimates for the return period that range from >2000 years (Ward, 1994) to nearly 9000 years (Jackson et al, 1995), respectively.

Hosgri Fault: The offshore San-Gregorio-Hosgri fault system extends to the south about 380 km from San Francisco Bay. The southern part of the Hosgri fault zone extends about 90 km from onshore Point San Simeon to south of Point San Luis, and shows evidence for Holocene displacement both on- and offshore (PG&E, 1988). Steritz and Luyendyk (1994) traced the Hosgri fault south from Purisima Point to Point Arguello with high-resolution and deep-penetration seismic reflection data. From here they interpret it to continue around Point Conception where it may connect with the North Channel fault system (Yerkes et al, 1981). Offshore of Santa Maria and Lompoc, the Hosgri images as a steeply dipping fault in the upper two seconds. It displays strike-slip offset features, but is clearly up on the east. PG&E (1988) conclude that displacement on the Hosgri fault is predominantly right-slip with a substantial reverse component. Steritz and Luyendyk could find no consistent piercing points to constrain the sense or amount of offset. The Hosgri fault zone approaches to within less than 100 km of the study area. Based upon a fault length of 60 km, and preferred Holocene slip rate and displacement per event of 3±2 mm/yr and 1-2 m, respectively (PG&E, 1988; Hanson et al, 1994; Hall et al, 1994), SCEC estimates a characteristic magnitude of M7.1 with a recurrence interval of about 2000 years. This fault may have been the source of the offshore M7.3 1927 Lompoc earthquake.

Palos Verdes and Newport-Inglewood Faults: The Palos Verdes fault extends from Santa Monica Bay at least 75 km to the south-southeast (Petersen and Wesnousky, 1994). It is mapped for about 15 km on the Palos Verdes Peninsular, and approaches within about 80 km of UCSB. Wesnousky (1986) and

Petersen and Wesnousky (1994) describe the sense of slip on this fault as right-reverse, with a vertical slip rate of 0.3 to 0.7 mm/yr. However, Rockwell (1995a) presents strong evidence based upon high-resolution seismic reflection data, borings and onshore trenching that the dominant sense of slip on the Palos Verdes fault is right-lateral at 2.5 to 3.5 mm/yr. Based on these recent interpretations, SCEC split the fault into two 55-km long segments and assigned a right-lateral slip rate of 3±1 mm/yr and a characteristic magnitude of M7.1 to both, with a recurrence interval of about 700 years. Right-lateral plate motion is also taken up on the parallel Newport-Inglewood fault, which was probably the source of the M6.4 1933 Long Beach earthquake. The slip rate on the northwesterly onshore segment of this fault is estimated as 1 mm/yr, and the characteristic magnitude is estimated as M6.8 by SCEC and M7.0 by Petersen et al (1995). However, Petersen et al estimate a recurrence interval of about 1700 years, significantly longer than the 470 years used by SCEC.

4.3 Earthquake Sources within the Western Transverse Ranges Province

In this section we describe known active faults and folds within the western Transverse Ranges province (**Figure 5**) and other potential nearby earthquake sources within the adjacent offshore borderland. The focus of this section is on active structures within 50 km of the study area, but we also discuss the seismic potential of these structures within the context of the broader regional style of faulting. This is particularly important for offshore and onshore faults in the Santa Barbara region, as these have been generally less well studied than earthquake sources located onshore to the east, within the Ventura and Los Angeles basins.

Shortening across the western Transverse Ranges province is mostly taken up on both north- and south-verging structures, which include folds, surface reverse faults and probably blind reverse and thrust faults (e.g., **Figure 6**). In addition, since the region is undergoing tectonic rotation, several of these structures also accommodate oblique or strike-slip components of motion. Within the western Transverse Ranges, there are several east-trending regional fault structures that represent the predominant earthquake hazard to the UCSB campus. These structures include the Santa Ynez, San Cayetano, More Ranch–Mission Ridge, North Channel/Pitas Point, Oak Ridge, and Malibu Coast/Channel Islands fault systems (**Figure 5**). Each of these active regional structures typically has associated with it an active fault and fold belt. For the purpose of identifying potential seismic sources in the western Transverse Ranges province, we first consider the onshore Ventura fault and fold belt, followed by the Santa Barbara fault and fold belt, and then offshore faults within the Santa Barbara Channel or associated with the Northern Channel Islands and California Continental Borderland. Active faults and folds are considered to be those known to deform Pleistocene and younger deposits.

4.3.1 Ventura Fault and Fold Belt

The Ventura fault and fold belt is a regional tectonic province characterized by numerous east-west-striking reverse faults and folds extending from the Topa Topa and Santa Ynez mountains to the north to the Santa Monica mountains to the south, and is bounded by the San Gabriel fault on the east (**Figure 5**). The on-land portion of the fault and fold belt extends westward into the Santa Barbara Channel.

Between the mountain ranges to the north and south, the Ventura basin is a deep structural trough that is bordered on the north by the north-dipping San Cayetano and Red Mountain reverse faults, and on the south, by the south-dipping Oak Ridge reverse or oblique reverse fault (Yeats, 1988; Huftile and Yeats, 1995). The Ventura fault and fold belt contains several structures known to be active in Holocene time, including the San Cayetano, Red Mountain, Pitas Point and Oak Ridge faults, the Ventura Avenue anticline, and potentially active structures, such as the Arroyo Parida fault. Direct evidence for past major earthquakes is, however, very limited. Nearly all the shortening across the Ventura fault and fold belt occurs on or north of the Oak Ridge fault (Yeats, 1983; Donnellan et al, 1993a, b). Because there appears to be relatively little Quaternary deformation in the Santa Ynez and Topa Topa mountains, this shortening thus appears to be taken up on the major faults that border the Ventura basin, on folds within and on the margins of the basin, and possibly on underlying blind faults. Slip rate estimates are available for the Oak Ridge, San Cayetano, Red Mountain, Ventura and Javon Canyon faults, but in general earthquake recurrence intervals are not well constrained.

San Cayetano Fault: SCEC divides the San Cayetano fault into a 24-km western segment and a 16-km eastern (Modelo lobe) segment, based upon the work of Huftile (1992). The western segment dips about 50°N near the surface (Huftile and Yeats, 1995). Microseismicity indicates that it may continue at a dip of 50° to 55° to at least 16 or 18 km depth (e.g., Jones and Simila, 1995). There is abundant evidence for Holocene activity, but there appears to have been no surface faulting in the last 200 years. Based on fluvial terrace deposits and offset alluvial fans, Rockwell (1988) estimated vertical slip rates ranging from 1.05±0.2 mm/yr to 3.6±0.4 mm/yr for the western segment of the fault, decreasing to zero in the Ojai Valley. He suggested that the long-term rate for the last 200 ka might be as high as 8.7±1.9 mm/yr. Huftile and Yeats (1995) and Huftile (1992) estimate rates of 3.6 to 5.8 mm/yr and 4.4 to 10.4 mm/yr for the western and Modelo lobe segments, respectively, based on displaced Pleistocene Saugus formation (dated at 500 ka). SCEC adopted a value of 4.5±1.5 mm/yr. Rockwell (1988) suggests that damaging earthquakes on the San Cayetano fault have a recurrence interval of 200 to 600 years.

Red Mountain Fault: South-verging displacement along the northern margin of the Ventura basin west of Sulfur Mountain is taken up on the Red Mountain fault (Huftile and Yeats, 1995), which has a mapped length of about 40 km and extends offshore. No large historical earthquakes are associated with the Red Mountain fault, but microseismicity shows that it is presently active. The fault dips at ~60°N to a depth of 3 km (based on borehole data), and may continue at a moderate angle to a depth of 18 km based on seismicity (O'Connell, 1995; Nicholson and Kamerling, 1997). Yeats (1988) suggests that the slip rate on the Red Mountain fault is similar to that on the Oak Ridge and San Cayetano faults, although the timing of displacement on this fault is poorly known. Based upon a balanced, retrodeformable cross section that includes the Saugus formation, Huftile and Yeats (1995) estimate 0.2 to 3.5 km of vertical displacement during the last 500 ka, yielding a dip-slip rate of 0.4 to 7.0 mm/yr.

Ojai Valley Blind Thrust: Between the north-dipping San Cayetano and Red Mountain faults there is no north-dipping fault that crops out to take up south-verging displacement along the northern

margin of the Ventura basin. Huftile and Yeats (1995) propose that this displacement is transferred from the Red Mountain fault to the San Cayetano fault via a moderately-dipping blind thrust beneath the Ojai Valley, Topa Topa Mountains and an associated fold. According to this model, the Lion fault is the surface expression of a passive back thrust (part of the Sisar décollement of Yeats, 1988), extending from the tip of the blind thrust along bedding within the Miocene Rincon formation at depth of about 7 km. A blind thrust in this location was first postulated by Namson and Davis (1988), but they propose that the detachment is a buried western extension of the San Cayetano fault. In their model, Lion Mountain within the Sulfur Mountain anticlinorium is a fault-bend fold above the blind thrust. Huftile and Yeats also ascribe folding of the Sulfur Mountain anticlinorium and displacement on the Lion fault in part to displacement on the blind thrust, but show that this displacement is difficult to resolve.

Onshore Oak Ridge Fault: The south-dipping Oak Ridge fault is traceable onshore from the Santa Susana Mountains to within 2 km of the coast, and its apparent offshore continuation can be traced on seismic reflection profiles to the middle of the Santa Barbara Channel. Onshore, the fault takes up north-verging displacement along the southern border of the Ventura basin. Recent work (Yeats, 1988, 1993) makes this the best characterized of the know active faults in the basin. East of South Mountain, near Santa Paula (**Figure 5**), the fault shows evidence for Pleistocene activity at the surface. Based on a balanced retrodeformable model that includes the Saugus formation, Levi and Yeats (1993) and Huftile and Yeats (1995) estimate the vertical slip rate of the fault at South Mountain to be 5 mm/yr, from which SCEC adopted a value of 4.9±1 mm/yr. The onshore fault is believed to be capable of producing M7.3 earthquakes and, assuming a displacement per event in the range of 2 to 3 m, this would give an average recurrence interval on the order of 500 years. Yeats and Huftile (1995) hypothesize, based primarily on gravity data, that a splay of the Oak Ridge fault extends to the east under the Santa Susana Mountains as a south-dipping blind reverse fault, and that this splay was the likely source of the 1994 M6.7 Northridge earthquake. Since the estimated slip rate on the fault in the Ventura basin is about three times higher than that under the Santa Susana Mountains, a rupture on the Oak Ridge fault within the basin—similar to the 1994 event—appears to be a distinct possibility.

The Oak Ridge fault is often assumed to have originated as a north-dipping Miocene normal fault (Namson and Davis, 1988; Shaw and Suppe, 1994; Huftile and Yeats, 1995), with the shallow part folded to become south-dipping and reactivated as a reverse fault. However, seismicity, subsurface geology and recent geodetic data suggest that the fault is now, and probably always has been a major through-going, south-dipping crustal feature (Hopps et al, 1992; Donnellan et al, 1993; Nicholson and Kamerling, 1995) suggesting that it probably originated as a south-dipping normal or oblique-normal fault. West of Santa Paula, the topographic expression of the Oak Ridge fault and evidence for Pleistocene vertical displacement die out abruptly (Yeats, 1988). Yeats and Taylor (1990) suggest that shortening along the E-W segments of the fault gains a left-lateral component along the NE-striking segment west of Santa Paula; a Pliocene seastack is displaced about 3.5 km left-laterally, and map restoration (unfolding) requires about 3-3.5 km of left slip. This slip can be inferred to be post 1 Ma

(Yeats and Taylor, 1990; Sorlien et al, 1995). Thus, the NE-striking segment can be considered a lateral tear fault or transfer zone, allowing the predominantly E-W-striking Oak Ridge reverse fault in the Ventura basin to step south to its offshore equivalent.

Ventura Avenue Anticline: The Ventura Avenue anticline is actively growing. Rates of uplift based on deformed terraces of the Ventura River suggest that the rate of uplift has decreased during the past 100,000 years from approximately 7 mm/yr to 4 mm/yr (Rockwell et al, 1988). In a similar model to that of Huftile and Yeats (1995), Namson and Davis (1988) model this anticline as a series of wedge-shaped imbricate thrusts that root into a Miocene décollement. The fold is complex and contains buried faults that may be capable of producing significant earthquakes. Although a relatively small structure, its importance to seismic hazard assessment in southern California may be significant. This is because the fold is currently growing without major or even minor earthquakes. This aseismic uplift of the anticline was first recognized by Sylvester (1995), and was subsequently confirmed by continued aseismic afterslip across the Ventura basin and San Fernando Valley following the 1994 Northridge earthquake (Donnellan et al, 1996). If further substantiated, this indicates that not all crustal strains measured geodetically in southern California are stored as elastic strain energy to be released in large earthquakes—as was assumed by Dolan et al (1995)—but that some of this deformation occurs aseismically, implying that the overall regional seismic hazard may be less than previously supposed.

Ventura and Javon Canyon Faults: South of the Red Mountain fault, the Javon Canyon fault shows evidence for four or five moderate earthquakes during the past 3500 years, for which a slip rate of about 1 mm/yr and an average recurrence interval of about 700 years are estimated (Sarna-Wojcicki et al, 1987). A prominent scarp just north of the city of Ventura is associated with the north-dipping Ventura fault. Petersen and Wesnousky (1995) report an estimated dip slip rate of 0.8 to 2.4 mm/yr during the last 5,700 to 15,000 years for this fault. However, the seismogenic potential of both these faults has been questioned. Trenches excavated across the Ventura fault onshore are inconclusive, and the scarp may be a fold surface associated with a deeper buried fault. Nevertheless, these faults still represent potential earthquake sources, especially farther west, largely because the offshore extension of the Ventura fault—the Pitas Point fault—exhibits seismicity and significant subsurface fault separation.

4.3.2 Santa Barbara Fault and Fold Belt

Most of the potentially active structures exposed at the surface within the Santa Barbara fault and fold belt are north-verging and are related to south-dipping reverse faults associated with surface folding. Although the major onshore fault system within the fault and fold belt, the More Ranch-Mission Ridge-Arroyo Parida fault system, and its bounding fault to the north, the Santa Ynez fault, are long (**Figures 5 and 7**) and exhibit evidence of Holocene slip (Keller et al, 1995), they have not been studied in detail and relatively little is known about them. Existing data do indicate, however, that slip rates on these fault systems are relatively low (less than 1 to 2 mm/yr), implying recurrence times for moderate and large earthquakes in the range of hundreds to thousands of years.

Santa Ynez Fault: The Santa Ynez fault can be traced continuously over a length of 160 to 180 km, and is therefore one of the longest faults west of the SAF (**Figure 7**). Based on an assumed segment length of 50 km, SCEC assigns a characteristic magnitude of M7.0 to it; although based on its overall length, this fault would be capable of producing M7.5 earthquakes. The fault trace is not very well defined except locally, where it is generally observed to dip steeply to the south. The sense of slip and total offset remain uncertain, but there is evidence for both left-lateral and reverse motion (c.f., Petersen and Wesnousky, 1994). Evidence for left-lateral Holocene displacement is presented by Darrow and Sylvester (1983, 1984), who suggest 5 to 10 m of left-lateral slip during the late Pleistocene to Holocene. Slickensides in Blue Canyon and Matilija Creek indicate left-slip (Sorlien, unpublished; Huftile and Yeats, 1995), and a fault-related furrow is associated with left-lateral gully deflections in Blue Canyon (Page et al, 1951), although systematic left deflections are not evident elsewhere. Petersen and Wesnousky (1994) give an estimated vertical slip rate of 0.1 to 0.7 mm/yr, and state that the observations allow a similar rate of left-lateral motion.

More Ranch-Mission Ridge-Arroyo Parida Fault System: The Santa Barbara coastal zone south of the Santa Ynez anticlinorium from Carpinteria west to Goleta (**Figure 7**) is dominated by active folding and faulting associated with the More Ranch-Mission Ridge-Arroyo Parida fault system. Virtually every topographically high area of the Santa Barbara region, including the Riviera, Mission Ridge, Hope Ranch, the Mesa and Campus Point, has been recently uplifted, and is on the up-thrown block of a potentially active reverse or oblique-reverse fault. Pleistocene and Holocene fault scarps range in height from about a meter to several tens of meters. Marine terraces are uplifted, faulted, folded or tilted and Pleistocene alluvial fan and stream deposits are similarly deformed. The dominant north-verging structure is an active fault system that consists of three geomorphic segments: the western segment is the **More Ranch fault,** the central segment is the **Mission Ridge fault**, and the eastern segment is the **Arroyo Parida fault**. The total length of this system is about 70 km. The Arroyo Parida fault near Ojai has an estimated vertical displacement of 0.37±0.02 mm/yr over the last 38 ka (Rockwell et al, 1984), and Petersen and Wesnousky (1994) quote a minimum vertical slip rate of 0.3 mm/yr on the More Ranch fault. The fault system has an estimated overall slip rate of 0.4-2.0 mm/yr and is believed to be capable of producing earthquakes greater than M6.5. This fault system is largest, most recently active onshore fault system that can be mapped in closest proximity to the UCSB campus.

4.3.2.1 Local UCSB Campus Faults and Structure

GIS-based mapping of active tectonic structures and surface geology in the Goleta area and in the immediate vicinity of the UCSB campus is shown in **Figures 9 and 10**. The main UCSB campus is located on a largely E-W-striking fault-bounded block that consists of a raised marine terrace situated between two low-lying areas: the Goleta slough to the north and the Santa Barbara Channel to the south (**Figure 10**). Faults responsible for the elevated campus region include the blind, north-dipping **North Channel fault** system located just offshore to the south (Hornafius et al, 1995) and the more steeply south-dipping **More Ranch fault** to the north (Olson, 1982; Gurrola et al, 1996). Over much of

the main UCSB campus, approximately 5 m of Quaternary marine terrace deposits overlie folded and tilted lower Sisquoc and Monterey formation. Age-dating of a single marine coral at 47±0.5 ka within the uplifted marine deposits yields a local vertical uplift rate of 1.2±0.1 mm/yr (Gurrola et al, 1996). The elevated campus terrace is sharply truncated to the east by the NNE-striking **Goleta Point fault** that may act to segment the More Ranch fault. The More Ranch fault is believed to act as a back thrust to the dominant North Channel fault system (Hornafius et al, 1995). Other secondary structures, such as the short NE-striking Campus fault, are probably minor subsidiary splays off the major faults at depth. A more detailed discussion of the UCSB campus structure and its implications for local seismic hazard and possible influence on local site response is given in sections 8 and 9.

4.3.3 Offshore Faults and Folds

Numerous active and possibly active faults have been identified within the Santa Barbara Channel making this area one of the largest single contributors to the seismic hazard of coastal Santa Barbara (e.g., **Figure 2**). Characterization of these faults has begun only recently, and is based largely on available public and proprietary marine seismic reflection and offshore well data. These data have the potential to dramatically improve our understanding of subsurface fault geometry and the slip rates of active offshore structures, but lack of research funding and limited access to some of the most critical datasets (such as detailed 3D seismic reflection surveys) have prevented rapid progress on this effort. The major faults within the Channel appear to be mostly continuations of fault systems mapped onshore. However, extending onshore interpretations of faulting and slip rates to offshore segments may not be straightforward, as illustrated by the apparent variations in style and slip observed along strike of the onshore Oak Ridge fault. Nevertheless, the most significant seismic hazard to UCSB is most likely to originate from offshore structures that border the northern Santa Barbara Channel, although the seismic potential of many of these offshore faults remains poorly resolved at present.

Offshore Oak Ridge Fault: The offshore Oak Ridge fault is mapped as continuous with the onshore Oak Ridge fault using public domain high-resolution seismic reflection data (Dahlen et al, 1990; Burdick and Richmond, 1982; Luyendyk et al, 1982; Yeats, 1989). The fault offsets a Quaternary abrasion terrace (Luyendyk et al, 1982; Dahlen et al, 1990) in the eastern part of the Santa Barbara Channel and can be traced to the central part of the channel (Richmond et al, 1981), where it merges with the WNW-striking Mid Channel trend (**Figure 5**). Shaw and Suppe (1994) present an alternative interpretation in which the Oak Ridge trend between the coast and the central channel is modeled as an axial fold surface above a bend in a deep active thrust fault. Kamerling and Nicholson (1995) and Stone (1996), however, present evidence from seismic reflection, well log and seismicity data that show this feature is indeed a steep south-dipping reverse or oblique-reverse fault having similar geometry to the Oak Ridge fault onshore. Wells drilled onshore in the Ventura basin and offshore in the Santa Barbara Channel penetrate steep to overturned strata, repeated section, a high-angle south-dipping fault, and require measurable vertical separation of several kilometers across this fault system. Moreover, 3D map restoration of deformed stratigraphic horizons suggests significant Pliocene and

younger reverse-left slip along the offshore segment of the Oak Ridge fault (Sorlien et al, 1996), consistent with the style of faulting observed onshore. Although poorly resolved, this offshore fault probably accommodates slip rates of 1–2 mm/yr and may be capable of producing earthquakes of M7.2.

Mid Channel Fault: A north-dipping fault (or faults) has been interpreted in the hanging-wall south of the Oak Ridge fault. This fault is called the Montalvo fault near the coastline (Yeats, 1989) or the Mid Channel fault a few kilometers farther west (Huftile and Yeats, 1995). Midway between Santa Cruz Island and Santa Barbara (**Figure 5**), a south-verging WNW-trending fold associated with the Mid Channel fault deforms the seafloor. This trend has been previously called the Mid Channel trend (Junger, 1979), and has been most active since about 1 Ma (Shaw and Suppe, 1994). The Oak Ridge fault merges with the Mid Channel trend south of Santa Barbara. If the offshore Oak Ridge fault is in fact an active reverse-left-slip fault (see above), then the south-verging Mid Channel fault and fold structure is most likely a back thrust to it, forming a wedge (Kamerling and Nicholson, 1995).

North Channel–Pitas Point-Red Mountain Fault System: This system of north-dipping faults defines the northern edge of the Santa Barbara Channel and includes the offshore part of the Red Mountain fault (**Figure 5**). The **Red Mountain fault** is easily mapped westward offshore to at least Fernald Point (Jackson and Yeats, 1982), and probably merges with the **North Channel fault** south of Santa Barbara. The **Pitas Point fault** has been interpreted to be the offshore extension of the Ventura fault, and also appears to merge with the Red Mountain/North Channel faults to the west. This onshore-offshore system is responsible for some of the most severe deformation in the Channel and may be capable of relatively frequent large earthquakes. Both the 1925 M6.3 and 1978 M5.9 Santa Barbara earthquakes likely originated on this structure—the 1978 event causing significant damage to the UCSB campus. The North Channel fault is imaged in 2D and 3D seismic surveys as a blind thrust that terminates about 1.5 km below the seafloor and dips 20°-40°N to about 3.7 km depth (**Figure 11**) (Hornafius et al, 1995). Seismicity studies suggest that this north-dipping fault system may continue beneath the coastal plain to intersect the steeply south-dipping Santa Ynez fault beneath the Santa Ynez anticlinorium (O'Connell, 1995; Nicholson and Kamerling, 1997). Because much of this complicated structure is blind, buried or underwater, little is know about this active fault system. Estimates of fault slip rate near its eastern end are approximately 1 to 3 mm/yr, and given its overall length, this structure could be capable of M7.2+ earthquakes. However, tear faults and other secondary features may act to segment the fault (Gurrola and Kamerling, 1996) so that smaller events may be more likely. Nevertheless, because of its physical extent, its proximity and location directly underneath the UCSB campus (see **Figure 20**), its style of faulting, and evidence for relatively recent activity, this fault system is considered to be the defining structure in terms of seismic hazard to the UCSB campus.

Hollywood-Malibu Coast-Pt. Dume–Santa Cruz Island Fault Trend: This trend extends from the northern margin of the Los Angeles basin to the western Santa Barbara Channel, and is about 200 km long (225 km if the left-lateral Raymond fault to the east is included). If this trend represents a continuous fault system, then it would seem to be capable of generating very large earthquakes. Its

greatest significance, however, is that it may indicate the presence of a larger, potentially more damaging, subparallel fault system (with which it merges at depth) that represents the southern frontal fault system to the western Transverse Ranges province as a whole (see below). Along this high-angle fault trend, left-lateral Holocene slip has been inferred on the onshore Hollywood-Malibu Coast section (Dolan and Sieh, 1992; Rzonca et al, 1991; Drumm, 1992; Dolan et al, 1993, 1995), on Santa Cruz Island (Patterson, 1979; Pinter and Sorlien, 1991) and on Santa Rosa Island (Sorlien, 1994; Dibblee, 1982). Dolan et al (1995) propose that the entire onshore section could rupture in a single large earthquake, but estimate a recurrence interval on the order of several thousands of years.

Serious questions arise, however, as to whether both the onshore and offshore segments could rupture together, and if such a rupture occurs, how far down-dip would such a rupture extend, as many of these high-angle strike-slip faults appear to be truncated at depth by low-angle north-dipping faults that crop out farther south. Moreover, even though there is evidence for similar components of left-slip along most of these fault segments, individual faults along the trend are poorly understood, and their continuity has not been demonstrated. At present, few geodetic measurements of regional crustal strain extend across this entire fault system, although GPS measurements are permissive of 1-3 mm/yr of left-lateral slip across the Santa Monica fault (A. Donnellan, oral communication, 1995).

Santa Cruz Island Fault: The Santa Cruz Island fault is the dominant on-land active structure in the northern Channel Islands. This fault is continuous for more than 100 km from northwest of San Miguel Island to east of Anacapa Island where it appears to merge with the Malibu Coast-Dume fault system in some complicated way (**Figure 5**). There is abundant evidence for left-lateral strike-slip on this fault (Patterson, 1979; Pinter and Sorlien, 1991). A trenched strand of the fault last moved between 33 ka and 5.5 ka (Pinter and Keller, 1994). To the east, the active Santa Cruz Island fault splits into multiple strands where a landslide, dated at ~13 ka, may be offset (Sorlien, 1994). Farther east on the island, the Potato Harbor and other subsidiary faults show evidence for Quaternary slip (Weaver and Meyer, 1969; Sorlien, 1994). Luyendyk et al (1982) identified a breached offshore anticline north of the Santa Cruz Island fault between Santa Cruz and Santa Rosa Islands. They believe this may be the offset equivalent to the northern part of the Christi Anticline located south of the fault onshore of Santa Cruz Island The left-lateral separation between the axial planes of the anticlines is 10 km. Luyendyk et al (1982) speculate that the anticline could have been formed as late as Early Miocene, which would yield an average lateral slip rate of 0.5 mm/yr on the Santa Cruz Island fault.

Santa Rosa Island Fault: The Santa Rosa Island fault intersects the Santa Cruz Island fault just west of Santa Cruz Island (Junger, 1976; Luyendyk et al, 1982). From this point the fault traces a gentle curve through the center of Santa Rosa Island westward, continuing south of San Miguel Island. The fault then makes a bend and is lost to the northwest of San Miguel Island (**Figure 5**) (Junger, 1979). Anderson et al (1949) suggested a left-lateral offset of 8 km on the Santa Rosa Island fault. The fault offsets the lowest well-developed marine abrasion platform, and both striations and deflected drainages indicate a component of left slip (Sorlien, 1994; Dibblee, 1982). Seven north-flowing streams

are deflected left between 250 and 1400 m, but the deflection of at least 3 of these streams is upstream from the fault. These stream deflections are interpreted to be tectonic (Rockwell, 1995b), and suggest a slip rate greater than 1 mm/yr. A minimum slip rate that can be inferred is 0.1 mm/yr (Sorlien, 1994).

Santa Monica-Channel Islands Thrust The southern edge of the western Transverse Ranges province was originally believed to lie along the Santa Monica-Malibu Coast faults, and on faults of the northern Channel Islands (e.g., Luyendyk et al, 1980; Crouch and Suppe, 1993), but long wavelength folding and uplift of the Santa Monica Mountains and northern Channel Islands indicates that this tectonic boundary lies farther south. This boundary is likely associated with a north-dipping thrust fault system that crops out offshore at or near the base of the Santa Monica coastline and the southern base of the northern Channel Islands. Two east-west-trending, down-to-the-south Quaternary faults are mapped south of Santa Cruz Island (Yerkes and Lee, 1979; Junger, 1979), and an east-west trending synclinal axis is mapped south of these faults (Junger, 1979) (**Figure** 5). A north-dipping fault is also imaged on a proprietary seismic reflection profile in the eastern Santa Barbara Channel (F. Victor, oral presentation, 1994). This structure is probably the master fault to the near onshore system east of Pt. Dume. These faults may be segments of a much longer fault associated with the scarp south of Santa Cruz Island. It is uncertain whether this trend continues west, south of Santa Rosa Island. No major east-west trending fault has been recognized in this area (Arleth, 1977; Field and Richmond, 1980), but small faults and folds that affect the sea floor are present (Junger, 1979; Field and Richmond, 1980).

The **Santa Monica thrust,** in conjunction with the offshore Anacapa fault, is believed responsible for the moderate uplift rates in the Santa Monica Mountains (Birkeland, 1972, Namson and Davis, 1990). The 1973 M6.0 Point Mugu earthquake may have occurred on the down-dip extent of this north-dipping structure, with many of its aftershocks illuminating faults in the hanging wall (Stierman and Ellsworth, 1976). Shaw et al (1994) and Shaw and Suppe (1994) suggest that Santa Cruz Island is being uplifted above a ramp on their hypothesized north-dipping **Channel Islands thrust** (see below). They infer that this thrust flattens out south of Santa Cruz Island and all its displacement is then taken up along the Santa Cruz Island fault as a back-thrust. However, this interpretation violates the evidence for predominantly left-slip motion on the Santa Cruz Island fault. Nevertheless, the evidence for folding and uplift of the northern Channel Islands does indicate the likely presence of a south-verging low-angle fault system. Other investigators (Davis et al, 1989; Hauksson and Jones, 1989; Dolan et al., 1994) infer a similar low-angle north-dipping **Santa Monica thrust** farther east, based on seismicity and on 2D fault-related fold models for the uplift of the Santa Monica Mountains. If these segments are all part of a single south-verging fault system, this fault could extend for over a mapped length of 220 km, have a down-dip width of at least 20 km, and would be capable of producing a truly great earthquake (e.g., Molnar, 1995; Seeber and Sorlien, 1996).

Channel Islands Thrust: The Channel Islands thrust is proposed to underlie much of the eastern Santa Barbara Channel based largely on simple 2D fault-related fold models (Shaw and Suppe, 1994). This structure is important to the analysis of seismic hazard in the Channel, and along the south coast

where UCSB is located, because this hypothesized basement thrust, if it exists, is not only estimated to be capable of generating potentially large earthquakes itself, but also because its existence would profoundly influence the way in which other crustal features in the Channel, such as the Oak Ridge, Pitas Point and Mid Channel trends, are interpreted. Based on their model, Shaw and Suppe (1994) estimate a slip rate of 1.3 mm/yr on this structure and infer that it is capable of producing a potential M7.2 earthquake with a recurrence interval of 1500 years. The problem is that this hypothesized basement thrust is not imaged on seismic reflection profiles; nor is there any other direct evidence for its existence other than the south-verging uplift of the northern Channel Islands. Central to the interpretation of Shaw and Suppe (1994) is the identification of the Oak Ridge trend as an axial fold surface above a ramp in the proposed thrust fault. However, this interpretation seriously violates observations of steep-to-overturned strata, measurable vertical separation, seismicity, and drillholes that define a major south-dipping fault along strike of the Oak Ridge trend (Kamerling and Nicholson, 1995; Stone, 1996).

Seeber and Sorlien (1996) have proposed an alternative interpretation and infer that the Channel Islands thrust is actually a reactivated listric normal (or normal-separation) fault. Slip rates inferred from folding and uplift are then based assuming an arcuate fault geometry and progressive limb rotation, rather than the classic 2D ramp-flat fault geometry assumed by Shaw and Suppe (1994). Although the slip rates calculated by Seeber and Sorlien (1996) are less than those inferred by Shaw and Suppe (1994), they find no evidence for major lateral ramps or other discontinuities that might act to segment the larger, deeper **Santa Monica–Channel Islands thrust** system, thereby raising the possibility of a very large earthquake on this structure.

Another major question concerns just how far north this structure—if it exists—extends beneath the Santa Barbara Channel. In one scenario, this fault truncates the Oak Ridge 'active axial fold surface' and links up with other north-dipping faults that underlie the Santa Ynez Mountains (Shaw and Suppe, 1994). Alternatively, this structure would be itself truncated by the south-dipping Oak Ridge fault (Kamerling and Nicholson, 1995), thereby separating the uplift and crustal shortening of the northern Channel Islands and Santa Monica Mountains from the uplift, folding and faulting farther north associated with the Santa Ynez and Topa Topa Mountains.

Faults in the California Continental Borderland. Using recent GPS measurements, a significant component of Pacific-North American transform plate motion is seen offshore in the California Continental Borderland. These data indicate that San Clemente Island is moving to the northwest at about 6 mm/yr with respect to San Diego (Larson, 1993). There are several northwest-striking faults within the California Borderland that may accommodate this motion. To the west, the San Clemente fault (**Figure 1**) is a major, seismically active fault with bathymetric evidence for right slip (Legg et al, 1989). The northwestern continuation of this fault is the Santa Cruz-Santa Catalina Ridge fault zone (**Figure 5**), which has been mapped in the shallow subsurface (Jennings, 1994; Burdick and Richmond, 1982; Junger and Wagner, 1977). This fault zone coincides with a significant seismicity trend, and is

probably the source of the 1981 M5.2 Santa Barbara Island earthquake (Corbett and Piper, 1981). Further inshore, the San Pedro basin fault is considered to be Quaternary-active (Jennings, 1994), and terminates at the Dume fault (Junger and Wagner, 1977). Additional plate boundary motion may be taken up by strike-slip faults with the San Diego Trough, however, there is still considerable uncertainty as to how any of this plate motion—whether on the San Clemente fault or on subsidiary faults located farther east—is actually accommodated or is transferred farther north to the predominantly E-W-striking southern frontal fault system of the western Transverse Ranges province.

5.0 SEISMICITY STUDIES RELATED TO EARTHQUAKE SOURCE HAZARDS

5.1 Historical Seismicity

The Santa Barbara area, including UCSB, has a known history of damaging earthquake activity. **Figure 12** shows inferred locations of major historical earthquakes in California (Ellsworth, 1990) and **Table 2** lists major earthquakes that have caused damage or were strongly felt in Santa Barbara (Olsen and Sylvester, 1975; Nicholson, 1992). These results are based on both published earthquake catalogs (Holden, 1898; Ellsworth, 1990), and eyewitness accounts of the resulting earthquake effects. The largest local earthquake occurred in December 1812. Most damaging in terms of dollar losses was the Santa Barbara earthquake of 1925. The sources of both these earthquakes remains unknown, although both are suspected to have occurred close to the coastline of the northern Santa Barbara Channel.

Information on pre-instrumental earthquakes typically relies mostly on felt reports. There are no reliable reports of surface rupture associated with any of the earthquakes in Santa Barbara or Ventura County, apart from the 1857 Ft. Tejon earthquake on the San Andreas fault. The felt reports reveal little about the locations of earthquakes, primarily because of the limited geographical distribution of the observers who were largely restricted to the east-west coastline. Thus, earthquake intensities cannot be accurately assessed north or south of the coast, and the limited number of people west of Santa Barbara before 1925 renders suspect assessments of historical seismicity there. Many earthquakes that were felt in the Santa Barbara area were not felt in Ventura or Santa Maria (and vice versa), judging largely from newspaper accounts. This indicates the presence of localized active faulting in each region of the western Transverse Ranges province, including the Santa Barbara Channel. A few large earthquakes were felt in two or more cities, but these accounts rarely permit the location of the earthquake to be interpreted.

Significant historical earthquakes that affected the Santa Barbara area are briefly described below. Each event is considered significant either because of its estimated size or location, or because it may reflect recent activity on a structure of importance to the evaluation of seismic hazard.

1812 earthquake-- The 21 December 1812 event is the largest historic earthquake to affect the Santa Barbara area. It is also the most significant earthquake about which we know the least, owing to the few people and structures in the Santa Barbara area at the time. The records of Mission Santa Barbara provide the best account. There are three primary issues concerning this earthquake: it's

location, its magnitude, and the nature of the water waves in the Santa Barbara Channel allegedly associated with it. Most investigators (Topozada et al, 1981; Evernden and Thompson, 1985; Ellsworth, 1990) conclude that the 1812 event was a subsea earthquake in the Channel having a magnitude greater than M7 (**Figure 12**), based both on intensity reports and on reports of a series of sea waves (McCulloch, 1985). The earthquake may also have involved two distinct ruptures spaced about 15 minutes apart (Ellsworth, 1990). The earthquake caused major damage to Mission Santa Barbara and to Mission La Purisimá near Lompoc, which was virtually destroyed. Sylvester (1978) argued that the seawaves may have been induced by a submarine landslide triggered by the earthquake, similar to tsunamis generated by subsea landslides triggered by the 1946 Alaska and 1975 Hawaii earthquakes (e.g., Hatori, 1976). This hypothesis was given added credence when a massive subsea landslide and turbidite flow previously identified with high-resolution seismic reflection data (Yerkes et al., 1981) was subsequently dated using intercalated varves at 1811 (±2 yr) (Schimmelmann et al., 1993). If this hypothesis is correct, then the earthquake itself need not have been a subsea event, although comparison of its felt area with modern events would still indicate a magnitude equal or greater than M7.0, and a location close to the western part of the northern Santa Barbara Channel coast line.

1857 Fort Tejon Earthquake: The M7.9 Fort Tejon earthquake of 9 January 1857 is the largest historic event in southern California. This event ruptured nearly 400 km of the **San Andreas fault** from Cholame Valley to Cajon Pass. Its magnitude of M7.9 is estimated from the measured length of fault rupture and fault displacement (up to 12 m near Ft. Tejon). No significant damage was reported to the Santa Barbara Mission, but many houses in the town were damaged and water was spilled from the Mission reservoir. Strong ground motion at Santa Barbara, however, likely lasted more than 90 seconds (Agnew and Sieh, 1978). The lack of major damage reported in Santa Barbara from this event appears to be largely the result of the small population and the small number of buildings in Santa Barbara at the time. The limited information together with the size and proximity of this event to the Santa Barbara area indicates that the UCSB site has most probably experienced large-amplitude, long-period, long duration ground motions in the past which could be easily suspected to reoccur in the future.

1925 Santa Barbara earthquake: The 29 June 1925 Santa Barbara earthquake was assigned an instrumental magnitude of M6.3 (Richter, 1958). Richter noted that "the epicenter remains uncertain, but records of aftershocks written at Santa Barbara beginning in July 1927, indicate an epicenter a short distance (not over 10 miles) west of the city, suggesting association with one of the known faults in the Ellwood oil field at the coast." This description would place the event at or near the UCSB campus. This event caused major damage to the downtown area of Santa Barbara. Sheffield Dam was also severely damaged and the reservoir emptied. Willis (1925) and some local historians believed that the earthquake occurred on the **Mesa fault**, which strikes mostly southeast through the city of Santa Barbara, but no indication of this exists beyond Willis' observation of high earthquake intensities along the fault. Olsen (1972) concluded that the highest intensities occurred close to the shoreline and in the center of the Santa Barbara graben, where alluvial fill is likely thickest, and that they

decreased away from the shoreline, toward the edges of the graben. The high intensities could therefore be explained by local site amplification and are not necessarily representative of proximity to the source. Another possibility is that the 1925 event, like the 1978 earthquake (see below), might have occurred on the blind, north-dipping **North Channel fault**.

1927 Lompoc earthquake-- The M7.3 earthquake of 4 November 1927 was the first event in the region large enough to be recorded world-wide. Its location is consistent with slip either on the offshore **Hosgri fault** (Gawthrop, 1978; Ellsworth, 1990) or beneath a series of active folds located farther west. Waveforms modeling suggests a predominantly reverse faulting mechanism (Helmberger et al, 1992). The earthquake produced a tsunami of about 2-3 m along the southern Central California coast. Aftershocks that continued for several years after the main shock were located along the Hosgri fault from Pt. Arguello north to Morro Bay (Wood et al, 1946). This earthquake confirms that active offshore faults exist, are capable of producing large damaging earthquakes that represent a significant seismic hazard, as well as acting as a potential source of local tsunamis.

5.2 Modern Earthquakes and Regional Monitoring

Expansion of the regional seismograph network operated by Caltech began in 1927. This allowed improved accuracy of earthquake locations in the Santa Barbara Channel and surrounding region starting in about 1932, with a steadily increasing accuracy and resolution up to the present. Earthquake epicenters are concentrated in the eastern half of the Santa Barbara Channel (**Figure 3**). Much of this activity has not been related to known or proposed faults, in part because large uncertainties in many hypocentral locations (especially for pre-1970 events) are likely to be greater than 5 km. Most of the events are located between depths of 5 and 18 km, similar to many other earthquakes in California.

1941 earthquake: The current location of the M5.9 30 June 1941 event is off the coast between Carpinteria and Ventura, possibly on the **Pitas Point fault**. Its size indicates that active faults with at least moderate earthquake capability exist in the eastern Santa Barbara Channel. Focal mechanisms of more recent earthquakes in this area exhibit strike-slip or oblique-reverse slip, and recent California earthquakes of similar size (e.g., 1986 M5.9 North Palm Springs; 1987 M5.9 Whittier Narrows) with oblique or reverse components of slip have generated high peak accelerations (in excess of 0.7g).

1968 earthquake- The M5.2 4 July 1968 earthquake was clearly located in the central Santa Barbara Channel and was part of an earthquake swarm that included at least 63 events (Sylvester et al, 1970). A composite focal mechanism of the 1968 earthquake and some of its larger aftershocks indicates predominantly right-slip on a steep NW-SE plane, or left-slip on a steep NE-SW plane (Sylvester et al, 1970). Neither nodal plane aligns with any of the major mapped offshore fault trends, which mostly strike east-west, however left-slip motion on a northeast-striking fault is consistent with the orientation of several cross faults identified within the western Transverse Ranges province (Gurrola and Kamerling, 1996). Based on this, and its proximity to a known discontinuity in the trend of major offshore faults and folds, it appears that the earthquake swarm may have occurred on a left-lateral, northeast-striking tear fault.

1978 earthquake: The hypocenter of the M5.9 19 August 1978 earthquake was located offshore of Santa Barbara at a depth of about 13 km (Corbett and Johnson, 1982). Damage was minor in the city but nearly $7 million in damage occurred in Goleta, 15 km farther west, mostly at the UCSB campus. This unusual damage distribution was attributed to the fact that several UCSB buildings had been exempted from local seismic-safety building codes, and because of possible directivity effects when the earthquake rupture propagated directly towards the UCSB campus. The distribution of damage in the epicentral region, the lack of any known surface rupture, the main-shock focal mechanism, and the observed distribution of the aftershock hypocenters all support the hypothesis that the earthquake occurred on a low-angle oblique-thrust fault that dips north at about 26° (Corbett and Johnson, 1982), rather than on a high-angle reverse fault as proposed by Yeats and Olson (1984). The most likely candidate appears to be the gently north-dipping **North Channel fault** (Hornafius et al, 1995).

This earthquake is important for several reasons. First, it is the only major earthquake in the Santa Barbara area for which adequate modern seismographic recordings exist. Second, it suggests that north-dipping blind or buried faults that extend directly under the Santa Barbara coast are active and capable of producing large damaging earthquakes. Third, the earthquake's focal mechanism indicates that one type of faulting in the Santa Barbara area is oblique-reverse. Several earthquakes throughout the western Transverse Ranges and in the offshore and near-shore regions of southern California exhibit oblique-reverse focal mechanisms (**Figure 13**), or this oblique strain appears to be partitioned into a mixture of strike-slip and reverse-slip faulting (Nicholson and Crouch, 1989). Earthquakes with a reverse component of slip can generate unusually high peak accelerations in the hanging wall block (Nason, 1973; Archuleta, 1992; Brune, 1996; Oglesby and Archuleta, 1997). UCSB is situated in the hanging wall of both the low-angle north-dipping **North Channel fault** and the steeply south-dipping **More Ranch fault**. And fourth, the fact that the 1978 event occurred on a oblique thrust fault suggests that other earthquakes, such as the 1812 or 1925 events, may also have occurred on similar structures in adjacent areas.

Continued monitoring of seismicity in the Santa Barbara–Ventura area also reveals important details about the general character and geometry of the active faults at depth. **Figure 14** shows a map and cross section of recent seismicity across the western Ventura basin and eastern Santa Ynez Mountains and includes the 1996 M4.1 Ojai earthquake sequence. Earthquake hypocenters and focal mechanisms define a planar south-dipping **Red Mountain fault**, and three faults within its hanging wall: (1) a steeply south-dipping strike-slip **Arroyo Parida fault**; (2) a steeply south-dipping predominantly strike-slip **Santa Ynez fault**; and (3) a curviplanar fault whose surface projection would also correspond with the surface trace of the **Santa Ynez fault**. The fact that there may be two separate faults at depth but which may alternate in outcrop along strike of the surface trace of the Santa Ynez fault may explain why the fault is mapped as steeply south-dipping farther west (Sylvester and Darrow, 1979; Dibblee, 1988; Keller et al., 1995), or north-dipping in this region or farther east (Dibblee, 1988; Namson and Davis, 1991; Huftile and Yeats, 1995). Geologic and seismicity studies would suggest,

however, that both faults associated with the Santa Ynez surface trace are presently active, are steeply-dipping, exhibit large strike-slip components, and extend to depths of 18-20 km. These results are inconsistent with several 2D balanced cross section models that assume the fault is predominantly reverse, dips at 35° to 40°, and extends only to depths of 7 to 10 km (**Figure 6**) (Namson and Davis, 1991, 1993; Anderson, 1993; Novoa and Suppe, 1994).

In summary, even within the short period of the available earthquake history of the region, the Santa Barbara area (including UCSB) has experienced repeated strong ground motion from earthquakes that are both local (1812, 1925, 1941, 1968, 1978), and as far away as 60 to 100 km (San Andreas fault in 1857, offshore Pt. Arguello in 1927, White Wolf fault in 1952). A number of these earthquakes are known to have occurred either directly in the Santa Barbara Channel (1941, 1968), or just offshore at depth along the Santa Barbara coast (1925?, 1978). Since the turn of the century, the Santa Barbara–Goleta–Carpinteria area has experienced a moderate, damaging event about once every 25 years.

Earthquake focal mechanisms and hypocenter distributions suggest that various types of active faults are present in and around the Santa Barbara area. This includes both high-angle and low-angle faults accommodating strike-slip, oblique-reverse, or reverse components of slip (**Figures 13 and 14**). This variety reinforces the need to consider blind reverse and moderate-to-low-angle detachment faults, in addition to more steeply dipping faults that offset the surface, as potential earthquake sources. Moreover, faults with reverse components of slip and dipping fault geometry can produce unusually large ground motions for their size (e.g., Brune, 1996; Oglesby and Archuleta, 1997), and some of these faults, such as the Santa Ynez fault and the Red Mountain/North Channel fault, likely extend to depths of 18 to 20 km beneath the Santa Ynez Anticlinorium (**Figure 14**) (O'Connell, 1995; Nicholson and Kamerling, 1997). This raises the possibility that even relatively short along-strike segments of these faults could produce major damaging earthquakes with large ground motions, especially in the hanging-wall block of the fault—and again—UCSB is situated in the hanging wall block of both the north-dipping **North Channel fault** and the steeply south-dipping **More Ranch fault**. Lastly, in addition to the hazard from local earthquakes, which is significant, large or great earthquakes (like 1857 and 1952) at large distances can generate large amplitude, long-period strong ground motions that may reach 0.15 - 0.25 g and that can be sustained for several tens of seconds.

6.0 GEODETIC STUDIES RELATED TO EARTHQUAKE SOURCE HAZARDS

The Santa Barbara Channel and onshore Ventura basin to the east (**Figure 5**) exhibit high rates of measured geodetic strain. **Figure 15** (top) shows the most recent geodetic velocity field (in mm/yr) for southern California as determined by SCEC using Global Positioning System (GPS) data collected since 1988 (Jackson et al., 1996). Based on earlier trilateration and GPS data collected between 1970 and 1988, Larsen et al (1993) determined near uniaxial convergence oriented N25° ± 5°E across the eastern Santa Barbara Channel (**Figure 15,** bottom) at a rate of 6.4±0.9 mm/yr. Larson and Webb (1992) and Feigl et al (1993) estimate similar shortening rates of 6±1 mm/yr oriented N16°±3°E and 4.9±1.0 mm/yr oriented

N32°E, respectively, across the eastern Channel. Onshore, GPS data (Donnellan et al, 1993a) indicate roughly north-south shortening rates across the Ventura basin in the range 7 to 10 mm/yr over a 4.6 yr period, with an average rate between the SAF and the coast of 7±2 mm/yr. It thus appears that most of the present convergence across the western Transverse Ranges as a whole is taken up across the Santa Barbara Channel and Ventura basin (Yeats, 1983; Donnellan et al, 1993a; Feigl, 1993).

The instantaneous shortening rates measured by GPS are about half those estimated in earlier geological model studies for the last 200-250 ka (25±5 mm/yr, Yeats, 1983; >20 mm/yr, Rockwell, 1988) and 2-3 Ma (17-26 mm/yr, Namson and Davis, 1988). However, Huftile and Yeats (1995) have recomputed an average long-term shortening rate across the Ventura basin of 10±3 mm/yr based on a revised age of 500 ka for the Top Saugus Formation, much closer to the instantaneous rate from GPS. Nevertheless, the geodetic results confirm that measured strain rates in the Santa Barbara–Ventura area are significant, and suggest average recurrence intervals for major, damaging earthquakes (such as the 1925 M6.3 and 1978 M5.9 events) on the order of decades to a few hundred years.

The NNE-SSW orientation of geodetic strain in the eastern Channel is consistent with the average N22°E orientation for P-axes of earthquake focal mechanisms within the eastern Channel (**Figure 13**) (Lee et al., 1979; Nicholson and Crouch, 1989; Larsen et al, 1993). In the central Channel (**Figure 15**), the strain analysis suggests a larger component of left-lateral shear, implying a possible change in deformation style between the eastern and central parts of the Channel. This is consistent with the structural style of the area, where the intensity of folding and faulting decrease westward along the northern margin, with an abrupt change in orientation west of the South Ellwood Oil field near UCSB.

Compression across this area largely results from north-south convergence produced as the right-lateral SAF, which bounds the north flank of the western Transverse Ranges, takes a large left step and changes strike from northwest to west-northwest (**Figure 1**). This is the 'big bend' of the SAF system. Recent research suggests that tectonic evolution of the Pacific–North American plate boundary caused by repeated capture of partially subducted microplates by the Pacific plate may be responsible for the rotation of the western Transverse Ranges and development of the big bend region (Nicholson et al, 1994). Paleomagnetic studies suggest that the western Transverse Ranges have undergone large clockwise rotations of at least 95° since about 16 Ma (e.g., Kamerling and Luyendyk, 1979, 1985; Hornafius et al, 1986; Luyendyk 1990, 1991). Stratigraphic control and isotope age dates of the samples (Hornafius, 1985; Liddicoat, 1990) imply that the rotation began in late Early Miocene time. Hornafius et al (1986) suggested that this rate of rotation has not been constant; however, Luyendyk (1990, 1991) demonstrated that with revised stratigraphic ages, the data can be interpreted equally well as showing a steady rate of rotation of ~6°/Ma since the Early Miocene. Molnar and Gibson (1994) analyzed Very Long Baseline Interferometry (VLBI) and GPS data from the western Transverse Ranges and found that they are currently rotating at about 6°/Ma, if the present rates are extrapolated to longer time intervals. Recent GPS measurements also indicate clockwise rotation of Ventura basin in the area of Santa Paula (Donnellan et al, 1993a, b), and more regional studies, such as shown in **Figure**

15 (top) (Feigl et al., 1993; Jackson et al., 1996), confirm that the western Transverse Ranges province is indeed rotating clockwise at a rate comparable to the long-term paleomagnetic average.

The geodetic results confirm that oblique motions, with a large reverse component, can be expected on active faults within the western Transverse Ranges province, and that strain rates are sufficiently high to produced large, damaging earthquakes every 100 to 300 years. Confirmation that the western Transverse Ranges have rotated in the past and are continuing to rotate today, emphasizes that active fault structures within this area have undergone a complex tectonic history, evolving from oblique-normal into strike-slip and oblique-reverse faults. This implies that the strain field has changed continually with time and is now different from the strain field under which many of the structures—which accommodate most of the seismogenic slip—originated, suggesting that these structures are unlikely to exhibit the simple geometry often adopted in 2D balanced cross section models (**Figure 6**).

7.0 OTHER POTENTIAL EARTHQUAKE-RELATED HAZARDS

7.1 Liquefaction Potential

Under certain conditions, strong ground motion from large earthquakes can cause saturated, unconsolidated sediments to liquefy. The basic principle involves recompaction and intergrain shearing of the sediment material under continued vibration that results in an increase in pore fluid pressure and the subsequent loss of shear strength. Should this occur, buildings that rely heavily on these sediments for support and are not anchored to deeper, stable soil or bedrock would be significantly damaged.

Most of the UCSB campus is situated on an elevated wavecut platform overlain by a few to several meters of unconsolidated Quaternary sediments. Most of these sediments are not sufficiently saturated to pose a significant risk of liquefaction, and many UCSB building foundations—especially structures over two stories like the Engineering I tower and Broida Hall—are indeed anchored by deep friction pilings. In the case of the Engineering I tower, 12-m deep concrete piers that extend approximately 8 m (25 ft) into the Sisquoc formation anchor the building's slab foundation (B. Hanna, personal communication, 1996). The potential for liquefaction to affect this structure is thus low. However, other UCSB campus sites, especially those north of the **More Ranch fault**, may be exposed to relatively high liquefaction risk. This is because many of these sites, such as UCSB Central Stores/Receiving, are located at lower elevations, close to the Goleta slough, where thicker, more saturated deposits of unconsolidated material are ponded against the scarp of the More Ranch fault. The Santa Barbara County Seismic Safety and Safety Element Report (1978) identifies the liquefaction potential along the coastal plain in the area of the Goleta Slough and Santa Barbara Airport as high.

The proper evaluation of liquefaction potential requires detailed geotechnical testing of the soils at each specific site, and sophisticated analyses of the dynamic response of these soils to expected earthquake ground motions. Such studies are part of the scope of the work for each critical campus structure under consideration by the CLC Campus Earthquake Hazard Program. Results of dynamic soil tests of samples retrieved from the CLC boreholes drilled at UCSB will be available in the **Phase II**

report, and estimates of expected earthquake ground motions will be conducted in the **Phase III**. A more detailed analysis of the liquefaction potential of the UCSB campus soils will then be possible.

7.2 Tsunami and Seiche Hazards

Earthquakes can produce potentially hazardous water waves and currents, either by displacement of the seafloor, or by triggering rapid submarine slides. The size of the tsunami produced is a function of the volume of water displaced and the configuration of the nearshore bathymetry. Most large tsunamis are typically caused by large seafloor displacements of up to several meters in deep (>2 km) water. Sources for destructive tsunamis can be either local or teleseismic, and both tsunamis (the initial wave) and seiches (reverberations within a closed or partially enclosed basin or other local bathymetric feature) could be created in this manner.

Along the southern California coast, the estimated hazard from tsunamis and seiches is typically considered relatively small, as the broad, shallow shelf of the continental borderland is believed to offer significant protection from most tsunami effects. The steep continental slope and seafloor topography of the outer borderland would tend to reflect and disperse much of the tsunami energy from teleseismic sources, while the shallow water depth of the inner borderland and Santa Barbara Channel is often thought insufficient to allow major tsunamis to be produced locally. However, these relatively low estimates of tsunami hazard from local sources are based largely on 1D calculations that do not take into account possible 3D basin and seiche effects. Several researchers have now begun to re-evaluate this problem. For example, McCarthy et al (1995) re-examined the possibility of near-shore tsunami generation along the California coast, and rate the potential in the Santa Barbara Channel as high. This rating reflects the existence of high-angle and low-angle reverse faults that border the Channel, suspected high-angle and low-angle faults underneath the Channel, and steep slopes that have produced large submarine slides within the Channel. The historical record also indicates that there is indeed a tsunami and seiche hazard along the Santa Barbara coast.

7.2.1 Historical Tsunamis Within the Santa Barbara Channel

While the historical record for the Santa Barbara area extends back only about 200 years (**Table 3**), there are indications of a tsunami hazard within the Santa Barbara Channel. For example, there are a number of reports of a tsunami following the 21 December 1812 earthquake. Although the accuracy of these tsunami reports, and even the existence of a tsunami, have been questioned, most researchers concede that a tsunami of some size probably did occur (e.g., Lander et al, 1993; Marine Advisors, 1965; Sylvester, 1978; McCulloch, 1985). Subsequent identification of a large underwater slide (Yerkes et al., 1981) along the north slope of the western Santa Barbara Channel, and its dating to within the time of the earthquake (1811±2 yr) (Schimmelmann et al, 1992) strongly indicates that a subsea slide triggered by the earthquake was the likely source of this tsunami. Estimates for the runup height along the northern Channel coast vary from 1 to 4 m, while accounts by indians living on Santa Rosa Island suggest that, at some point, water may have retreated off the island by several hundred meters (Heizer, 1955). It is unclear, however, whether this observation was the effect of a leading depression tsunami or

permanent uplift or tilting of the island—the latter would require that the 1812 earthquake was located near Santa Rosa Island.

Another important historical tsunami apparently occurred to the southeast of the Santa Barbara Channel in Santa Monica Bay. A magnitude 5.2 earthquake on August 30, 1930 is reported to have triggered a 6 to 7 m wave that caused one drowning , necessitated the rescue of several others, and significantly damaged the Santa Monica Pier (Lander et al, 1993). It is not known to what extent the enclosed nature of the Santa Monica basin may have contributed to the wave height, but because the Santa Monica basin is similar in its physical characteristics to the Santa Barbara Channel, this event warrants serious consideration. Other significant events include a tsunami following the 1927 Lompoc earthquake, which produced 2 to 3 m waves along the west coast of Santa Barbara County, and five tele-tsunamis observed in the Channel that ranged in wave heights from 1.5 to 4 m. In addition, at least one prehistoric Chumash Indian site excavated near the Santa Barbara harbor exhibits evidence for possible flooding and tsunami(?) effects at least twice during its occupation (Rogers, 1929).

The average height above mean sea level of the main UCSB campus is about 16 m. The hazard to the campus associated with these reported historical tsunamis along the Santa Barbara coast—if they were to reoccur today—is minimal, although the hazard in adjacent low-lying areas, such as Goleta Beach, would be significant. What is difficult to estimate is whether unusual 3D basin effects, coupled with a relative strong tsunamigenic source (such as a massive underwater landslide), could produce an unusually large tsunami locally along the Santa Barbara coast, and if so, would this water wave continue to reverberate within the Santa Barbara Channel as a seiche.

8.0 LOCAL UCSB SOURCE AND SITE CHARACTERIZATION STUDIES

As part of the CLC project, several geologic, geophysical, and geotechnical studies were undertaken or reviewed to help characterize the local site response of the UCSB campus to strong ground motions. These studies generally focused on details of local topography, fault geometry and fault slip rates to better assess the hazard from local seismogenic sources; the character of the subsurface structure and seismic velocity beneath the campus to evaluate seismic-wave propagation effects; and local array seismic monitoring to help identify any unusual campus site amplification or focusing effects from local and near regional sources.

8.1 UCSB Campus Geomorphology and Shallow Structure from Foundation Studies

In active tectonic regimes like the western Transverse Ranges, geomorphology often reveals important clues regarding the style, rate, and characteristics of the local deformation (Keller and Pinter, 1996). **Figure 16** shows a 3D perspective view looking north across the UCSB campus topography. The first-order observation is that UCSB is situated on a relatively flat, uplifted area sharply bounded by relatively steep slopes. The campus sits about 15 m (50 ft) above mean sea level. The flat campus region is a wave-cut platform or marine terrace uplifted between active faults that control the relatively steep escarpments. To the south is the **North Channel fault** system (**Figure 11**)

that dips north beneath the campus. To the north, is the **More Ranch fault** that dips steeply south; and to the east, the campus is truncated by the northeast-striking, steeply dipping **Goleta Point fault** (**Figure 10**). Thus, each of the major local active faults has a clear topographic expression, and can be readily identified.

The actual surface of the wave-cut platform is overlain by unconsolidated sediments consisting mostly of sand and fine-grained silt. **Figure 17** shows a structure contour map that represents the elevation of the top of the wave-cut platform above mean sea level. This surface is defined by a set of coreholes drilled for various UCSB building foundation studies. A 3D perspective side view of campus topography, the top of the wave-cut platform, and the foundation boreholes is shown in **Figure 18.** The campus boreholes typically penetrate about 5 m (15 to 16 ft) of Quaternary marine terrace deposits above lower Sisquoc Formation of early Pliocene age. The unconformity at the top of the wave-cut platform thus represents a considerable missing section in both time and stratigraphic thickness as a result of uplift and erosion. Dating of a single corral found at the base of the terrace deposits indicates an age of 47 ka (Gurrola, 1996). Given the known variations in mean sea level, this yields an average rate of recent uplift of the marine terrace of about 1 mm/yr.

8.2 Previous Studies Related to UCSB Subsurface Structure, Faults, and Site Response

Although topography and shallow borehole data suggest a relatively simple structure to the UCSB campus consisting of Quaternary sediments overlying a relatively flat, raised marine terrace, deep test wells drilled for hydrocarbon exploration indicate that the subsurface crustal structure beneath UCSB is more complicated. **Figure 19** shows one of several approximately north-south vertical cross sections through the UCSB campus (Olson, 1982). The cross section shows subsurface structure in the upper 2100 m (8000 ft) based on the stratigraphy correlated between the deep wells. The data indicate the presence of several approximately east-trending fault-related folds that are sharply truncated to the north by the steeply-dipping **More Ranch fault**. South of the fault, wells that drill beneath UCSB penetrate several thousand feet of folded Lower Sisquoc (Tsq), Monterey (Tm), Rincon (Tr), and Vaqueros (Tf) Formations before bottoming in Sespe (Ts). North of the fault, Quaternary Santa Barbara Formation (Qsb) rests, for the most part, directly on Monterey Formation of Miocene age, suggesting a marked reversal in the dip-slip component—from normal to reverse separation—across the steeply south-dipping primarily strike-slip More Ranch fault. Other faults suggested by the subsurface geology, such as the **Coal Oil Point fault**, are likely hanging-wall splays off the blind north-dipping **North Channel fault (Figure 11)**. **Figure 20** shows a simplified schematic cross section of how these faults and folds may interact at depth, and what kind of pre-existing structure may have been present prior to shortening (Hornafius et al., 1995). In this model, convergence is largely accommodated by reactivating older normal-separation faults and subsequent basin inversion, a style that is very characteristic of the western Transverse Ranges province (Nicholson and Kamerling, 1997).

In terms of local source and site effects, **Figures 18, 19 and 20** provide a fairly comprehensive overview of the major controlling factors that would affect expected strong ground motions at UCSB.

Although large earthquakes could be expected from the **Santa Ynez fault** to the north, and the offshore **Oak Ridge fault** to the south, the active faults that are most likely to represent the greatest seismic hazard to UCSB are the **North Channel** and **More Ranch faults**. Because of their proximity and location beneath UCSB, details of their geometry, slip rate, expected earthquake recurrence intervals and rupture dynamics will have critical influence on the how and what strong ground motions would be predicted from these sources. Thus, whether the fault is planar, listric, or has some other curviplanar shape (e.g., **Figure 20**), as well as the direction of propagation, the sense of slip, the location of possible segmentation boundaries and which fault splays are involved in the rupture will all play important roles in predicting the range of possible strong ground motions when these specific local source zones are modeled. How these seismic waves may or may not be affected by the geometry of the hanging-wall folds (e.g., **Figure 19**) must also be considered (Gao et al., 1995); while the strong contrast in material strengths between the wave-cut platform and the overlying Quaternary terrace deposits (e.g., **Figure 18**) suggest a possible uniform amplification of seismic wave energy across the UCSB campus.

It is for these very earthquake hazard related issues that individuals at UCSB have been attempting to better document the local UCSB source and site characteristics, and why many of these previous and CLC-sponsored studies were undertaken. Thus, details of the geometry of the **North Channel fault** are being mapped using available offshore 3D seismic survey and other marine geophysical data (**Figure 11**) (Hornafius et al., 1995); the tectonics, geomorphology and surface geology are being mapped and incorporated into a GIS database (**Figures 9** and **10**) (Gurrola et al., 1995); paleoseismic studies including trenching (**Figure 21,** top) and age-dating of marine terrace deposits have been undertaken to better determine near-surface fault location, dip, slip rates and uplift rates (Gurrola, 1996); and the shallow (**Figure 18**) and deep (**Figure 19**) borehole data discussed above were compiled to investigate the characteristics of important local subsurface structure and fault geometry that may influence the propagation of seismic wave energy.

8.3 Shallow Seismic Refraction Profiling

Other critical parameters in the estimation of strong ground motion are the seismic velocities, and the depth, geometry, and impedance contrasts of various velocity discontinuities for the material beneath the UCSB campus. In an attempt to better define the variation in velocity structure across the UCSB campus, the CLC project conducted several shallow-penetration seismic refraction profiles (e.g., **Figure 21,** bottom). Both P-wave and S-wave refraction surveys were performed. Locations of the seismic refraction lines are shown in **Figure 4**. **Figure 22** is an example of P-wave data collected by the 24-channel digital recording system provided by UCR, one of the four CLC partner campuses. The vertical source used was a 10-lb sledge hammer. Signals were recorded out to offsets of over 100 meters. The data in **Figure 22** suggest a low-velocity near-surface layer about 5 m thick (350 to 500 m/s) above a fairly homogeneous layer with velocity 1400 m/s, increasing slightly to 1500 m/s at the far offsets.

These results are entirely consistent with earlier shallow P-wave refraction studies conducted as part of foundation tests for the UCSB Recreation Center (**Figure 23**) and the known material properties

and geometry of the regional subsurface geology derived from the shallow and deep borehole data (e.g., **Figures 18 and 19**). The previous studies confirm the presence of a relatively thin, uniform layer of low-velocity Quaternary sediments that overlies, for the most part, low-velocity lower Sisquoc Formation. Where it has been drilled onshore and just offshore near the UCSB campus, the lower Sisquoc is a fairly massive, homogeneous diatomaceous siltstone with unusually low density (~2.0 g/cc), low permeability (~1 md), high porosity (up to 70%), and a few scattered chert lenses. A minimum of over 370 m (1200 ft) of lower Sisquoc is present beneath the UCSB campus (**Figure 19**). The unusually high porosity but low permeability produces a rock with high storativity and low transmissivity. Thus, it is not surprising that the Sisquoc Formation defines the top of the ground water table beneath the UCSB campus, or that the P-wave velocity measured in this saturated rock is close to that of water. Also, given the uniformity of the well logs for the lower Sisquoc drilled just offshore, it is not surprising that the seismic velocity of the lower Sisquoc does not increase very rapidly with depth.

In terms of seismic hazard studies and the local site response to strong ground motion, it is the shear wave velocity that is the most important. **Figure 21** (bottom) shows UCSB students conducting a shear-wave study adjacent to Engineering I, the CLC-designated structure. Additional profiles were conducted near the site of the CLC deep boreholes located between Webb and Broida Hall, and on the far side of the campus near the UCSB Recreation Center (**Figure 4**). The shear-wave source was a gas-driven, hydraulic twin sliding hammer-anvil system designed and constructed by Craig Pearson (LANL). A one-ton van was used to provide coupling (**Figure 21,** bottom). Unfortunately, owing to the nature of the shallow subsurface geology beneath UCSB, the shear-wave data were not very useful. Because of the apparently low-velocity of the unconsolidated marine terrace deposits (~200 m/s), the first dominant arrival after cancellation of the P-wave energy was either an air-wave or a surface wave trapped in a slightly faster upper layer of compacted sediments (~350 m/s), not the S-wave. This near-surface low-velocity zone created by the dry unconsolidated, uncompacted sandy sediments above the wave-cut terrace prevented good, clear unambiguous first S-wave arrivals from being identified, especially when the refraction studies were conducted adjacent to campus buildings and sidewalks that caused additional multi-pathing, secondary reflections and other undesired coherent energy. All that really could be derived from the shear wave data was that the thin layer of marine terrace deposits known from the boreholes (**Figure 18**) and the P-wave refraction studies (**Figure 23**) has unusually low shear-wave velocity (< 330 m/s), and that—where sampled at the mid to far offsets—the lower Sisquoc Formation also exhibited a relatively low shear-wave velocity that was not much higher (~400 m/s). This gave minimum near-surface Vp/Vs velocity ratios of 2 to 3 in the upper 20 m or so, which is not unusual for these kinds of conditions (Nicholson and Simpson, 1985).

8.4 Cone-Penetration Soil Tests and In-situ Velocity Measurements

In an attempt to acquire more detailed *in situ* measurements of engineering interest, the CLC project conducted cone-penetration tests (CPT) at three locations around the Engineering I building, and two locations closer to Webb Hall, near where the deep CLC boreholes were drilled. The CPT soundings

provide geotechnical information on the variation with depth in tip resistance (Qc), sleeve friction (Fs), pore pressure (Ut) and transmissivity (that is derived from transient pore-pressure dissipation time). These values can be combined to provide an estimation of the soil type, water table depth, and *in situ* permeability. **Figure 24** (top) shows the CPT truck in operation and **Figure 25** shows an example of CPT data collected and the inferred soil types in the UCSB CPT hole #1 located next to the Woodhouse Laboratory (Gregg In Situ, Inc., 1996). The data show a dry near-surface sandy-silt layer above a dry sand layer with high tip resistance (Qt) typical of unconsolidated beach deposits. This sequence directly overlies a more compact uniform layer encountered at a depth of ~4.7 m (~15 ft) with high sleeve resistance. This is the more consolidated Sisquoc Formation. Within 0.5 m of the top of the Sisquoc, pore pressure rapidly rises, indicating saturated conditions and the top of the water table.

As predicted by the previous borehole studies (**Figure 17**) and the shallow refraction studies (**Figure 23**), the base of the marine terrace deposits was almost uniformly encountered at a depth of 4.3 to 4.9 m in the vicinity of the Engineering I building (Gregg In Situ, Inc., 1996). The cone used in CPT is 3.81 cm (1.5 in) in diameter and is pushed into the ground using an hydraulic system. The system used at UCSB (**Figure 24**, top) had the capability of providing a maximum force equivalent to 20 tons of thrust. Depth of penetration is determined either by penetration refusal or by the maximum depth of interest specified in the contract. Typically, for seismic studies, the maximum depth specified is 30 to 45 meters. In the UCSB CPT hole #1, depth to refusal was about 22 m (84 ft) and about 19 m (63 ft) in CPT borehole #3, where the cone tip likely encountered a hard chert lens. Refusal was not encountered in either CPT borehole #2 or #4 that were pushed to 45 m (~150 ft). This result was not unexpected given the massive, relatively homogeneous nature of the lower Sisquoc where it has been drilled elsewhere.

The CPT system used also allows for the acquisition of in situ downhole shear-wave velocity measurements. Results obtained in the UCSB CPT hole #1 are shown as an example in **Figure 26**. The data confirm the preliminary results of the S-wave refraction studies, and show a surface layer about 2 m thick with shear-wave velocity of about 275 m/s that overlies a sand layer about 3 m thick with shear-wave velocity about 185 m/s. These unusual low velocities, and the shallow low-velocity zone explains the difficulty in distinguishing the S-wave arrival from surface waves in the refraction results and the difficulty in effectively transmitting S-wave energy to deeper depths and far offsets. This sedimentary layer of marine terrace deposits overlies the more consolidated, but still relatively low-velocity Sisquoc Formation with shear-wave velocities that start at about 365 m/s (1200 ft/s) and generally increase slowly with depth.

In March 1997, two deep (~75 m) UCSB boreholes were drilled to permit wire-line logging, soil and rock core sampling, and the installation of uphole and downhole seismic equipment to record strong and weak ground motion. **Figure 24** (bottom) shows the drill rig in operation adjacent to Webb Hall. Because of potential interference from construction of the new Marine Science Institute building, the location of the deep drilling was moved from the original proposed site adjacent to the Woodhouse Laboratory over to the north side of the geology building (**Figure 4**). Details of the drilling, the

dynamic tests of the soil samples and rock cores retrieved, and the installation, calibration, and monitoring of the uphole and downhole seismic monitoring equipment will be discussed in the **Phase II** report. Results of the *in situ* P- and S-wave suspension velocity measurements conducted in the UCSB deep borehole #2 are shown in **Figure 27** (Agbabian and Associates, 1997). The data confirm previous results from industry sonic well logs, and from the refraction and *in situ* CPT studies that show the lower Sisquoc to be a fairly homogeneous formation with velocities slowly increasing with depth from about 1400 to 1600 m/s for the P-wave, and from about 350 to 500 m/s for the S-wave over the depth range of 5 to 75 m. The anomalous high-velocity layer at a depth of about 57 m is likely a chert lens that is significantly thicker (about 1 to 2 m) than others encountered in the well based on analysis of the borehole cuttings.

8.5 Local Array Monitoring of Earthquake Activity.

In addition to GIS-based mapping of active onshore and offshore faults and folds (**Figures 9, 10, and 11**); improved estimates of campus uplift and near-surface fault slip rates (**Figure 16** and **Figure 21**); analysis of regional microseismicity (**Figure 14**); compilation of campus subsurface structure contour maps (**Figure 17**) and cross sections (**Figure 19**) from shallow and deep borehole data; shallow seismic refraction studies (**Figure 22**); cone-penetration tests (**Figure 25**); and *in situ* downhole velocity measurements (**Figures 26 and 27**), the CLC project also conducted portable array monitoring of local seismicity to evaluate amplitude variations of weak ground motion across the UCSB campus. Several portable digital instruments maintained as part of the SCEC Portable Broad-band Instrument Center were installed and operated by ICS staff and undergraduate students at UCSB for a period of about 5 months. Seismic recording included both 3-component velocity and acceleration data. Locations of the seismic monitoring stations within the main UCSB campus area, including a site at the base of the Engineering I tower, are shown in **Figure 4.** Additional stations were operated at West Campus, at the Santa Barbara Airport, and at several other more regional sites north of the Santa Ynez Mountains.

During operation of the local portable array, two significant earthquakes occurred: one was the 1996 M4.1 Ojai earthquake north of Ventura (**Figure 28**) and the other was the 1997 M3.6 earthquake just offshore of Santa Barbara (**Figure 29**). This was indeed fortunate, as these were the only two earthquakes larger than M3 in the Santa Barbara–Ventura area since 1988. The seismic data show a fairly consistent pattern across the UCSB campus. For the 1996 event, amplitudes were typically higher (by about 30%) at the Engineering I site than at other campus sites that recorded the earthquake (**Figure 28**), while little variation in seismic frequency was observed. During the 1997 earthquake, however, an unusual high-amplitude pulse was seen on the N-S component at Environmental Health and Safety (**Figure 29**). This unusual response may be the result of the fact that this site is located between the north and south branches of the **More Ranch fault,** with the large pulse possibly representing an unusual trapped, fault-zone guided wave. In any case, the seismic monitoring did confirm that unusual site effects are indeed possible and present in the UCSB campus area.

8.6 Initial Seismic Data Recorded at the UCSB CLC Borehole Installation:

The two 75-meter boreholes at UCSB were instrumented with sensors at the bottom of each hole, and data recording by both downhole and surface sensors began by July of 1997. One of the boreholes contains a three-component Wilcoxon accelerometer package. This instrument is capable of recording ground motion from the micro-g (μg) level (weak motion) to 0.5 g (strong motion). While this instrument covers a wide dynamic range in ground motion, there was concern that a large local earthquake could generate even larger accelerations than 0.5 g. The relatively slow shear-wave velocity in the Sisquoc formation and its three-dimensional shape could cause amplification of the ground motion even at the level of the borehole instruments. The second borehole was therefore instrumented with a three-component Kinemetrics force balance accelerometer (FBA) which can record ground accelerations up to 1.0 g. The FBA was determined to have some internal problems after the installation, and a new borehole and instrument were provided by Kinemetrics in September 1997 to rectify the situation. At the surface of the boreholes, a vault was constructed which contains both three-component Wilcoxon and FBA instruments.

The Wilcoxon accelerometer data (both downhole and surface) are digitized by a Quanterra recorder and monitored in real-time by the USGS/Caltech Southern California Seismic Network (SCSN). Earthquakes are digitally recorded both locally onto a disk drive at UCSB and, at the Southern California Earthquake Center (SCEC) Data Center where the data are available for retrieval to all researchers via the internet. The FBA data (both downhole and surface) are digitized and recorded by a Kinemetrics K2 recorder at UCSB.

Examples of earthquake records that will be provided by this project are shown in **Figures 30 and 31.** A M3.3 Northridge aftershock which occurred on August 21, 1997 was recorded both in the borehole and at the surface (**Figure 30**). The ground acceleration (measured in micro-g) is plotted as a function of time on the same scale for all six components: three from the downhole borehole instrument (top) and three from the surface sensor (bottom). The peak-to-peak acceleration is about three times larger (75 μg) at the surface than it is at 75-m depth (25 μg). This earthquake is over 100 km from the UCSB station. A second example is a M3.2 earthquake near Santa Paula, CA, approximately 70 km from the UCSB station (**Figure 31**). Again, the surface accelerations are amplified by a factor of ~3 with respect to those found at the base of the borehole. With the ability to record events in the magnitude 3-4 range out to distances of up to 100 km, we expect to have collected within several months a substantial data set of weak-motion records to use in analytical modeling of the near-surface wave propagation and local site response.

9.0 ISSUES RELATED TO UCSB EARTHQUAKE SOURCE AND SITE CHARACTERIZATION

9.1 Offshore Faults and Folds

The location, geometry, and slip rate of faults that underlie or border the Santa Barbara Channel is a major issue relevant to the earthquake hazard at UCSB. Some of these faults extend directly beneath the UCSB campus. These faults, like the **North Channel fault**, are likely to produce the largest earthquakes in closest proximity to the site; and therefore they represent the greatest seismic hazard. These structures are also the least well resolved. It appears that many of these offshore faults are continuations of major onshore structures (e.g., Oak Ridge, North Channel, Channel Islands fault systems), which would provide the opportunity to conduct more detailed studies of these faults onshore. The problem is that several of the major fault structures do in fact change character offshore, and many of the techniques used to identify and characterize onshore faults are not available for use offshore. Offshore studies typically rely on interpretation of seismic and other sub-seafloor and seafloor data, while onshore the near-surface trace can be trenched using paleoseismic techniques to infer past slip events and fault slip rates. The different interpretations for the Oak Ridge, Pitas Point and Mid Channel trends illustrate the difficulty in discriminating faults from fault-related fold structures and other offshore features, and have lead in the past to widely different assessments of fault geometry and capability. We believe, however, that consistent, reliable interpretation and characterization of offshore faults and folds can in fact be made, especially when care is taken to properly correlate subsurface stratigraphy and geology with the available seismic data (Kamerling and Nicholson, 1995). The extremely dense coverage of both commercial multi-channel deep-penetration seismic reflection data, public domain shallow-penetration high-resolution seismic reflection data, and the numerous wells drilled in the Santa Barbara Channel provide much better subsurface information than is generally available onshore. However, until recently, much of these data were proprietary and not generally available for such seismic hazard studies. As a result, a significant amount of offshore data have yet to be fully exploited. This is why many important features of active offshore fault and fold structures are still largely inferred using indirect analysis.

9.2 Blind Faults, Regional Fault Models, and Subsurface Fault Geometry

Blind faults present a particularly difficult problem in seismic hazard analysis because they represent significant earthquake sources that cannot be sampled or evaluated directly by surface studies. Many fault parameters, such as depth, dip, areal extent, geometry and fault slip rate, critical to hazard assessment are inferred from near-surface measurements, or extrapolated using various fault-related fold models. Because many important features are inferred, this significantly increases the uncertainty in the earthquake hazard assessment. In the western Transverse Ranges, the problem is exacerbated by uncertainty in the characteristic geometry of active blind faults. This uncertainty stems from a poor understanding of the fundamental style of tectonic deformation in the region—thin-skinned (e.g. Yeats, 1981; Namson and Davis, 1988; Shaw and Suppe, 1994; Dolan et al, 1995) or thick-skinned (Yeats, 1993; Kamerling and Nicholson, 1994; Yeats and Huftile, 1995; Huftile and Yeats, 1995).

In the thick-skinned model, moderately to steeply dipping reverse, oblique-reverse or strike-slip faults that extend through the thickness of the seismogenic brittle crust (to depths of 18 to 20 km) are sources of earthquakes like the 1994 Northridge event, and accommodate a substantial part of the regional crustal convergence. These would include, for example, the **Santa Ynez, San Cayetano, Red Mountain,** and **Oak Ridge fault** systems. In the thin-skinned models, reverse faults typically extend at moderate to low dips into the mid and lower crust and are simple convergent structures that root into large-scale, sub-horizontal basement detachments. According to this model, these detachment faults are the primary structures on which crustal shortening is taken up, yet is unclear from the models whether these detachments are themselves potential sources of moderate and large earthquakes, or whether they are largely aseismic and only certain parts are seismogenic, like the thrust ramp responsible for 1987 Whittier Narrows event. In these models, many of the major regional fault structures would only extend at moderate dips to depths of 7 to 12 km (Namson and Davis, 1991, 1993; Shaw and Suppe, 1994; Novoa and Suppe, 1995), reducing the implied hazard. However, these results from the thin-skinned models violate observations of more steeply dipping fault geometry ($\geq 70°$) and deep crustal faulting observed in outcrop, well data and seismicity (Kamerling and Nicholson, 1995; O'Connell, 1995; Stone, 1996; Nicholson and Kamerling, 1997), and are inconsistent with the regional tectonic geomorphology (Yeats and Huftile, 1995).

Yeats (1995) points out that many characteristic features of well-defined thin-skinned tectonic zones, such as the Himalayas, are not clearly observed in the western Transverse Ranges, and argues that seismicity shows that the dips of major reverse faults do not shallow into basement detachments. Huftile and Yeats (1995) argue that recent observations of earthquakes as deep as 28 km under the Ventura basin (Bryant and Jones, 1992) are not consistent with the thin-skinned model. The shortening rate across the Ventura basin based on a thick-skinned model is closer to the geodetic rate (Donnellan et al, 1993a, b) than that estimated using the thin-skinned model. There are also significant problems regarding several shallow thrust ramps defined by Shaw (1993), Shaw and Suppe (1994) and Davis et al (1989). For example, these authors require the Palos Verdes fault to be a west-dipping reverse fault; however, Rockwell (1995a) shows the Palos Verdes fault to be a major right-lateral strike-slip fault.

Another major difficulty with the thin-skinned models and the application of many 2D balanced cross section techniques to the western Transverse Ranges region is that the deformation is assumed to be solely within the plane of the section and largely accommodated by folding and low-to-moderately dipping thrust faults with fixed, planar footwall geometry. There are no rotations and no oblique or strike-slip components of slip. These features of the 2D models completely ignore the fact that regional deformation within the western Transverse Ranges and offshore Santa Barbara Channel is still accommodated primarily by crustal rotations and oblique or strike-slip motion on more steeply dipping reactivated faults which do not always exhibit planar footwall geometry in map or cross section (Nicholson and Kamerling, 1997). Such distinctions, such as the dip, depth, and geometry of faulting, are extremely important when attempting to predict strong ground motions from local or near-regional

earthquake sources (e.g., Brune, 1996; Oglesby and Archuleta, 1997) or even in terms of estimating fault slip rates of subsurface faults (Seeber and Sorlien, 1996). These characteristics are particularly important to estimating the seismic hazard to the UCSB campus because of its unusual location in the hanging wall of both the north-dipping **North Channel fault** and the south-dipping **More Ranch fault.**

9.3 Cross Faults, Tear Faults, and Fault Segmentation

Well mapped faults are often believed to be segmented at depth based either upon mapped geometrical discontinuities or previous rupture history. Within the regional San Andreas fault system, several northeast-trending secondary faults can be identified that may act to segment the larger first-order northwest-striking fault structures (Nicholson et al., 1986b). Within the western Transverse Ranges province, these secondary cross faults displace the major east-west trending faults and folds (Yeats, 1983; Shaw and Suppe, 1994; Huftile and Yeats, 1995; Gurrola and Kamerling, 1996) and appear to act primarily as tear-faults or lateral ramps, usually with left-lateral displacement. The importance of these faults is that they may act to segment the major east-trending faults and thus limit the size of expected fault rupture and earthquake magnitudes. For example, the predominantly reverse 1970 M6.7 San Fernando (Whitcomb et al, 1973), 1978 M5.9 Santa Barbara (Corbett, and Johnson, 1982), 1987 M6.0 Whittier Narrows (Hauksson and Jones, 1989) and 1994 M6.7 Northridge earthquakes (Seeber and Armbruster, 1995) all appear to be bounded, at least in part, by well defined aftershock zones with strike-slip focal mechanisms. Segmentation is especially important for estimating the hazard from local faults because it not only limits the characteristic size of earthquake a fault may produce, but it may also limit the distance a rupture may propagate towards a particular area of interest.

Unfortunately, the degree to which such secondary cross faults or other geometrical discontinuities may act as barriers to arrest or segment future earthquake ruptures (or to serve as points where large earthquakes may initiate) is poorly understood. The great 1857 M7.9 Fort Tejon earthquake on the SAF and, more recently, the 1992 M7.3 Landers event in the Mojave Desert clearly show that a single earthquake can rupture several fault segments, or even several clearly distinct mapped fault systems.

Segmentation of blind faults is particularly problematical. The overall dimensions of many of these structures are rarely known, and their seismogenic potential is not well understood. It has been assumed by some that only the dipping ramps of the detachments are seismogenic (Shaw and Suppe, 1996), but this is entirely speculative. Moreover, it is still undetermined whether the high-angle, generally south-dipping faults, like the **Oak Ridge fault** and **Santa Ynez fault**, truncate or are themselves truncated by the generally north-dipping low-to-moderately dipping blind faults, such as the **Channel Islands thrust**, the **Santa Monica thrust**, or the **North Channel fault**. Additional uncertainties arise when deciding whether segmentation boundaries that control more steeply dipping faults within the hanging wall block, may actually influence or affect dynamic rupture at depth on blind low-angle detachment surfaces.

Many of the faults in the Western Transverse Ranges, particularly those in the Santa Barbara fault and fold belt and the eastern Santa Barbara Channel are poorly defined and consequently will be

difficult to argue either for or against segmentation. This is of particular concern for very long trends like the **Santa Monica-Pt. Dume-Santa Cruz Island fault** trend, which, if it ruptured as a whole would generate a very large earthquake. Long faults onshore such as the **More Ranch–Mission Ridge–Arroyo Parida fault** system appear to be segmented; yet again, it is unclear whether this segmentation would affect slip on the deeper **North Channel–Red Mountain–Pitas Point fault** system. More field work will be necessary to better establish the characteristic behavior of individual fault segments and what might constitute rupture lengths for various fault systems. At present, the along-strike lengths of thrust ramp sections are assumed to correspond to the lengths of the fault-related near-surface fold structures (e.g., Shaw and Suppe, 1994; Davis and Namson, 1994; Dolan et al, 1995). Dolan et al state that there is as yet no sound basis for segmenting thrust ramps along strike, but assume that they are segmented by "lateral ramps" that are defined by discontinuities in the fold trends. Shaw and Suppe (1994) segment their proposed **Channel Islands thrust** based on a series of tear faults identified from fold trends in the overlying cover rocks, while Seeber and Sorlien (1996) see no evidence that such discontinuities affect the regional long-wavelength folding, and argue that the **Santa Monica–Channel Islands thrust** is a continuous fault at depth and should be considered capable of producing a truly great earthquake.

9.4 Fault Slip Rates and Earthquake Recurrence

The most significant advance in seismic hazard analysis embodied in the methodology of Nicholson (1992), Ward (1994), and SCEC is the integration of geologic, seismicity and geodetic data to estimate earthquake recurrence rates. However, these data sets are not entirely compatible. Geologic data average slip rates over thousands to millions of years, while geodetic strain rates are essentially instantaneous. The seismicity record is only about 150 years long, and may not be representative of earthquake recurrence over the long-term. SCEC points out two main inconsistencies that result from their integration of the data sets. The first is that the SCEC integrated source model predicts rates of occurrence of earthquakes ≥M6 and ≥M7 that are about twice as high as those observed since 1850. The second is that whereas the geologic slip rate data and geodetic data concentrate strain accumulation on the major strike-slip faults of the San Andreas system, the seismicity data indicate that strain release is distributed over a much broader plate boundary zone. The major basis for this discrepancy is the assumption that all accumulated geologic or geodetic strain is stored elastically and released in large earthquakes. Recent studies by Gratier et al (1994) on pressure solution–deposition creep, by Sylvester (1995) on aseismic folding and uplift, and by Donnellan et al (1996) on continued aseismic afterslip of the 1994 Northridge event suggest a number of other mechanisms for the accommodation of regional strain within the western Transverse Ranges without necessarily producing significant seismicity. Thus, it remains unclear whether a discrepancy does indeed exist, and if so, is it a problem with the *model* of how long-term strain is assumed to accumulate and to be released, or is it a problem that the limited *observations* of earthquakes in southern California are not representative of the long-term average.

How this issue is resolved has significant implications for how fault slip rates, earthquake recurrence rates, and maximum earthquake magnitudes are estimated for various fault systems, especially blind faults within the western Transverse Ranges region where UCSB is located. This is because of the methods and large uncertainties in how these parameters are determined or inferred. For example, central to the uncertainty in any earthquake source model is the inherent tradeoff between maximum magnitude and slip rate when neither is well constrained directly by data. A moment rate budget can be met either by frequent moderate earthquakes or by relatively infrequent large earthquakes. Thus, it is possible to account for much of the discrepancy between observed moment release rates and those predicted by the SCEC model either by assuming that the rate of future moderate earthquakes will significantly increase (by a factor of two), or by increasing the maximum magnitude estimated for various fault systems, although this latter would require the occurrence of an earthquake bigger than any known earthquake to have occurred in California in the past. This problem is particularly acute for blind faults, for which rupture areas and slip rates are highly uncertain and, to date, largely inferred from simple 2D models. Slip on blind faults not accounted for in the current geologic slip rate estimates is a potential source of the discrepancies.

Another apparent inconsistency in the SCEC model is that the seismogenic thickness estimated by matching the geodetic and seismic moment rates gives a maximum earthquake depth of about 14 km. However, several recent damaging earthquakes in California have nucleated deeper than this depth, including the 1989 M7.1 Loma Prieta and 1994 M6.7 Northridge events, and many major faults within the western Transverse Ranges province exhibit seismic activity to depths greater than 18 km, including the **Oak Ridge, Santa Ynez** and **Red Mountain faults**. Also, large parts of hypothesized basement detachments from certain 2D models are located below 14 km. Although increasing the seismogenic thickness exacerbates the discrepancy between the geodetic estimates of earthquake recurrence and the observed seismicity, allowing for aseismic slip on faults, especially low-angle blind detachments at depth, would reduce the discrepancy. In addition, although recurrence rates for certain types of fault zones in the integrated SCEC model are based on unweighted averages of the estimated geologic, seismic and geodetic moment rates, these estimates are not independent. The thickness of the seismogenic crust used in computing moment rates from geodetic strain measurements is estimated by constraining the total geodetic moment rate to match the seismic rate (see Ward, 1994), and this thickness is also used to compute geologic moment rates. Therefore, both the geologic and geodetic rates are constrained by the historical seismicity catalog, even though the resulting recurrence estimates are inconsistent with the catalog. The general agreement between the strain patterns predicted by the geologic and geodetic data is expected, since partitioning of the geodetic strain rate is strongly controlled by geologic estimates of slip rates determined for the major faults (Ward, 1994).

Estimates of slip rates on individual surface faults are ideally based upon detailed paleoseismic studies. To date, such studies have been carried out on only a few faults within the western Transverse Ranges; for blind or offshore faults, these techniques are generally unavailable and more indirect

methods must be used. These indirect methods typically rely primarily on 2D balanced cross sections, and are therefore highly model dependent. Crustal shortening rates are estimated from balanced cross sections by retrodeforming the section back to a given time horizon assuming a certain geometrical relationship between faults and their inferred fault-related folds. However, the thin- and thick-skinned models differ in the way the observed slip rates translate to shortening rates (Yeats, 1993) and vice-versa. If, as assumed in the thin-skinned model, surface faults, such as the **Red Mountain** and **Oak Ridge fault** flatten to horizontal detachments, then measured dip-slip rates translate directly into horizontal shortening rates on the detachments. In the thick-skinned model, the faults extend into the lower crust at moderate-to-steep dip so that the shortening rate is only the horizontal component of the slip rate (slip rate × cosine of the dip). Yeats (1993) and Huftile and Yeats (1995) show that the crustal shortening rate across the Ventura basin estimated from the thick-skinned model agrees fairly well with the GPS data of Donnellan et al (1993a, b). Estimates using the thin-skinned model are typically too large by a factor of about two.

Slip rates estimated from published 2D balanced cross section models also rely on the assumption that crustal layers remain parallel and that there is little or no motion out of the plane of the section: i.e. no strike-slip displacement, no rotation and no progressive limb rotation (Namson and Davis, 1988, 1990, 1992; Shaw and Suppe, 1994). These assumptions are not valid for the western Transverse Ranges tectonic province, where significant rotations, strike-slip displacements, and progressive limb rotations are well known to occur and where much of shortening has inverted basins of Miocene age with large variations in formation thicknesses (Nicholson and Kamerling, 1997). The net result are published 2D balanced cross section models that incorrectly identify the dip, depth, geometry, or slip rate of faults, or completely fail to properly identify the presence (or absence) of major active faults all together.

The accuracy of the indirect methods to estimate fault slip not only depend on the validity and reliability of the model assumptions and fault geometry used, these shortening rates also depend heavily upon the dating accuracy of the horizons used. For example, uncertainty remains as to whether the age of the top of the Saugus formation, used by Huftile and Yeats (1995) in estimating the shortening rate across the Ventura basin, is 500 or 250 ka. Limited drill-hole sampling can lead to considerable uncertainties in dating horizons, especially if these horizons are time transgressive. Problems also arise when correlating well logs and chronostratigraphy to seismic data, if the data are not correlated correctly, projected too far, or too much reliance is given to seismic reflections as imaging structure, without independent confirmation from drilling.

9.5 Subsurface Structure, Hanging-wall Geometry and Local Site Amplification

With respect to the CLC-designated building and the UCSB campus, there are several important issues regarding local source and site characteristics that may strongly effect the estimation of strong ground motion. Because the UCSB campus is situated in the hanging wall directly above the **North Channel fault** and adjacent to the **More Ranch fault**, the specific geometry of these faults relative to UCSB campus buildings presents an unusual challenge in ground motion estimation. There are several

critical issues that are related to either a possible source, path or site effect. First, a building situated on the hanging wall of a fault can be subject to very large accelerations because the fault subtends a large solid angle at the site. The site can thus potentially receive radiation from many different parts of the fault simultaneously that can constructively interfere to produce very large accelerations (Archuleta, 1992; Oglesby and Archuleta, 1993; Abrahamson and Somerville, 1994). Second, a building located at or close to the up-dip extension of the fault plane maximizes the directivity effect due to a propagating rupture (e.g., Archuleta and Hartzell, 1981; Archuleta, 1984). This can greatly enhance the amplitude of the ground motions from large earthquakes, particularly at longer periods (>1.0 s). The largest peak velocities observed from earthquakes have been typically associated with the component of ground motion that is most affected by rupture directivity. Third, earthquakes with a reverse component of slip and less than vertical dip typically generate unusually large ground motions in the hanging wall towards the fault. This is believed to be a geometrical result of seismic wave energy being trapped and focused towards the thrust tip (Nason, 1973; Brune 1996). UCSB is situated updip near the thrust tip of the North Channel fault.

Fourth, unusual surface or subsurface structure can focus or defocus seismic energy. Although UCSB is situated on a relatively flat raised marine terrace (**Figure 16**), analysis of subsurface well data suggested that several campus locations, including the CLC-designated building, are situated directly above a buried synclinal fold (**Figure 19**) (Olson, 1982). This concave-upwards shape can potentially act as lens to focus seismic energy beneath UCSB. A similar subsurface geometry has been proposed to explain some of the unusually large ground motions observed at Santa Monica during the 1994 Northridge earthquake (Gao et al., 1995). And fifth, the large impedance contrast in seismic velocity at the interface between the shallow unconsolidated marine terrace deposits and the deeper Sisquoc Formation could potentially cause significant local site amplification, although this effect is largely minimized by being shallower than the Engineering I building foundation pilings. Local recordings of weak ground motions from local and near-regional earthquakes (**Figures 28** and **29**) do show some unusual variations in amplitude across the UCSB campus, but how systematic these variations might be for strong ground motions has yet to be determined.

Although we as yet do not fully understand how each of these particular factors of source, propagation, and site effect may combine to affect the expected ground motions at UCSB from a large local earthquake, subsequent CLC project studies that include uphole and downhole seismic monitoring, laboratory tests of soil and rock cores taken from the UCSB campus, and model studies of source and site-specific ground motions in 3D, are specifically designed to address this issue. More complete descriptions and documentation of the results from drilling, logging, monitoring and testing of cores from the UCSB deep drillholes will be available in the **Phase II** report, and results of the model studies to predict source- and site-specific earthquake ground motions will be available in the **Phase III** report.

10.0 ACKNOWLEDGMENTS

This project was funded by the UC Office of the President, LLNL – University Campus Directed Research and Development, UCSB Office of the Vice Chancellor for Research, UCSB Office of the Executive Vice Chancellor, and UCSB Office of the Vice Chancellor for Administrative Services. A large part of the regional hazard studies of this report was prepared under a previous UCSB-LLNL collaborative effort funded by the Minerals Management Service. We thank our colleagues who contributed substantially to the previous draft report, including Bill Foxall, Marc Kamerling, Ed Keller, Grant Lindley, Bruce Luyendyk, Chris Sorlien, and Art Sylvester. We thank Francois Heuze (LLNL) and our other CLC collaborators, including Steve Day (SDSU), Scott Elrick (UCR), Bernard Minster (UCSD), Steve Park (UCR), Mladen Vucetic (UCLA), Jeff Wagoner (LLNL), Frank Wyatt (UCSD) and Heming Xu (UCSD), for their assistance. We thank our UCSB colleagues, including Bill Hanna, Chris LaVino Kaplan, Everett Kirkelie, John Murphy, and Ron Strahl, for facillitating various CLC on-campus studies, and we especially thank Bill Hanna for providing us with important subsurface information of UCSB. We thank Chris Kaplan, Mary Ray, Steve Howson, Richard Colla, Dan Coon, Terry Gibson, Dan O'Connell, Bob Pizzi, and Mrs. Henry Wang for their assistance and permission to monitor earthquakes at various sites both on and off campus. The shear-wave generator used in the S-wave refraction studies was provided to the CLC project courtesy of Professor Eugene Herrin at Southern Methodist University, Dallas, Texas. We also appreciate discussions and contributions by Dan O'Connell (US Bureau of Reclamation), and Mary Templeton (CalState Fullerton) on various aspects of local seismicity and shallow refraction studies, respectively, and—as always—we acknowledge the expert technical assistance of Aaron Martin.

11.0 REFERENCES

Abrahamson, N., and Somerville, P. G., 1994, Effects of Hanging Wall and Footwall on Ground Motions During the 1992 Northridge Earthquake, Abstract, Eos Transactions of the American Geophysical Union, vol. 75, no. 44, p. 167.

Agbabian and Associates (1997). Preliminary report of suspension velocity logging in the UCSB CLC-2 borehole, Pasadena, CA.

Agnew, D. C., and Sieh, K. H., 1978, A documentary study of the felt effects of the great California earthquakes of 1857, Bulletin of the Seismological Society of America, vol. 68, p. 1717-1729.

Anderson, D.S. (1993). Structural synthesis of Santa Maria basin and northern Santa Barbara Channel for Bradbury Dam seismotectonic evaluation, Santa Barbara County, California, A Report to the U.S. Bureau of Reclamation, 14 pp plus 2 plates.

Anderson, R. E., Redwine, L. E., and McGovney, P. E., 1949, Geology of Northern Santa Rosa Island, Abstract, American Association of Petroleum Geologists Bulletin, vol. 33, p. 2062.

Archuleta, R. J., 1984, A faulting model for the 1979 Imperial Valley earthquake, J. Geophys. Res., vol. 89, p. 4559-4585.

Archuleta, R. J., 1992, How earthquakes can generate extreme accelerations, EOS, vol. 73, 388.

Archuleta, R.J., and Hartzell, S.H., 1981, Effects of fault finiteness on near-source ground motion, Bulletin of the Seismological Society of America, vol. 71, p. 939-957.

Arleth, K. F., 1977, Marine structural geology and geologic evolution south of Santa Rosa and San Miguel Islands, California, M. S. Thesis, San Diego State University.

Atwater, T., 1970, Implications of plate tectonics for the Cenozoic evolution of western North America: *Geological Society of America Bulletin*, v. 81, p. 3515-3536.

Atwater, T., 1989, Plate tectonic history of the northeast Pacific and western North America, *in* Winterer, E.L., Hussong, D.M., and Decker, R.W., eds., The Eastern Pacific Ocean and Hawaii: Boulder, Colorado, Geological Society of America, The Geology of North America, v. N, p. 21–71.

Bird, P. and R.W. Rosenstock, 1984, Kinematics of present crust and mantle flow in southern California, Geol. Soc. Am. Bull., 95, 946-957.

Birkeland, P. W., 1972, Late Quaternary eustatic seal-level changes along the Malibu coast, Los Angeles County, California, Journal of Geology, vol. 80, p. 432-448.

Brune, J. (1996). Particle motions in a physical model of shallow angle thrust faulting, Proc. Indian Acad. Sci. (Earth Planet. Sci.), v. 105, n.2, p.L197–L206.

Bryant, A.S. and L.M. Jones, 1992, Anomalously deep crustal earthquakes in the Ventura basin, southern California, J. Geophys. Res., 97, 437-447.

Burdick, D. J., and Richmond, W. C., 1982, A Summary of geologic hazards for proposed OCS Oil and Gas Lease Sale 68, Southern California, U. S. Geological Survey Open-File Report 82-33, 38 pp.

Çemen, I., 1989, Near-surface expression of the eastern part of the San Cayatano fault; A potentially active thrust fault in the California Transverse Ranges, J. Geophys. Res.,94, 9665-9677.

Clarke, S. H., Greene, H. G. and Kennedy M. P., 1985. Identifying potentially active faults and unstable slopes offshore, in Evaluating Earthquake Hazards in the Los Angeles Region- an Earth-Science Perspective, J. I. Ziony, ed., U.S. Geological Survey Professional Paper 1360, p. 347-374.

Corbett, E.J. (1984). Seismicity and crustal structure studies of southern California: Tectonic Implications from improved earthquake locations, Ph.D. Dissertation, Caltech, 231 p.

Corbett, E. J., and Johnson, C. E., 1982, The Santa Barbara, California, earthquake of 13 August 1978, Bulletin of the Seismological Society of America, vol. 72, pt A, no. 6, p. 2201-2226.

Crouch, J. K., and Suppe, J., 1993, Late Cenozoic tectonic evolution of the Los Angeles basin and inner California borderland: A model for core complex-like crustal extension, Geological Society of America Bulletin, vol. 105, no. 11, p. 1415-1434.

Dahlen, M. Z., Osborne, R. H., and Gorsline, D. S., 1990, Late Quaternary history of the Ventura mainland shelf, California, Marine Geology, vol. 94, p. 317-340.

Darrow, A.C., and Sylvester, A.G, 1983, Activity of the central reach of the Santa Ynez fault, USGS Open-file Report, Contract no. 14-08-0001-19787.

Darrow, A.C., and Sylvester, A.G, 1984, Activity of the central reach of the Santa Ynez Fault: Continuation of investigations, USGS Final Technical Report, Contract no. 14-08-0001-21367.

Davis, T.L., J. Namson and R.F. Yerkes, 1989, A cross section of the Los Angeles area: Seismically active fault and fold belt, the 1987 Whittier Narrows earthquake, and earthquake hazard, J. Geophys. Res., 94, 9644-9664.

Davis, T. L., and Namson, J. S., 1994, A balanced cross-section of the 1994 Northridge earthquake, Southern California, Nature, vol. 372, no. 10, p. 167-169.

Dibblee, T.W., Jr., 1982, Geology of the Channel Islands, Southern California, in: D. L. Fife and J. A. Minch, eds., Geology and Mineral Wealth of the California Transverse Ranges, Mason Hill Volume, South Coast Geological Society, Santa Ana, California, p. 27-39.

Dibblee, T. W. Jr, 1988, Geologic Map of the Tranquillon Mtn. and Point Arguello, Lompoc and Surf, Solvang and Gaviota, Santa Rosa Hills and Sacate, Santa Barbara County, California, H. E. Ehrenspeck, ed., Dibblee Geological Foundation, Santa Barbara, California

Dolan, J. F., and Sieh, K. E., 1992, Paleoseismology and geomorphology of the northern Los Angeles basin: Evidence for Holocene activity on the Santa Monica fault and identification of new strike-slip faults through downtown Los Angeles, EOS, Trans. AGU, vol. 73, no. 43, p. 589.

Dolan, J. F., Sieh, K. E., Guptill, P., Miller, G., Rockwell, T., and Smirnoff, T., 1993, Structural geology, fault kinematics, and preliminary paleoseismologic results from the Hollywood fault: New data from continuously cored borings and geotechnical trenches, Hollywood, California, Abstract, EOS Transactions American Geophysical Union, vol. 74, no. 43, p. 427.

Dolan, J.F., K. Sieh, T.K. Rockwell, R.S. Yeats, J. Shaw, J. Suppe, G.J. Huftile, and Gath, E.M., 13 January 1995, Prospects for larger or more frequent earthquakes in the Los Angeles metropolitan region, Science, vol. 267, p. 1994.

Donnellan, A., Hager, B. H., and King, R. W., 1993, Discrepancy between geological and geodetic deformation rates in the Ventura basin, Nature, vol. 366, p. 333-336.

Donnellan, A., Hager, B. H., King, R. W., and Herring, T. A., 1993, Geodetic measurement of deformation in the Ventura basin region, Southern California, Journal of Geophysical Research, vol. 98, no. B12, p. 21,727-21,739.

Donnellan, A. and G.A. Lyzenga (1996) Northridge postseismic deformation: Inferences from continuous and campaign GPS observations, EOS (Trans. AGU), v. 77, n. 46, p.F147.

Drumm, P., 1992, Holocene displacement of the central splay of the Malibu Coast fault zone, Latigo Canyon, Malibu, in B. Pipkin and R. Proctor, eds., Engineering Geology Practice in Southern California, Star Publishing Company, Belmont, California, p. 247-254.

Elliott, W., and Kamerling, M., 1995, Seismic hazards in the Santa Barbara Channel using high resolution seismic refection data and dated horizons from ODP 893 [abstract]: EOS, Transactions, American Geophysical Union, v. 76, no. 46, Fall Meeting, p. F417.

Ellsworth, W. L., 1990, Earthquake History, 1769-1989, in Wallace, R. E., ed., The San Andreas Fault System, California, U.S. Geological Survey Professional Paper 1515, p. 152-187.

Evernden, J. G., and Thompson, J. M., 1985, Predicting seismic intensities, in J. I. Ziony, ed., Evaluating Earthquake Hazards in the Los Angeles Region - An Earth-Science Perspective. U.S. Geological Survey Professional Paper 1360, p. 151-202.

Feigl, K. L., Agnew, D. C., Bock, Y., Dong, D., Donnellan, A., Hager, B. H., Herring, T. A., Jackson, D. D., Jordan, T. H., King, R. W., Larsen, K. M., Murray, M. H., Shen, Z., and Webb, F. H., 1993, Space geodetic measurement of crustal deformation in central and southern California, 1984-1992, Journal of Geophysical Research, vol. 98, no. B12, p. 21,677-21,712.

Field, M. E., and Richmond, W. C., 1980, Sedimentary and structural patterns on the northern Santa Rosa–Cortez Ridge, Southern California, Marine Geology, vol. 34, p. 79-97.

Frankel, A., et al, 1996, National seismic hazard maps, U.S. Geol. Surv. Open-file Report 96-532, 110 p.

Gao, S., H. Liu, P.M. Davis and L. Knopoff, Localized amplification of seismic waves and correlation with damage due to the Northridge earthquake: Evidence for focusing in Santa Monica, Bull. Seismol. Soc. Am., v. 86, n. 1B, p. S209–S230, 1996.

Gawthrop, W. H., 1978b, The 1927 Lompoc, California earthquake, Bulletin of the Seismological Society of America, vol. 68, p. 1705-1716.

Goter, Susan K., 1992, Southern California earthquakes, United States Geological Survey, National Earthquake Information Center, Open-File Report OFR 92-533, Map scale 1:375,000.

Gratier, J.-P., 1995, Displacement field and geometric compatibility using computational restoration of folded and faulted strata: Application to the last 3-4 Ma in the Ventura and Los Angeles basins, EOS, Transactions American Geophysical Union, vol. 76, no. 46, p. F143.

Gratier, J.-P., T. Chen and R. Hellman, 1994. Pressure solution as a mechanism for crack sealing around faults, in The Mechanical Involvement of Fluids in Faults, S. Hickman, R. Sibson, and R. Bruhn, eds., U.S. Geological Survey Open-file Report 94-228, p. 279–300.

Gregg In Situ, Inc. (1996). Presentation of cone penetration data, University of California at Santa Barbara, CLC Campus Earthquake Project, A Report to LLNL, Signal Hill, CA.

Gurrola, L.D., 1996, Dating of emergent marine terraces and rate of uplift for the western Santa Barbara fold belt, California, Geol. Soc. Am. Abstracts w/Prog., v. 28, n. 7, p. A-301.

Gurrola, L.D., D. Valentine, and E.A. Keller, Earthquake hazard of the Santa Barbara fold belt, California, SCEC Annual Progress report, p. C27–C30, 1996.

Gurrola, L. D., and Kamerling M., 1996, Segmentation of principal east-west trending reverse/thrust faults and earthquake nucleation sites in the western Transverse Ranges, California: *EOS (Trans. AGU)*, **v. 77**, p. F512,

Hadley, D., and H. Kanamori, 1977, Seismic structure of the Transverse Ranges, California, Geol. Soc. Am. Bull., 88, 1469-1478.

Hadley, D., and H. Kanamori, 1978, Recent seismicity of the San Fernando region and tectonics of the west-central Transverse Ranges, California, Bull. Seis. Soc. Am., 68, 1449-1457.

Hall, N.T., T.D. Hunt and P.R. Vaughan, 1994, Holocene behavior of the San Simeon fault zone, south-central coastal California, Geol. Soc. Am. Spec. Pap. 292, 167-190.

Hanson, KL., J.R. Wesling, W.R. Lettis, K.I. Kelson, and L. Mezger, 1994, Correlation, ages, and uplift rates of Quaternary marine terraces: South-central coastal California, Geol. Soc. Am. Spec. Pap. 292, 45-72.

Hatori, T., 1976, Wave source of the Hawaii tsunami in 1975 and the tsunami behavior in Japan, Journal of the Seismological Society of Japan vol. 29, p.355-364.

Hauksson, E., and L.M. Jones, 1989, The 1987 Whittier Narrows earthquake sequence in Los Angeles, southern California: Seismological and tectonic analysis, J. Geophys. Res., 94, 9569-9589.

Helmberger, D. V., Somerville, P. G., and Garnero, E., 1992, The location and source parameters of the Lompoc, California earthquake of 4 November 1927, Bulletin of the Seismological Society of America, vol. 82, no. 4, p. 1678-1709.

Henyey, T. L., et al, 1979, A sea-floor seismic monitoring network around an offshore oil field platform and recording of the August 13, 1978 Santa Barbara earthquake, Offshore Tech. Conf., Proc.; no. 11, vol. 4, p. 2219-2223.

Hileman, J. A., Allen, C. R., and Nordquist, J. M., 1973, Seismicity of southern California region, California Institute of Technology, Division of Geology and Planetary Sciences No. 2385, p. 487.

Holden, Edward S., 1898, Catalogue of Earthquakes on the Pacific Coast 1769 to 1897, Smithsonian Miscellaneous Collections No. 1087 for distribution by the Lick Observatory, p. 253.

Hopps, T.E., H.E. Stark, and R.J. Hindle, Subsurface geology of Ventura Basin, California, *Ventura Basin Study Group Report*, 45 pp., 17 structure contour maps and 84 structure panels comprising 21 cross sections, Rancho Energy Consultants, Inc., Santa Paula, CA, 1992.

Hornafius, J. S., 1985, Neogene tectonic rotation of the Santa Ynez Range, western Transverse Ranges, California, suggested by paleomagnetic investigation of the Monterey Formation, J. Geophys. Res., 90, 12503-12522.

Hornafius, J. S., Luyendyk, B. P., Terres, R. R. and Kamerling, M. J., 1986, Timing and extent of Neogene tectonic rotation in the Western Transverse Ranges, California, Geological Society of America Bulletin, vol. 97, p. 1476-1487.

Hornafius, J. S., B. P. Luyendyk, and M. J. Kamerling, 1995, Seismic images of the North Channel fault near Santa Barbara, CA, SCEC Workshop on Thrust Ramps and Detachment faults in the Western Transverse Ranges, Univ. Calif. Santa Barbara, Jan., 1995, p. 11.

Huftile, G.J., 1992, Convergence rates across the Ventura basin, California, Ph.D. dissertation, Oregon State Univ., Corvallis.

Huftile, G.J., H. Tsutsumi, C.L. Schneider and R.S. Yeats, Geologic evidence for thick-skinned deformation in the Western Transverse Ranges, California, *SCEC Workshop on Thrust Ramps and Detachment Faults in the Western Transverse Ranges*, p. 12, UC Santa Barbara, January, 1995.

Huftile, G.J., and R.S. Yeats, 1995, Convergence rates across a displacement transfer zone in the western Transverse Ranges, Ventura basin, California, J. Geophys. Res., 100, 2043-2067.

Huftile, G. and R.S. Yeats, Deformation Rates across the Placerita (Northridge Mw = 6.7 aftershock zone) and Hopper Canyon segments of the western Transverse Ranges deformation belt: Bulletin of the Seismological Society of America, **v. 86**, no. 1B, p. S3-S18, 1996.

Jackson et al, 1995, Seismic Hazards in Southern California: Probable Earthquakes, 1994-2024, The Phase II Report, Southern California Earthquake Center, Bull. Seismol. Soc. Am., 1996.

Jackson, J., and Molnar, P., 1990, Active faulting and block rotations in the Western Transverse Ranges, California: Journal Geophysical Research, v. 95, p. 22073-22087.

Jackson, P. A., and Yeats, R. S., 1982, Structural evolution of Carpinteria basin, Western Transverse Ranges, California, American Association of Petroleum Geologists Bulletin, vol. 66, p. 805-829.

Jennings, C. W., 1994, Fault activity map of California and adjacent areas, California Division of Mines and Geology, Sacramento, Calif.

Jones, T.A., and G.W Simila, Seismicity and tectonics of the Western Transverse Ranges: Ventura basin to the San Fernando Valley, SCEC Workshop on Thrust Ramps and Detachment faults in the Western Transverse Ranges, Univ. Calif. Santa Barbara, Jan., 1995, p. 14.

Junger, A., 1976, Offshore structure between Santa Cruz and Santa Rosa Islands, in Howell, D. G., ed., Aspects of the geologic history of the California continental borderland, American Association of Petroleum Geologists Miscellaneous Publication 24, p. 418-426.

Junger, A., 1979, Maps and seismic profiles showing geologic structure of the northern Channel Islands platform, California continental borderland, U. S. Geological Survey Miscellaneous Field Studies Map MF-991, 5 maps, 16 pp.

Junger, A., and Wagner, H. C., 1977, Geology of the Santa Monica and San Pedro basins, California Continental Borderland, U. S. Geological Survey Map MF-820.

Kamerling and Nicholson, 1995, Fault geometry of blind thrusts along the Oak Ridge trend in the Santa Barbara Channel, SCEC 1994 Annual Report, v.2, p. C12-C15.

Kamerling, M.J. and C. Nicholson, Reliability of 2-D kinematic models to infer deep structure in the western Transverse Ranges, California, *Eos (Trans. AGU)*, **v. 76**, n.46, p. F349 (1995).

Kamerling, M. J., and Luyendyk, B. P., 1979, Tectonic rotations of the Santa Monica Mountains region, western Transverse Ranges, California, suggested by paleomagnetic vectors, Geol. Soc. Am. Bull., vol. 90, p. 331-337.

Kamerling, M. J., and Luyendyk, B. P., 1985, Paleomagnetism and Neogene tectonics of the northern Channel Islands, California, Journal of Geophysical Research, vol. 90, no. B14, p. 12485-12502.

Keller, E. A., Johnston, D. L., Laduzinsky, D. M., Rockwell, T. K., Seaver, D. B. and Zepeda, R. L., 1988, Source and seismic potential associated with reverse fault and related folding, Rep. U. S. Geol. Surv. Contrib. 14-08-0001-G1165, University of California, Santa Barbara, 148 pp.

Keller, E.A, L.D. Gurrula, J.G. Metcalf, and T.W. Dibblee, Jr., Earthquake Hazard of the Santa Barbara Fold Belt, California, *SCEC Workshop Field-Trip Guidebook*, UC Santa Barbara, January, 1995.

Keller, E.A. and N. Pinter, 1996, *Active Tectonics – Earthquakes, Uplift, and Landscape*, Prentice Hall, Upper Saddle River, N.J., 338 pp.

Kennett, James P., 1995, Latest Quaternary benthic oxygen and carbon isotope stratigraphy: Hole 893A, Santa Barbara Basin, California: *in* Kennett, J. P. Baldauf, J. G., and Lyle, M., eds., Proceedinfgs of the Ocean Drilling Program, Scientific Results, v. 146, Pt. 2. p. 3-18.

Lander, J. F., Lockridge, P. A., and Kozuch, M. J., 1993, Tsunamis Affecting the West Coast of the United States 1806-1992, NGDC Document No. 29, US Dept. Of Commerce, National Geophysical Data Center, Boulder, Colorado.

Larsen, S., D. C. Agnew and B. H. Hager, 1993, Strain accumulation in the Santa Barbara Channel, 1970-1988, J. Geophys. Res., 98, 2119-2133.

Larson, K. M., 1993, Application of the global positioning system to crustal deformation measurements 3. Results from the southern California Borderlands, Journal of Geophysical Research, vol. 98, no. B12, p. 21,713-21,726.

Larson, K.M. and Webb, F. H.,1992, Deformation in the Santa Barbara Channel from GPS measurements, 1987-1991, Geophys. Res. Let., 19, 1491-1494.

Lee, W.H.K., R.F. Yerkes, and M. Simirenko, 1979, Recent earthquake activity and focal mechanisms in the western Transverse Ranges, California, U.S. Geol. Surv. Circular 799–A, 37 pp.

Legg, M. R., Luyendyk, B. P., Mammerickx, J., De Moustier, C., and Tyce, R. C., 1989, Sea beam survey of an active strike-slip fault: The San Clemente Fault in the California continental borderland, Journal of Geophysical Research, vol. 94, no. B2, p.1727-1744.

Levi, S., and R.S. Yeats, 1993, Paleomagnetic constraints on the initiation of uplift on the Santa Susana fault, Western Transverse Ranges, California, Tectonics, 12, 688-702.

Liddicoat, J. C., 1990, Tectonic rotation of the Santa Ynez Range, California, recorded in the Sespe Formation, Geophysical Journal International, vol. 102, p. 739-745.

Luyendyk, B. P., Hajic, E. J., Crippen, R. E., and Simonett, D. S., 1982, Side scan sonar and high resolution reflection maps of the Santa Barbara Channel seafloor, UCSB, California Sea Grant College Program Report no. T-CSGCP-006.

Luyendyk, B. P., Kamerling, M. J., Terres, R. R., and Hornafius, J. S., 1985, Simple shear of southern California during the Neogene, Journal Geophysical Research, vol. 90, p.12454-12466.

Luyendyk, B.P., 1990, Neogene-age fault slip in the continental transform zone in Southern California, Ann. Tectonic., vol. 4, p. 24-34.

Luyendyk, B.P., 1991, A model for Neogene crustal rotations, transtension and transpression in Southern California, Bull Geol. Soc. Amer., vol. 103, p. 1528-1536.

Marine Advisors, Inc., 1965, Examination of tsunami potential at the San Onofre nuclear generating station, Report A-163, La Jolla, California, p. 59.

McCarthy, R. J., Bernard, E. N, and Legg, M. R., 1995, The Cape Mendocino earthquake: A local tsunami wakeup call? 2nd International Workshop on Wind and Earthquake Engineering for Offshore and Coastal Facilities, Paper Preprints, University of California at Berkeley, Berkeley, California.

McCulloch, D. S., 1985. Evaluating tsunami potential, in J. I. Ziony, ed., Evaluating Earthquake Hazards in the Los Angeles Region - An Earth-Science Perspective, U.S. Geological Survey Professional Paper 1360, Washington D. C., p. 375-413.

McGill, S.F., and K.E. Sieh, 1991, Surficial offsets on the central and eastern Garlock fault associated with prehistoric earthquakes, J. Geophys. Res., 96, 21957-21621.

McGill, S.F., and K.E. Sieh, 1993, Holocene slip rate of the central Garlock fault in southeastern Searles Valley, California, J. Geophys. Res., 98, 14217-14231.

McWayne, E. H., and Sorlien, C. C., 1994, History of faulting and folding in western Santa Barbara Channel, California, EOS, Transactions American Geophysical Union, vol. 75, no. 44, p. 622.

Molnar, P. (1992). Active deformation of the western Transverse Ranges, SCEC Final Report, 125 p.

Molnar, P., 1995, A review of active deformation of the western Transerse Ranges and its relevance to the active tectonics and earthquake history of Mongolia, SCEC Workshop on Thrust Ramps and Detachment Faults in the Western Transverse Ranges, Univ. Calif. Santa Barbara, Jan., 1995, p. 16.

Molnar, P., and Gibson, J. M., 1994, Very long baseline interferometry and active rotations of crustal blocks in the western Transverse Ranges, California, Bull Geol. Soc. Amer., vol. 106, p. 594-606.

Nason, R. (1973). Increased seismic shaking above a thrust fault, in San Fernando, California, Earthquake of February 9, 1971, US Dept. of Commerce, Washington, DC, v. III, p.123–126.

Namson, J., and Davis, T, 1988, Structural transect of the Western Transverse Ranges, California: Implications for lithospheric kinematics and seismic risk evaluation, Geology, vol. 16, p. 675-679.

Namson, J., and Davis, T. L., 1990, Late Cenozoic fault and fold belt of the southern Coast Ranges and Santa Maria basin, California, A.A.P.G. Bulletin, vol. 74, no. 4, p. 467-492.

Namson, J., and Davis, T., 1992, Late Cenozoic thrust ramps of southern California, Final Report for 1991 Contract, Southern California Earthquake Center.

Namson, J.S. and W.R. Lettis, 1993. Balanced cross section through the westrn Transverse Ranges in the vicinity of Bradbury Dam, a Report to the U.S. Bureau of Reclamation, 9 pp plus 2 plates.

Nicholson, C., Seismic Hazard Analysis of the El Estero Water Treatment Facility in Santa Barbara, California, A Report to the City of Santa Barbara, 30 pp. (1992).

Nicholson, C., 1995, A new tectonic model for the evolution of the Western Transverse Ranges and its implications for crust and mantle structure, SCEC Workshop on Thrust Ramps and Detachment Faults in the Western Transverse Ranges, Univ. Calif. Santa Barbara, Jan., 1995, p. 18.

Nicholson, C. and J.K. Crouch, Neotectonic structures along the central and southern California margin: Predominantly a thrust regime?, *Seismol. Res. Lett.*, **60**, 23-24 (1989).

Nicholson, C. and M.J. Kamerling, Reliability of 2-D kinematic fold models to infer deep fault structure in the western Transverse Ranges, California, *Proceedings of the Northridge Earthquake Research Conference*, 8 pp (1997).

Nicholson, C., L. Seeber, P. Williams and L.R. Sykes. Seismic evidence for conjugate slip and block rotation within the San Andreas fault system, southern California, *Tectonics*, **5**, 629-648 (1986b).

Nicholson, C. and D.W. Simpson, Changes in Vp/Vs with depth: Implications for appropriate velocity models, improved earthquake locations and material properties of the upper crust, *Bulletin Seismological Society of America*, **75**, 1105-1123 (1985).

Nicholson, C., C.C. Sorlien, T. Atwater, J.C. Crowell and B.P. Luyendyk, Microplate capture, rotation of the western Transverse Ranges, and initiation of the San Andreas transform as a low-angle fault system, *Geology*, **v. 22**, p.491–495 (1994).

Novoa, E., J. Suppe, K. Mueller, and J. Shaw, 1995, Axial surface mapping of active folds in the Santa Barbara Channel, SCEC Workshop on Thrust Ramps and Detachment Faults in the Western Transverse Ranges, Univ. Calif. Santa Barbara, Jan., 1995, p. 19.

O'Connell, D., Earthquake locations, focal mechanisms, and GPS near Ventura, Western Transverse Ranges, California: The crust has a thick skin, *EOS (Trans. AGU)*, **76**, n.46, p. F141 (1995).

Oglesby, D.D. and Archuleta, R.J., 1997, A faulting model for the 1992 Petrolia earthquake: Can extreme ground acceleration be a source effect?, J. Geophys. Res., v. 102, in press.

Olsen, P. G., 1972, Seismic microzonation in the city of Santa Barbara, Proceedings of the International Conference of Microzonation, Seattle, Washington, p. 395-408.

Olsen, P. G., and Sylvester, A. G.,1975, The Santa Barbara earthquake 29 June 1925, California Geology 28, p. 123-132.

Olson, D.J. (1982). Surface and subsurface geology of the Santa Barbara–Goleta metropolitan area, Santa Barbara County, California, Masters Thesis, Oregon State University, 71 pp plus 14 plates.

Page, B.M., J.G. Marks and G.W. Walker, 1951, Stratigraphy and structure of mountains northeast of Santa Barbara, California, AAPG Bull., 35, 1727-1780.

Pacific Gas and Electric (PG&E), 1988. Final report of the Diablo Canyon long-term seismic program, Pacific Gas and Electric Company, Docket Nos. 50-275 and 50-323.

Patterson, Roy H., 1979, Tectonic Geomorphology and neotectonics of the Santa Cruz Island Fault Santa Barbara County, California, MA thesis, University of California, Santa Barbara, 141 pp., 1 map.

Petersen, M.D., and S.G. Wesnousky, 1994, Fault slip rates and earthquake histories for active faults in southern California, Bull. Seis. Soc. Am., 84, 1608-1649.

Petersen, M.D., C.H. Cramer, W.A. Bryant, M.S. Reichle, and T. Toppozada, 1996, Preliminary seismic hazard assessment for Los Angeles, Ventura, and Orange counties, California affected by the January 17, 1994 Northridge earthquake, Bull. Seis. Soc. Am., v. 86, n.1, part B, p. S247–S262.

Pinter, N., and Keller, E. A., 1994, Latest Pleistocene to Holocene rupture history of the Santa Cruz Island fault, Final Technical Report, U. S. Geological Survey No. 1434-92-G-2208.

Pinter, N., and Sorlien, C. C., 1991, Evidence for latest Pleistocene to Holocene movement on the Santa Cruz Island fault, California, Geology, vol. 19, p. 909-912.

Plafker, G. and Galloway, J. P., 1989, Lessons learned from the Loam Prieta, California, Earthquake of October 17,1989, U. S. Geological Survey Circular 1045, p. 48.

Richmond, W. C., Cummings, L. J., Hamlin, S., and Nagaty, M. E., 1981, Geological hazards and constraints in the area of proposed OCS oil and gas lease sale 48, southern California, U.S. Geological Survey Open-File Report 81-307, 37 p.

Richter, C. F., 1958, *Elementary Seismology*, Freeman Press, San Francisco, CA, 768 pp.

Rockwell, T., 1988, Neotectonics of the San Cayetano fault, Transverse Ranges, California, Geological Society of America Bulletin, vol.100, p. 500-513.

Rockwell, T., 1995a, Rates and styles of surface deformation associated with the San Cayatano and Elysian Park thrust systems, SCEC Workshop on Thrust Ramps and Detachment Faults in the Western Transverse Ranges, Univ. Calif. Santa Barbara, Jan., 1995, 20.

Rockwell, T., 1995b, Paleoseismic studies in the Los Angeles area, SCEC 1994 Annual Report, v.2: 1994 Progress Report from SCEC Scientists, C26-C27.

Rockwell, T., Keller, E., and Dembroff, G.R., 1988, Quaternary rate of folding of the Ventura Avenue anticline, Western Transverse Ranges, California, Geol. Soc. .Am. Bull., .00, 850-858.

Rogers, D.B. (1929). *Prehistoric Man of the Santa Barbara Coast*, Santa Barbara Museum of Natural History, Santa Barbara, CA.

Rzonca, G. F., Spellman, H. A., Fall, E. F., and Shlemon, R. J., 1991, Holocene displacement of the Malibu Coast Fault Zone, Winter Mesa, California: Engineering geologic implications, Bulletin of the Association of Engineering Geologists, vol. 28, no. 2, p. 147-158.

Santa Barbara County Seismic Safety and Safety Element Report, 207 pp (1978).

Sarna-Wojcicki, A. M., Lajoie, K. R., and Yerkes, R. F., 1987, Recurrent Holocene displacement on the Javon Canyon fault- A comparison of fault-movement history with calculated average recurrence intervals: in Recent Reverse Faulting in the Transverse Ranges, California, U.S.G.S. Professional Paper 1339, p. 125-135.

Schimmelmann, A., C.B. Lange, W.H. Berger, A. Simon, S.K. Burke, and R.B. Dunbar (1992). Extreme climatic conditions recorded in the Santa Barbara basin laminated sediments: the 1835–1840 Macoma event, Marine Geology, v. 106, p.279–299.

Scott, J.S., Hauksson, E., Vernon, F., and Edelman, A., 1994, Wave propagation in the Los Angeles basin: observations and modeling of Northridge earthquake aftershocks, EOS, vol. 75, p. 175.

Seeber, L. and J.G. Armbruster, The San Andreas fault system through the Transverse Ranges as illuminated by earthquakes, *J. Geophys. Res.*, **v. 100,** p.8285–8310, 1995.

Seeber, L. and C.C. Sorlien, Listric thrusts in the western Transverse Ranges, California, *Geol. Soc. Am. Bull*, 12 pp., submitted 1996.

Shaw, J.H., 1993, Active blind-thrust faulting and strike-slip fault-bend folding in California, Ph.D. dissertation, Princeton Univ., 216 p.

Shaw, J. H., and Suppe, J., 1994, Active faulting and growth folding in the eastern Santa Barbara Channel, California, Geological Society of America Bulletin, vol. 106, p. 607-626.

Shaw, J. H., Hook, S. C., and Suppe, J., 1994, Structural trend analysis by axial surface mapping, American Association of Petroleum Geologists Bulletin, vol. 78, p. 801-812.

Sieh, K., M. Stuiver and D. Brillinger, 1989, A more precise chronology of earthquakes produced by the San Andreas fault in southern California, J. Geophys. Res., v. 94, n. B1, p. 603–623.

Simila, G.W., P. Armand and B. Van Waggoner, 1987, Seismicity of the San Cayatano fault, Western Transverse Ranges, (abs.), Seis. Res. Let., 58, 28.

Somerville, P., and Cornell, A., 1992, Site seismic hazard and ground motion; in, Iwan, Wilfred D., ed., Proceedings of the international workshop on seismic design and reassessment of offshore structures Dec. 7-9, 1992: Pasadena, CA, USA, 135-138.

Sorlien, C. C., 1994, Faulting and uplift of the northern Channel Islands, California, in, Halvorson, W. L., and Maender, G. J., eds., The Fourth Channel Islands Symposium: Update on the Status of Resources, Santa Barbara Museum of Natural History, Santa Barbara, California, p. 281–296..

Sorlien, C.C, Structure and Neogene evolution of offshore Santa Maria basin and western Santa Barbara Channel, California, Ph.D. Dissertation, University of California at Santa Barbara, 219 pp., 1994.

Sorlien, C.C., J.P. Gratier, B.P. Luyendyk, J.S. Hornafius, and T.E. Hopps, 1995, Finite displacement field across the Oak Ridge fault: Restoration of a folded and faulted layer near onshore and offshore Ventura basin, California, SCEC Workshop on Thrust Ramps and Detachment faults in the Western Transverse Ranges, Univ. Calif. Santa Barbara, Jan., 1995, p. 24-27.

Sorlien, C. C., Seeber, L., Pinter, N., and Geiser, P. A., 1995, Listric faults and related folds, uplift, and slip, Supplement to EOS, Transactions American Geophysical Union, vol. 76, no. 46, p. F-625

Stein, R.S., and W. Thatcher, 1981, Seismic and aseismic deformation associated with the 1952 Kern county, California, earthquake and relationship to Quaternary history of the White Wolf fault, J. Geophys. Res., 86, 4913-4928.

Steritz, J., and B. P. Luyendyk, Hosgri fault zone, offshore Santa Maria basin, California. In Alterman, I. B., McMullen, R.B., Cluff, L.S., and D.B. Slemmons eds., Seismotectonics of the central California Coast Ranges. Geol. Soc. Amer. Spec. Paper. 292, 191-210, 1994.

Stierman, D. J., and Ellsworth, W. L., 1976, Aftershocks of the February 21, 1973 Point Mugu, California earthquake, Bulletin of the Seismological Society of America, vol. 66, no. 6, p. 1931-1952.

Stone, Donald S., Structural trend analysis by axial surface mapping: Discussion: AAPG Bulletin, v. 80, no. 5, p. 770-779, 1996.

Suppe, J., 1983, Geometry and kinematics of fault-bend folding, American Journal of Science, vol. 283, p. 684-721.

Suppe, J., *Principles of Structural Geology*, Prentice-Hall, Englewood Cliffs, NJ, 537 p., 1985.

Suppe, J., R.E. Bischke and J.H. Shaw, Evaluation of the use of compressive growth structure in earthquake hazard assessment, *U.S. Geol. Surv. Open-file Report 91-352*, NEHRP Technical Reports XXXII, p. 192–195, 1991.

Suppe, J. and D.A. Medwedeff, Geometry and kinematics of fault-propagation folding, *Eclogae Geol. Helv.*, **v.83/3,** p. 409–454 (1990).

Sylvester, A. G. 1978, Where in Santa Barbara County, California, was the earthquake of 21 December, 1812?, Earthquake Notes, vol. 49, p. 36-37.

Sylvester, A., Aseismic growth of Ventura Avenue anticline (1978 to 1991): Evidence for anelastic strain release in Ventura basin, southern California, *Eos (Trans. AGU)*, **v.76,** p. F141, 1995.

Sylvester, A.G. and A.C. Darrow, 1979, Structure and neotectonics of the western Santa Ynez fault system in southern California, Tectonophysics, v. 52, p. 389–405.

Sylvester, A. G., Smith, S. W., and Scholz, C. H., 1970, Earthquake swarm in the Santa Barbara Channel, 1968, Bulletin of the Seismological Society of America 60, p. 1048-1063.

Toppozada, T. R., Real, C. R., and Parke, D. L., 1981, Preparation of isoseismal maps and summaries of reported effects for pre-1900 California earthquakes, California Division of Mines and Geology Open-File Report 81-11 SAC, 182 pp.

Tsutsumi, H., Yeats, R. S., Hummon, C., Schneider, C. L., and Huftile, G. J., 1994, Subsurface analysis of the active trace of the Santa Monica fault and the northern extension of the Newport-Inglewood fault zone, Los Angeles basin, California, EOS, Trans. AGU, vol. 75, no. 44, p. 622.

U. S. Geological Survey, 1974, Final Environmental Statement Proposed Plan of Development Santa Ynez Unit Santa Barbara Channel, off California, vol. 1, 422 pp.

U.S. Geological Survey and SCEC, 1994, The magnitude 6.7 Northridge, California, Earthquake of 17 January 1994, Science, vol. 266, p. 389-397.

Wallace, R.F. (ed.), 1990, The San Andreas fault system California, U.S. Geol. Survey Prof. Pap. 1515, 283 p.

Ward, S. N., 1994, A multidisciplinary approach to seismic hazard in southern California, Bull Seis. Soc. Am., 84, 1293-1309.

Weaver, D. W., and Meyer, G. L., 1969, Stratigraphy of northeastern Santa Cruz Island, in D. W. Weaver, assisted by D. P. Doerner, and B. Nolf, Geology of the Northern Channel Islands: AAPG and SEPM Pacific Section, Special Publication, p. 95-104.

Weaver, D. W., and Nolf, B., 1969, Geology of Santa Cruz Island, in D. W. Weaver, assisted by D. P. Doerner, and B. Nolf, Geology of the Northern Channel Islands: AAPG and SEPM Pacific Section, Special Publication, map.

Wells, D.L., and K.J. Coppersmith, 1994, New empirical relationships among magnitude, rupture length, rupture width, rupture area, and surface displacement, Bull. Seis. Soc. Am., 84, 974-1002.

Wesnousky, S.G., 1986, Earthquakes, Quaternary faults, and seismic hazards in California, J. Geophys. Res., 91, 12587-12631.

Whitcomb, J. H., Allen, C. R., Garmany, J. D. and Hileman, J. A., 1973, San Fernando earthquake series: Focal mechanisms and tectonics, Reviews of Geophysics and Space Physics, vol. 11, p. 693-730.

Willis, B., 1925, A study of the Santa Barbara earthquake of June 29, 1925, Bulletin of the Seismological Society of America, vol. 15, p. 255-278.

Wood, H.O., 1947, Earthquakes in southern California with geologic relations: Part 2, Bulletin of the Seismological Society of America, v. 37, p. 217–258 plus 4 maps.

Wood, H. O., Heck, N. H., and Eppley, R. A., 1966, Earthquake history of the United States, part 2, stronger earthquakes of California and western Nevada (revised through 1963), U.S. Coast and Geodetic Survey Publication, p. 41, 48.

Yeats, R. S., 1981, Quaternary flake tectonics of the CaliforniaTransverse Ranges, Geology, 9, 16-20.

Yeats, R. S., 1983, Large-scale Quaternary detachments in Ventura basin, southern California, Journal of Geophysical Research, vol. 88, no. B1, p. 569-583.

Yeats, R. S., 1988, Late Quaternary slip rates on the Oak Ridge Fault, Transverse Ranges, California: Implications for seismic risk, Journal of Geophysical Research, vol. 93 no. B10, p.12137-12150.

Yeats, R. S., 1989, Oak Ridge fault, Ventura basin, California, U. S. Geological Survey Open File Report OFR 89-343, 30 pp.

Yeats, R. S., 1993, Converging more slowly, Nature, vol. 366, p. 299-301.

Yeats, R. S., 1995, Thin-skinned vs thick-skinned interpretation of sesimogenic reverse faults, SCEC Workshop on Thrust Ramps and Detachment faults in the Western Transverse Ranges, Univ. Calif. Santa Barbara, Jan., 1995, 29-30.

Yeats, R. S., and Huftile, G. J., 1995, The Oak Ridge fault system and the 1994 Northridge earthquake, Nature, 373, 418-420.

Yeats, R.S., and Olson, D. J., 1984, Alternate fault model for the Santa Barbara, California, earthquake of 13 August 1978, Bulletin of the Seismological Society of America vol. 74, p. 1545-1554.

Yeats, R. S., W.H.K. Lee and R.F. Yerkes, 1987, Geology and seismicity of the eastern Red Mountain fault, Ventura county, California, in, Recent Reverse Faulting in the Transverse Ranges, California, eds., D.M. Morton and R.F Yerkes, U.S.G.S. Prof. Pap. 1339, 161-168.

Yeats, R. S., Huftile, G. J., and Grigsby, F. B., 1988, Oak Ridge fault, Ventura fold belt, and the Sisar décollement, Ventura basin, California, Geology, vol. 16, p. 1112-1116.

Yeats, R. S., and Taylor, J. C., 1990, Saticoy oil field-U.S.A. Ventura basin, California, in E. A. Beaumont and N. H. Foster, eds., Structural Traps III, Tectonic Fold and Fault Traps, Treatise of Petroleum Geology, Atlas of Oil and Gas Fields, American Association of Petroleum Geologists, Tulsa, Oklahoma, p. 199-215.

Yerkes, R. F. and Lee, W. H. K., 1979, Faults, fault activity, epicenters, focal depths and focal mechanisms, 1970–75 earthquakes, western Transverse Ranges, California, U.S. Geol. Surv. Misc. Field Stud. Map MF-1032.

Yerkes, R. F., Greene, H. G., Tinsley, J. C., and Lajoie, K. R., 1981, Seismotectonic setting of the Santa Barbara Channel area, southern California, U.S. Geological Survey Miscellaneous Field Studies Map MF-1169, 25 pp.

Ziony, J.I. and L.M. Jones, Map showing late Quaternary faults and 1978–84 seismicity of the Los Angeles region, California, U.S. Geol. Surv. Map MF–1964, scale 1:250,000, 1989

TABLE 1

ACTIVE OR POTENTIALLY ACTIVE FAULTS WITHIN 100 KM OF THE UCSB CAMPUS AND THEIR EARTHQUAKE POTENTIAL

Abbreviated Fault Name	Primary Style of Faulting*	Site Distance (km)	Maximum Credible Magnitude	Peak Site Acceleration (g)	Estimated Slip Rate (mm/yr)	Estimated Recurrence Interval (yr)
Arroyo Parida –More Ranch – Mission Ridge	LS	1	6.7-7.0	0.70+	0.4-2.0	750-3000
Big Pine	LS	35	7.2	0.20	0.8-2.0	1000-2700
Casmalia – Orcutt – Little Pine	Rv?	20	6.5-6.8	0.25	0.2-0.4	2900
Channel Islands–Santa Monica	O-Rv?	20?	7.2-7.5	0.40+	1.2-3.0	600-1400
West Garlock	LS	95	7.2-7.5	0.15	7.0-11.0	530
Hosgri	O-Rv-RS	70	7.1-7.5	0.15	1.0-5.0	650-2000
Los Alamos	Rv	15	6.8-7.0	0.30	0.7-1.0	1500
Malibu Coast – Pt.Dume	LS	70	7.0-7.5	0.15	1.0-3.0	700-3000?
Mesa – Rincon – Lavigia	O-Rv-LS	10	6.5	0.30+	0.3-0.5?	1000-2000?
North Channel – Pitas Point	O-L-Rv	5	6.8-7.2	0.75+	1.0-3.0	300-1500
Offshore Oak Ridge	O-L-Rv	20	6.9-7.2	0.40+	1.6-3.0	400-1200
Onshore Oak Ridge	O-L-Rv	50	7.2-7.5	0.25	3.5-6.0	300-600
Ozena – South Cuyama	O-Rv?	50	6.8	0.15	?	?
Pine Mountain	LS?	50	7.0	0.20	1.5-3.5	500-1500
Pleito	Rv?	70	7.0-7.2	0.10	1.4-2.0	750-1470
Red Mountain	O-Rv	20	6.8-7.2	0.20–0.30+	0.9-3.5	510-870
San Andreas	RS	70	7.5-8.0	0.15-0.25	35	150-350
San Cayetano	O-Rv	63	6.8-7.3	0.17	3.6-5.6	200-600
Santa Cruz-Santa Catalina Ridge – San Clemente Island	RS	70	6.5-7.0	0.10	1.0-5.0	350-2000
Santa Cruz Is – Santa Rosa Is – Anacapa Island	LS	43	6.8-7.3	0.30	1.0-1.7	530-1200
San Gabriel	RS	90	7.0	0.10	1.0-5.0	1250
Santa Susana	O-Rv	100	6.8-7.3	0.10	4.3-7.0	630
Santa Ynez	O-R-LS	10-12	7.0-7.5	0.40-0.60	0.4-2.0	670-3200
Simi – Santa Rosa	O-Rv?	70	6.7-7.0	0.10	0.5-1.5	950
White Wolf	O-L-Rv	90	7.2-7.5	0.15	3.0-8.5	300-850

* LS – Left Slip; RS – Right Slip; O-L – Oblique-Left; O-R – Oblique-Right; Rv – Reverse.

TABLE 2

SEISMICITY AND INFERRED GROUND MOTIONS AFFECTING THE SANTA BARBARA AREA, 1812–1992.

Date	Magnitude	Location	Epicentral Peak Intensity Modified Mercalli Scale (MM)	Damage	Measured or Inferred Peak Acceleration (g)	Peak Acceleration at Santa Barbara (g)	Distance to Santa Barbara (km)
24 Mar. 1806	??	??	??	Damage to Mission Santa Barbara and the Royal Presidio.	??	0.05–0.10	??
21 Dec. 1812	7.1+	34°12'N 119°54'W Santa Barbara Channel?	X–XI	Destroyed La Purisima Mission (near Lompoc), severe damage to Santa Barbara Mission; tsunami.	0.60+	0.20–0.40	< 50
09 Jan. 1857	8.2+	35°42'N 120°18' San Andreas Fault	X+	Ruptured 300 km of the San Andreas fault; intensity VI-VII at Santa Barbara; >90 s of shaking.	0.80+	0.10+	60–190
27 July to 12 Dec. 1902	6.0?	34°44'N 120°17'W near Los Alamos	VIII–X	Several earthquakes that totally destroyed Los Alamos; drove population away.	0.40–0.50	0.05	60
29 June 1925	6.3	34°18'N 119°48W Santa Barbara	VIII-IX	Estimated $6–20 million, 80% of commercial buildings in Santa Barbara damaged or destroyed.	0.50–0.60	0.40–0.60	< 3
29 June 1926	5.5?	34°18'N 119°48'W Santa Barbara	VIII	Moderate damage to downtown Santa Barbara. Late aftershock of 1925 earthquake.	0.30	0.20	< 3
04 Nov. 1927	7.3	34°42'N 120°48'W off Pt. Arguello	VIII+	Tsunami (2 m) generated along coast; slight damage reported in Santa Barbara.	0.60+	0.10	100
30 June 1941	5.9	34°20'N 119°38'W offshore Carpenteria	VII	$100,000 damage to downtown Santa Barbara.	0.40–0.50	0.10	10
21 July 1952	7.7	35°00'N 119°01'W Kern County	XI	$400,000 damage to downtown Santa Barbara; reported liquefaction effects along Laguna Street.	0.80+	0.15	85
05 July 1968	5.2	34°07'N 119°42'W Santa Barbara Channel	VI	Earthquake swarm; largest event caused about $12,000 damage in Santa Barbara-Goleta.	0.20	0.07–0.10	15
13 Aug. 1978	5.9	34°24'N 119°41'W off Goleta Point	VII-VIII	$7.3 million in damage, chiefly to UCSB campus.	0.44	0.28	< 5

Table 3

Well-Documented Tsunamis within or near the Santa Barbara Channel

Date	Source	Comments
21 Dec. 1812	Tectonic uplift or submarine slide within the channel caused by the 1812 earthquake	The size of this event is uncertain, but may have been substantial. Some question whether a tsunami occurred at all, although reports of a tsunami extend from Gaviota to Ventura. See Lander et al. (1993), Marine Advisors (1965), Sylvester (1978), and McCulloch (1985).
31 May 1854	Submarine slide (?) within the channel following a moderate earthquake	One report of a heavy swell in Santa Barbara following an earthquake (Trask, 1856; Lander et al., 1993)
10 May 1877	M 8.3 earthquake off coast of Chile	Report of ocean rising and falling 12 feet at Gaviota, western Santa Barbara Channel (Lander et al., 1993).
4 Nov. 1927	M 7.2 earthquake west to northwest of the Santa Barbara Channel	Produced a tsunami reported up to 6 feet in height along the western shore of Santa Barbara County (Byerly, 1930; Satake and Sommerville, 1992; Lander et al., 1993). No reports of a tsunami within the channel.
30 Aug. 1930	M 5.2 earthquake near Santa Monica Bay; probable submarine slide	20-foot waves produced at Santa Monica, Venice, and Redondo Beach; one fatality (Lander et al., 1993). No reports of a tsunami within the channel.
3 Oct. 1931	M 7.9 Solomon Islands earthquake	1.5 inch marigram recorded in Santa Barbara (Lander et al., 1993).
2 Mar. 1933	M 8.3 earthquake off coast of Japan	2 to 3 inch marigram at Santa Barbara (Lander et al., 1993).
1 April 1946	M 7.8 earthquake at the Aleutian Islands	Produced a 6-foot range in water height at Santa Barbara and was also noticed at Ventura and Carpinteria. (Lander et al., 1993).
22 May 1960	M 8.6 earthquake off coast of Chile	Nine-foot range in water height; twelve boats broke loose at Santa Barbara, causing some damage (Lander et al., 1993).
28 Mar. 1964	M 8.4 earthquake, Prince William Sound, Alaska	Five-foot swells; minor damage (Lander et al., 1993).

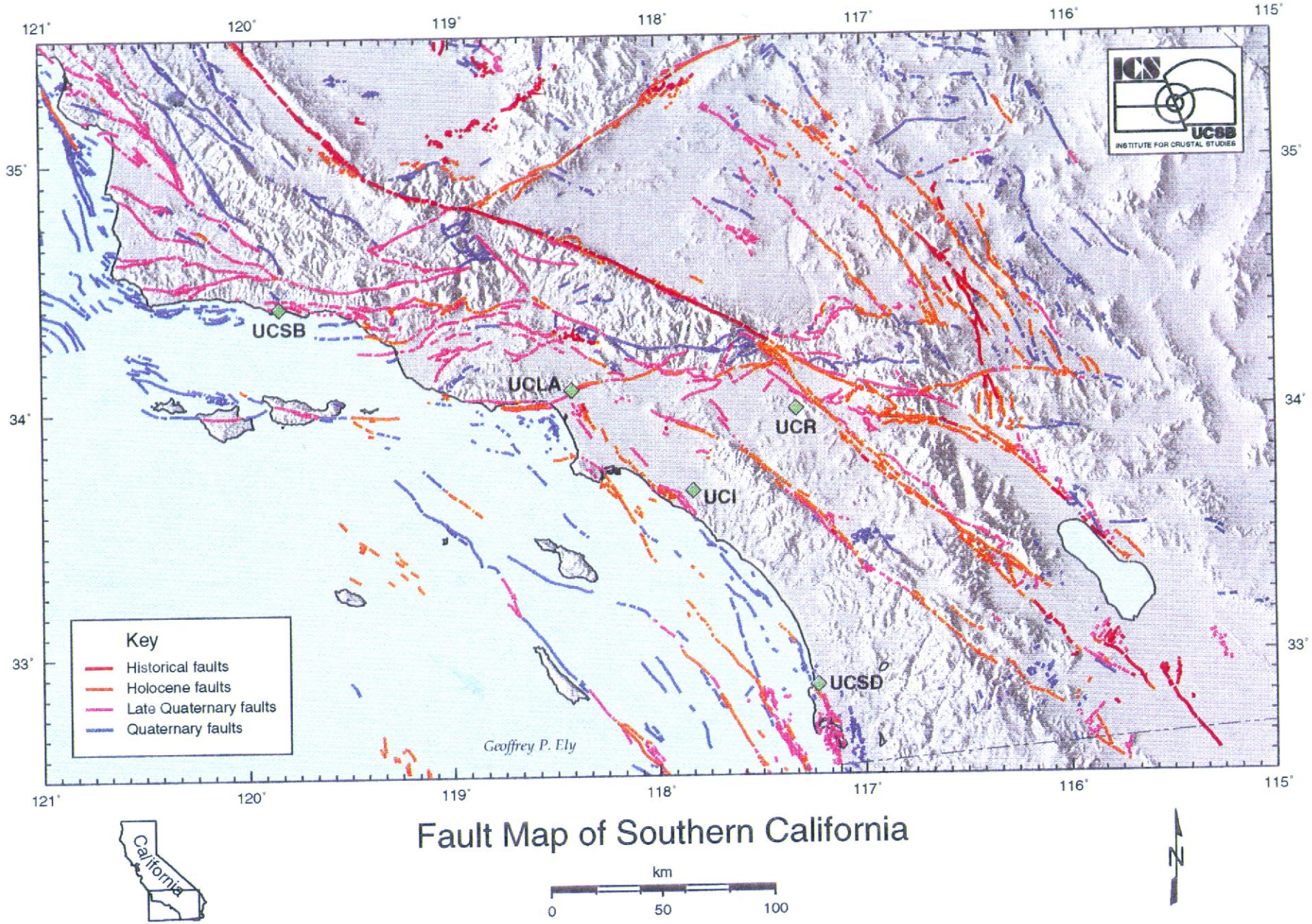

Figure 1. Active fault map of southern California (CDMG, 1994) showing UC campus locations.

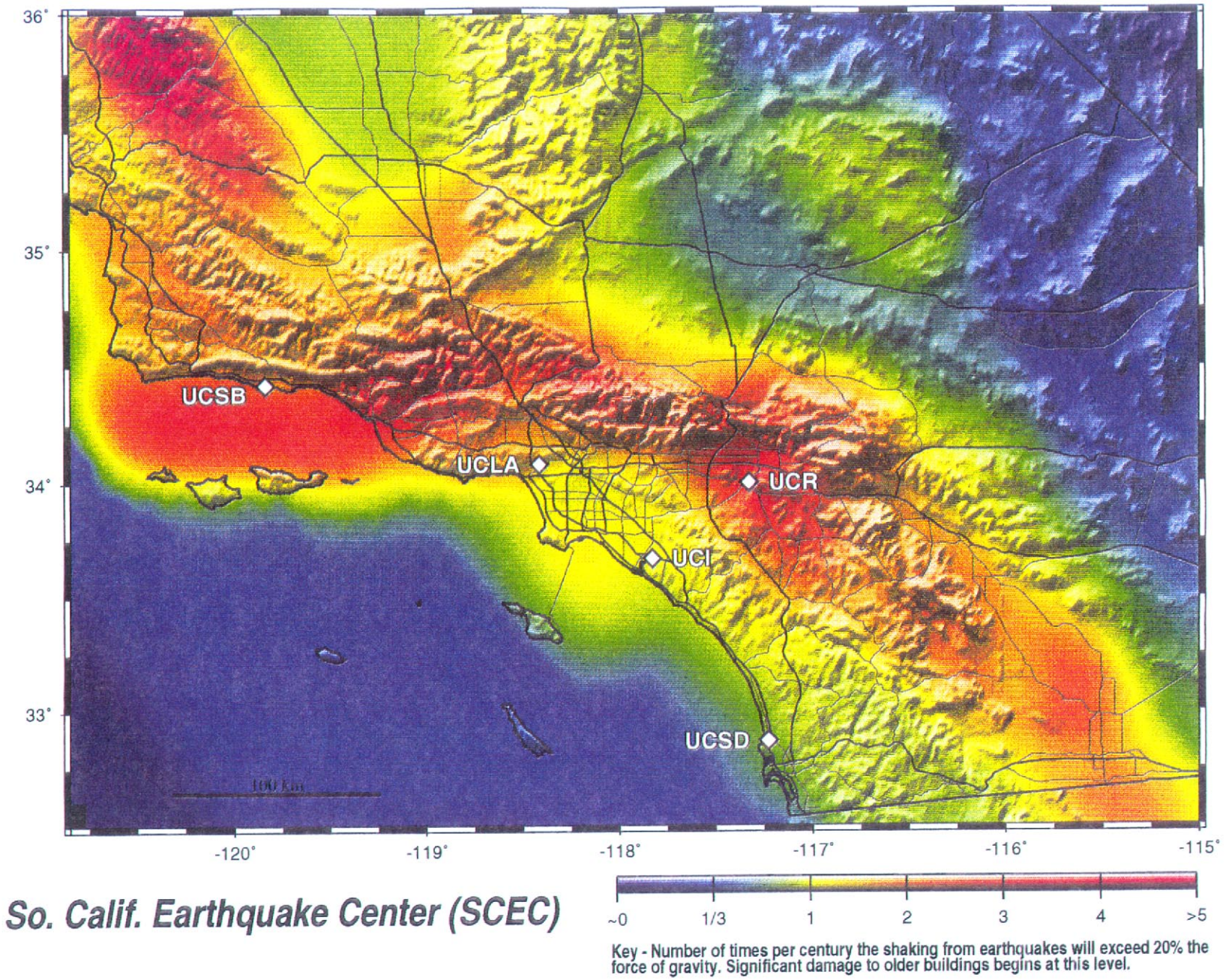

Figure 2. Probability of exceedence of 0.2g in 50 years for southern California, as determined by SCEC (Jackson et al., 1995).

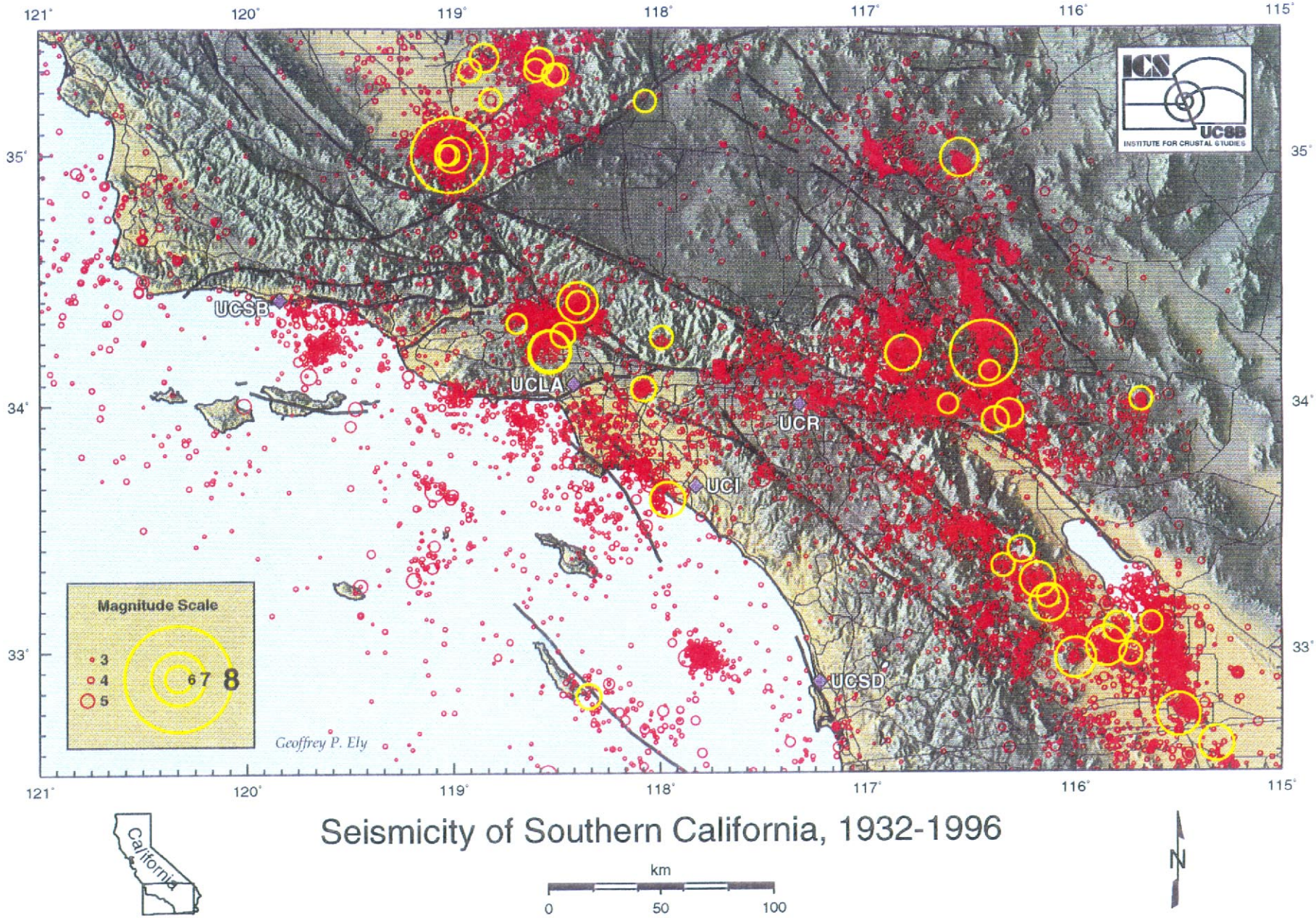

Figure 3. Seismicity of southern California (1932-1996). Data provided by SCEC.

Figure 4. UC Santa Barbara campus showing locations of Engineering I, Broida, Webb, seismic refraction profiles (red lines), seismic stations (triangles), CPT sites (circles), and the CLC deep drill site (square).

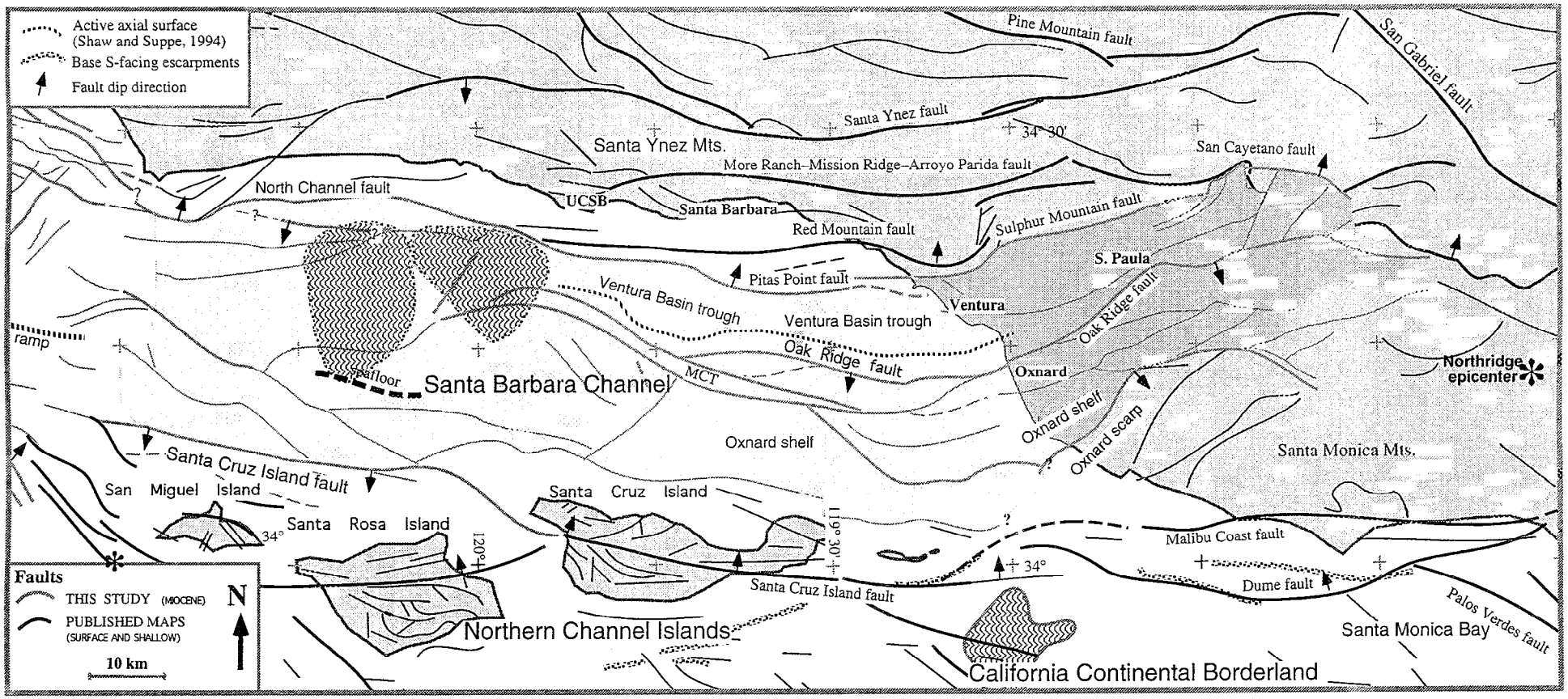

Figure 5. Regional fault map of the western Tranverse Ranges region (Sorlien, 1995).

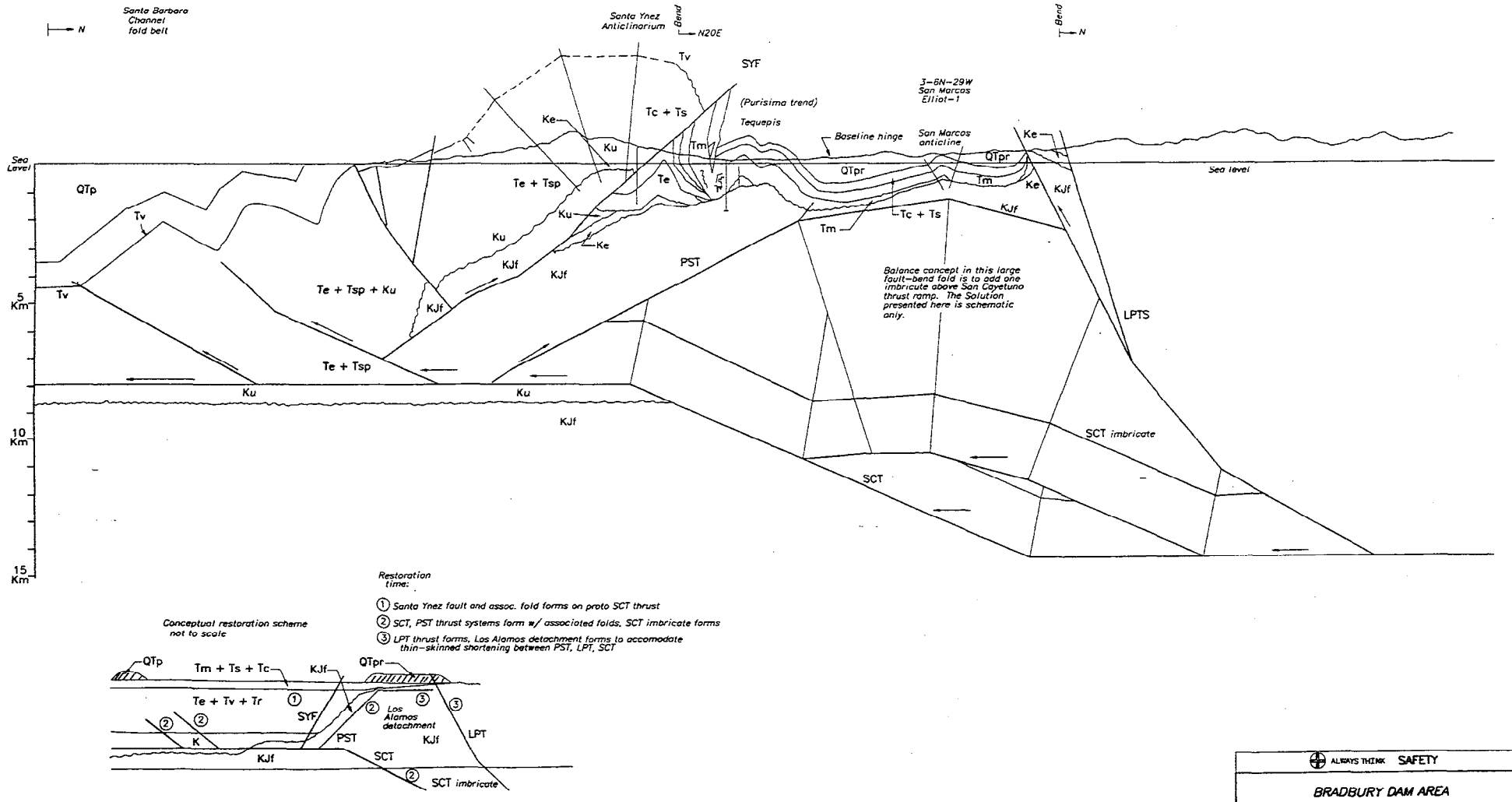

Figure 6. Revised 2D fault-propagation fold model of the western Tranverse Ranges region (Anderson, 1993). Geology modified from Namson and Lettis (1993). SCT – San Cayetano thrust.

Geologic Map of the Santa Barbara-Goleta-Carpinteria Area

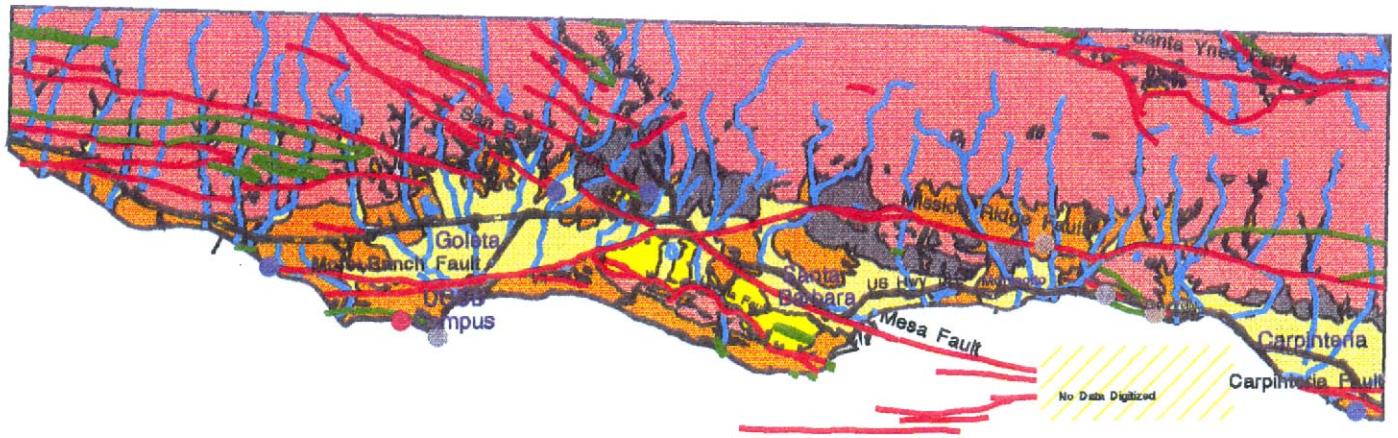

Legend

Geologic Structures
- Folds
- Faults

Geology
- Qbs
- Qal
- Qls
- Qg
- Qoa
- Qog
- Qca
- Qsb
- Qsbp
- Pre-Quaternary

Study Sites
- Fault Exposure
- Fossil Locality
- Geomorphic Feature
- Wavecut Platform

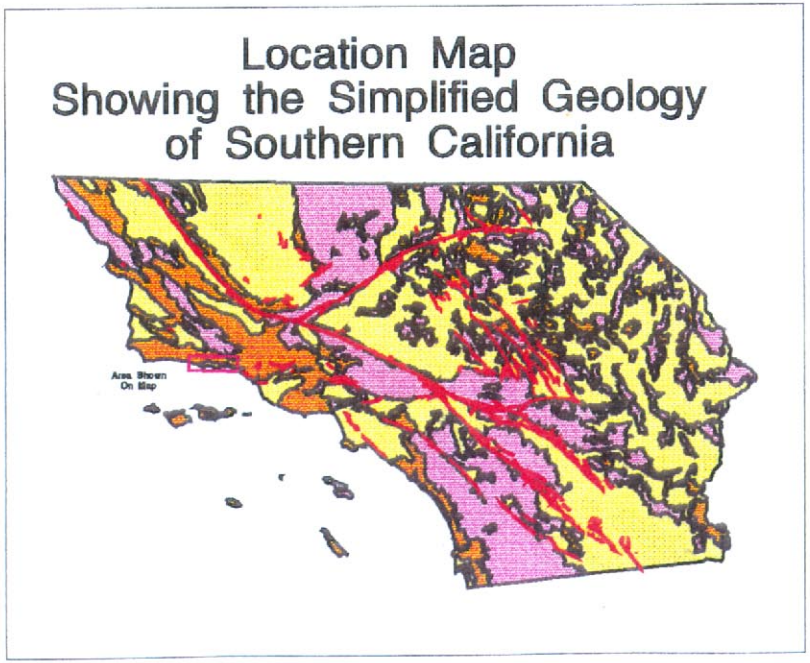

N

- Stream
- Streets

5 0 5 10 15 Kilometers

5 0 5 10 Miles

Figure 7. Location map (insert) and regional GIS geologic map of the Santa Barbara-Goleta-Carpenteria area (Gurrola et al., 1996).

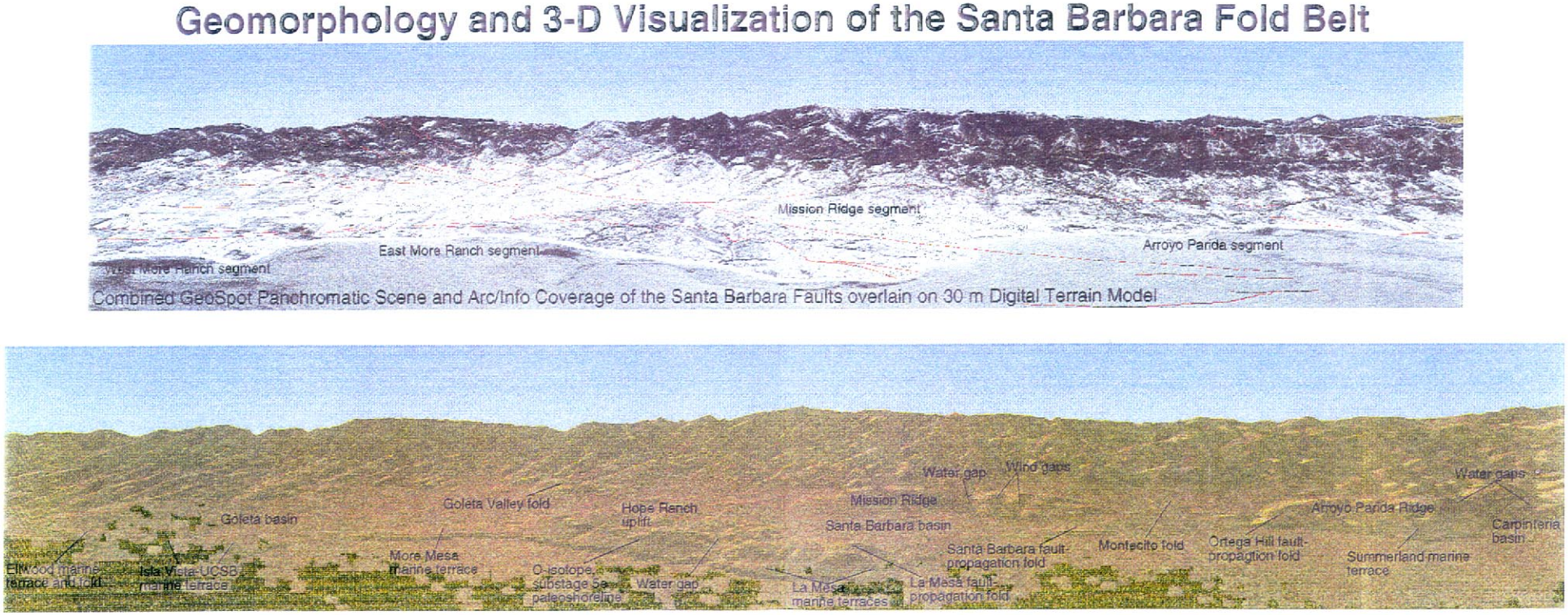

Tectonic geomorphology of the Santa Barbara Fold Belt. View is looking north towards the Santa Ynez Mountains. Coastal coverage is approximately 30 km with no vertical exaggeration. Mapping by Larry D. Gurrola and Tom Dibblee, Jr. All visualizations created in Erdas Imagine at the UCSB Map and Imagery Library by David Valentine.

Figure 8. 3D perspective of the Santa Barbara fault and fold belt geomorphology (Gurrola, 1996).

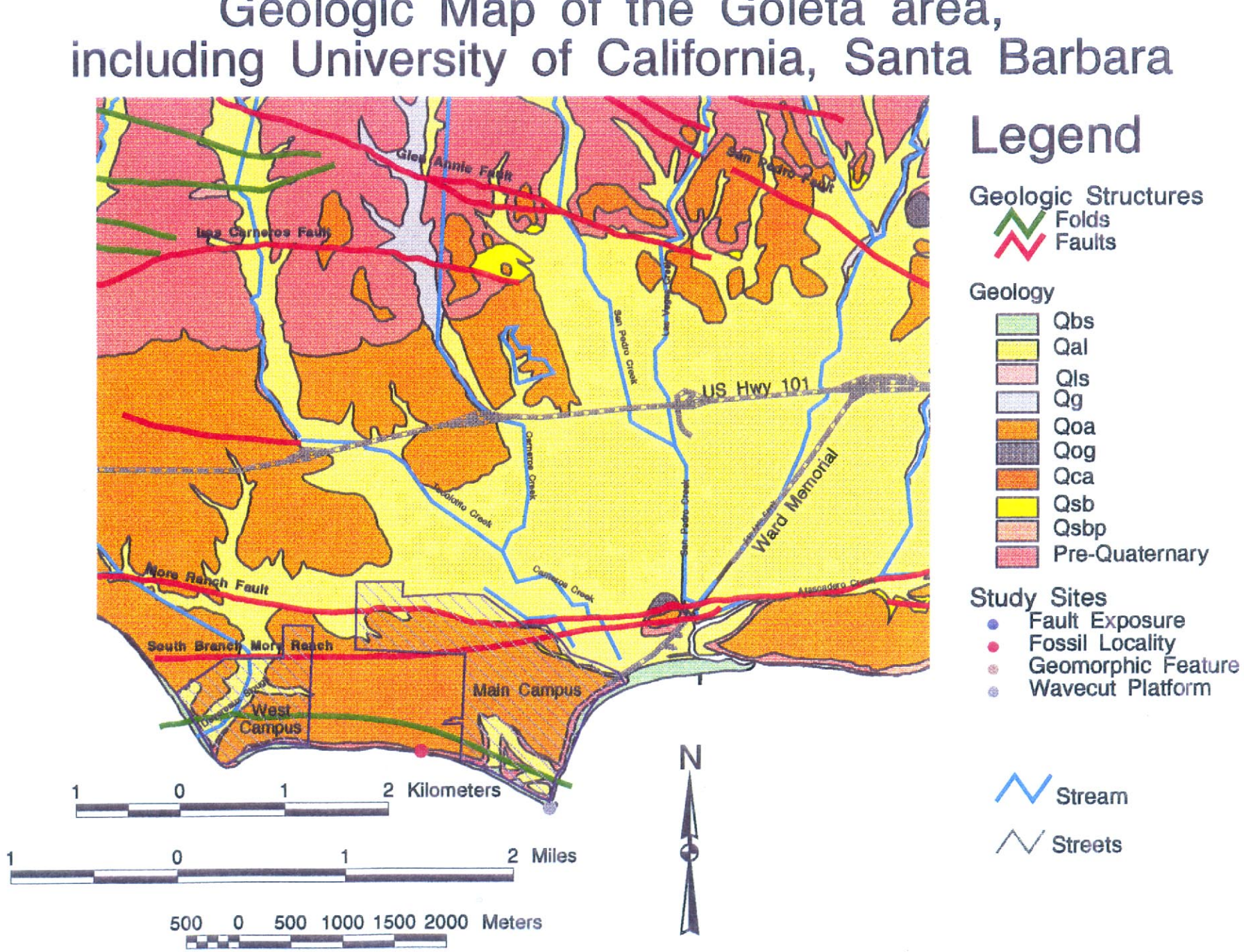

Figure 9. Local GIS geologic map of the Goleta-UCSB campus region (Gurrola et al., 1996).

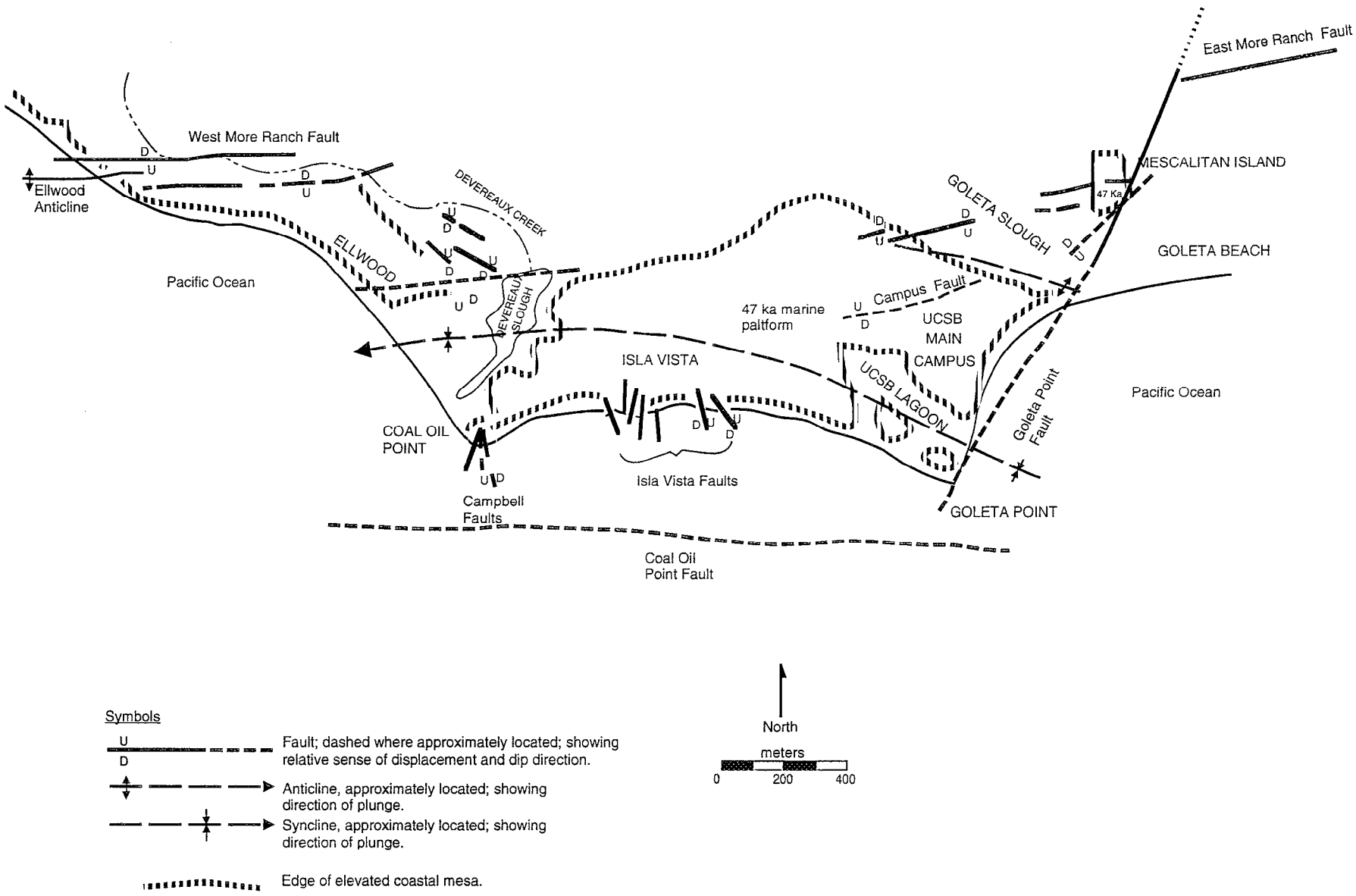

Figure 10. Local tectonic structure map of the UCSB campus region (Gurrola, 1996).

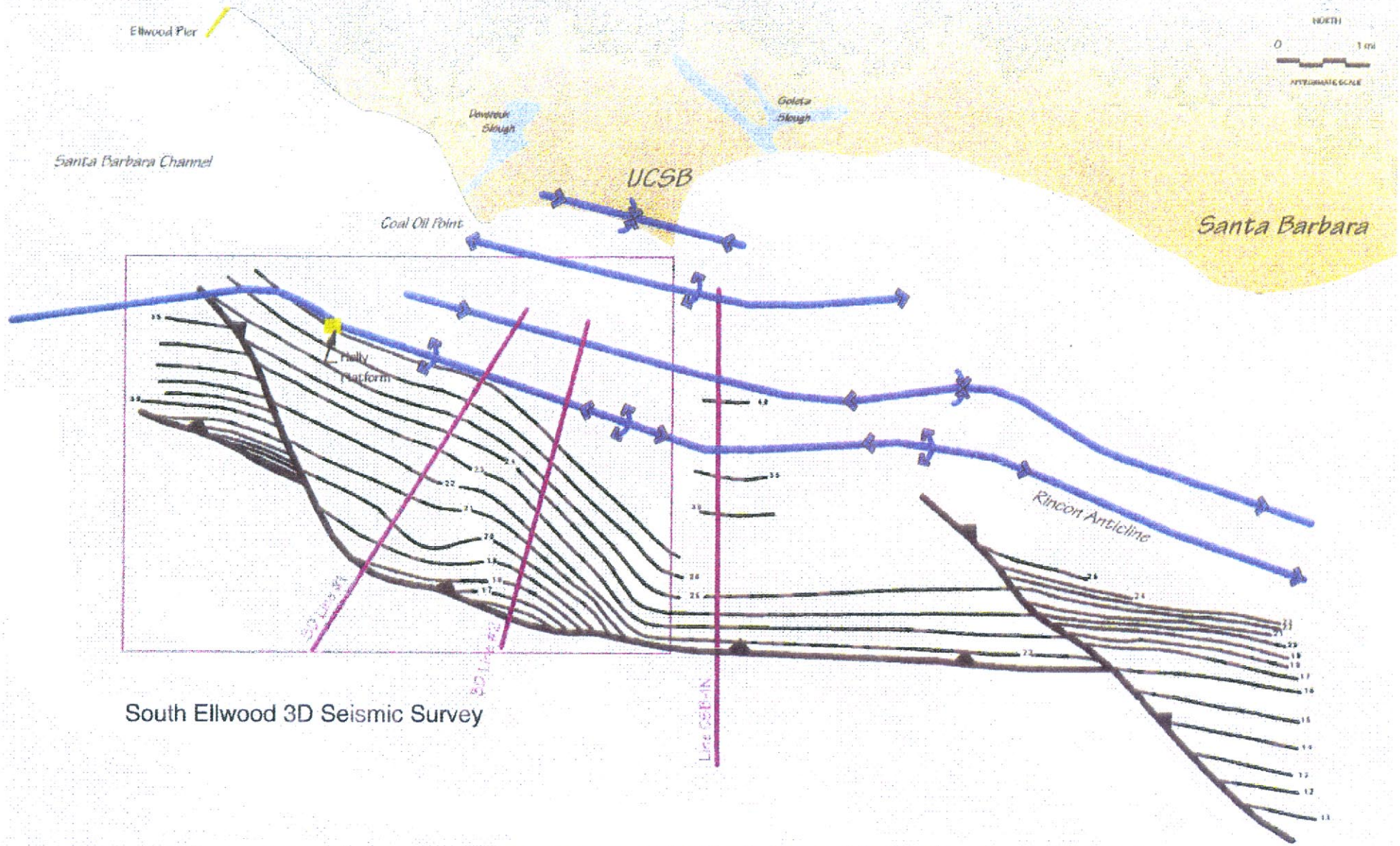

Figure 11. Two-way travel-time structure contour map of the North Channel fault (Hornafius et al., 1995).

Two-Way Time Structure Map on the North Channel Fault

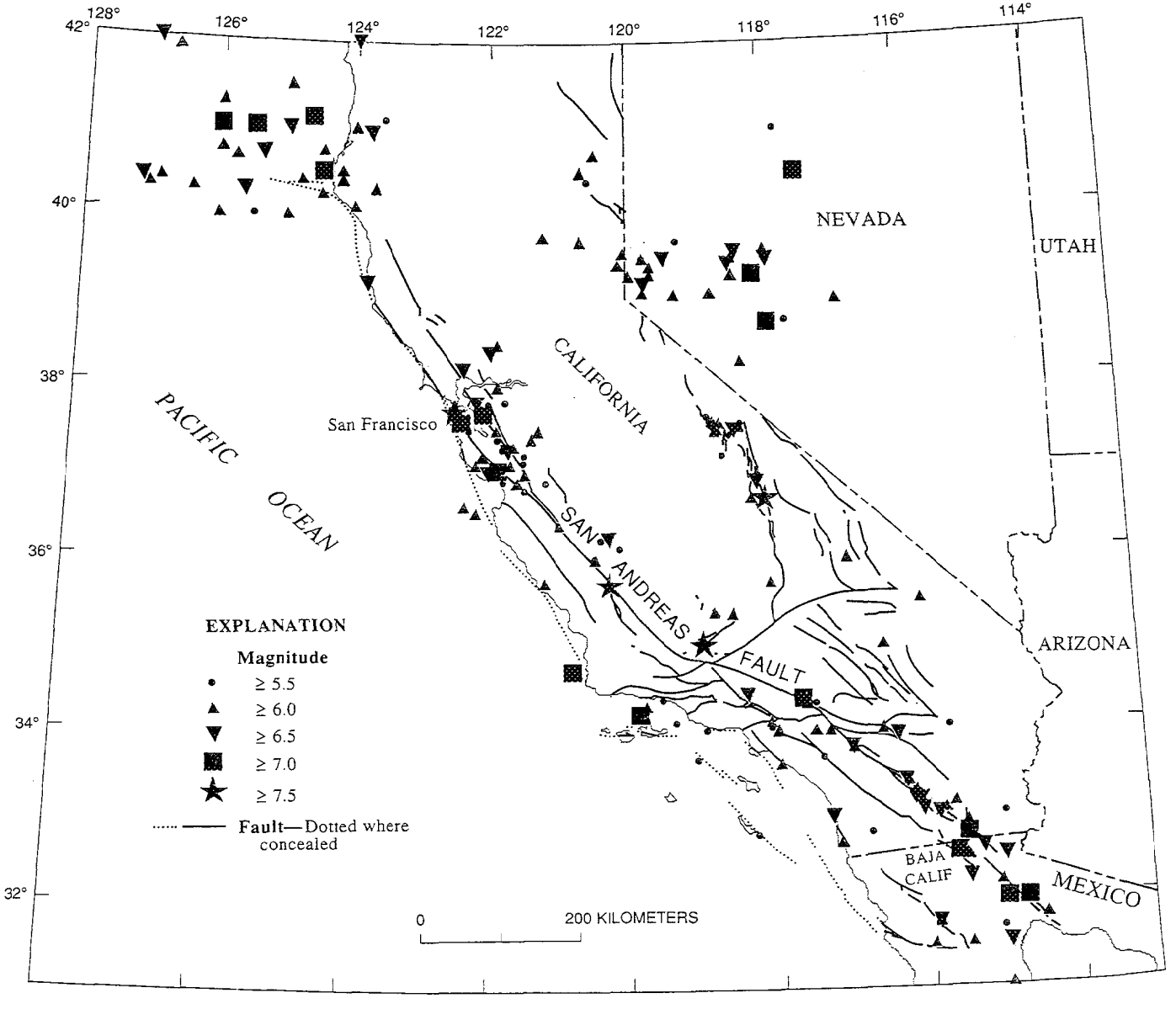

Figure 12. Historical seismicity in California, Nevada and northern Baja California (1769–1989). Earthquake symbols and size scale with magnitude (Ellsworth, 1990).

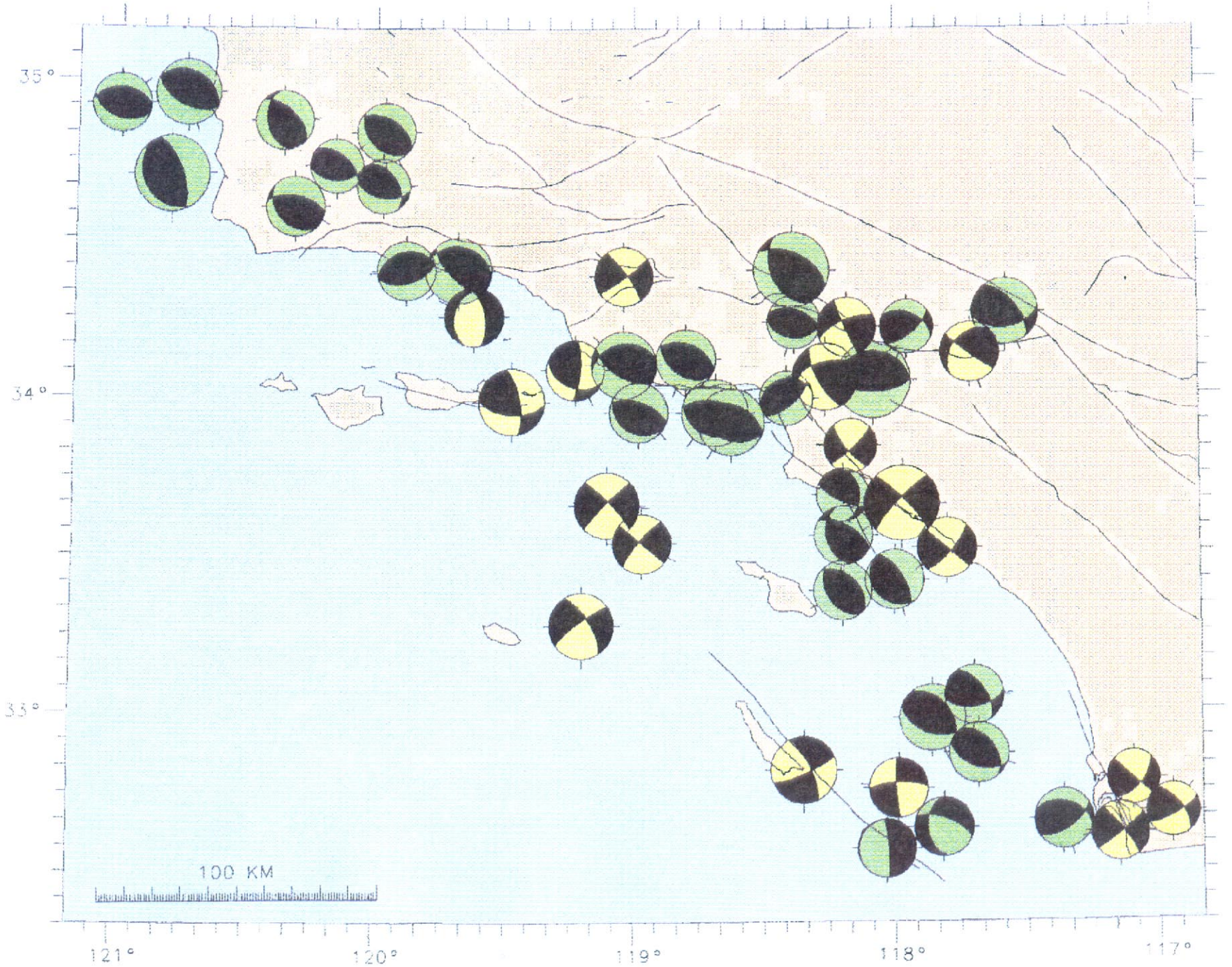

Figure 13. Significant earthquake focal mechanisms along coastal California (1927-1988) [Nicholson and Crouch, 1989]. Focal mechanisms are color coded according to faulting type: green (reverse to oblique-reverse); yellow (strike-slip to normal).

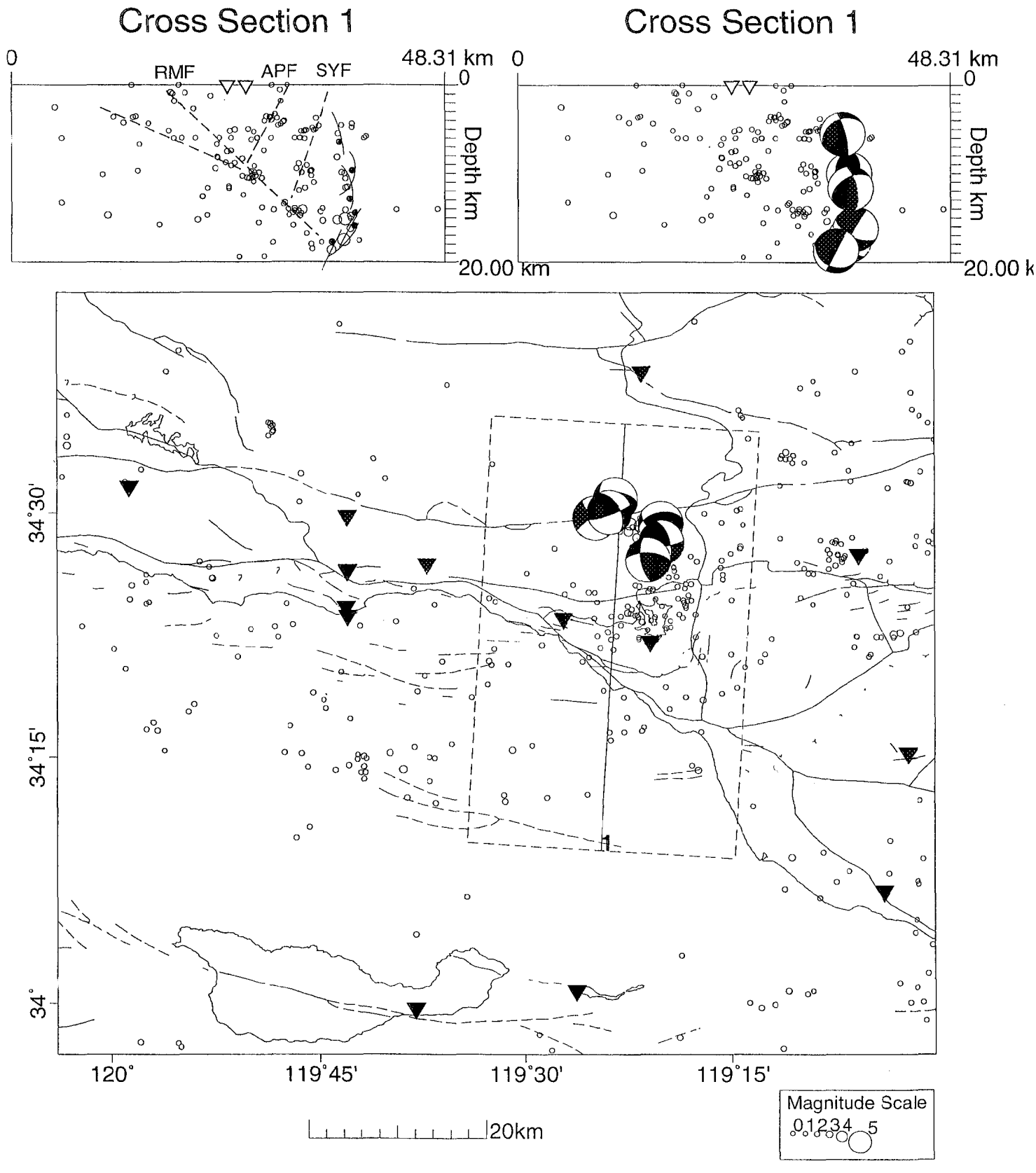

Figure 14. Map and cross sections of recent seismicity (1994-1996) in the Santa Barbara-Ventura area and the 1996 M4.1 Ojai Valley earthquake sequence. Focal mechanisms are upper-hemisphere projection in map view and front-projection in cross section. Seismicity appears to be closely associated with the Red Mountain (RMF), Arroyo Parida (APF) and Santa Ynez faults (SYF). Aftershocks of the Ojai earthquake define a curviplanar fault in the footwall of the SYF whose projection would also coincide with the approximate surface trace of the Santa Ynez fault.

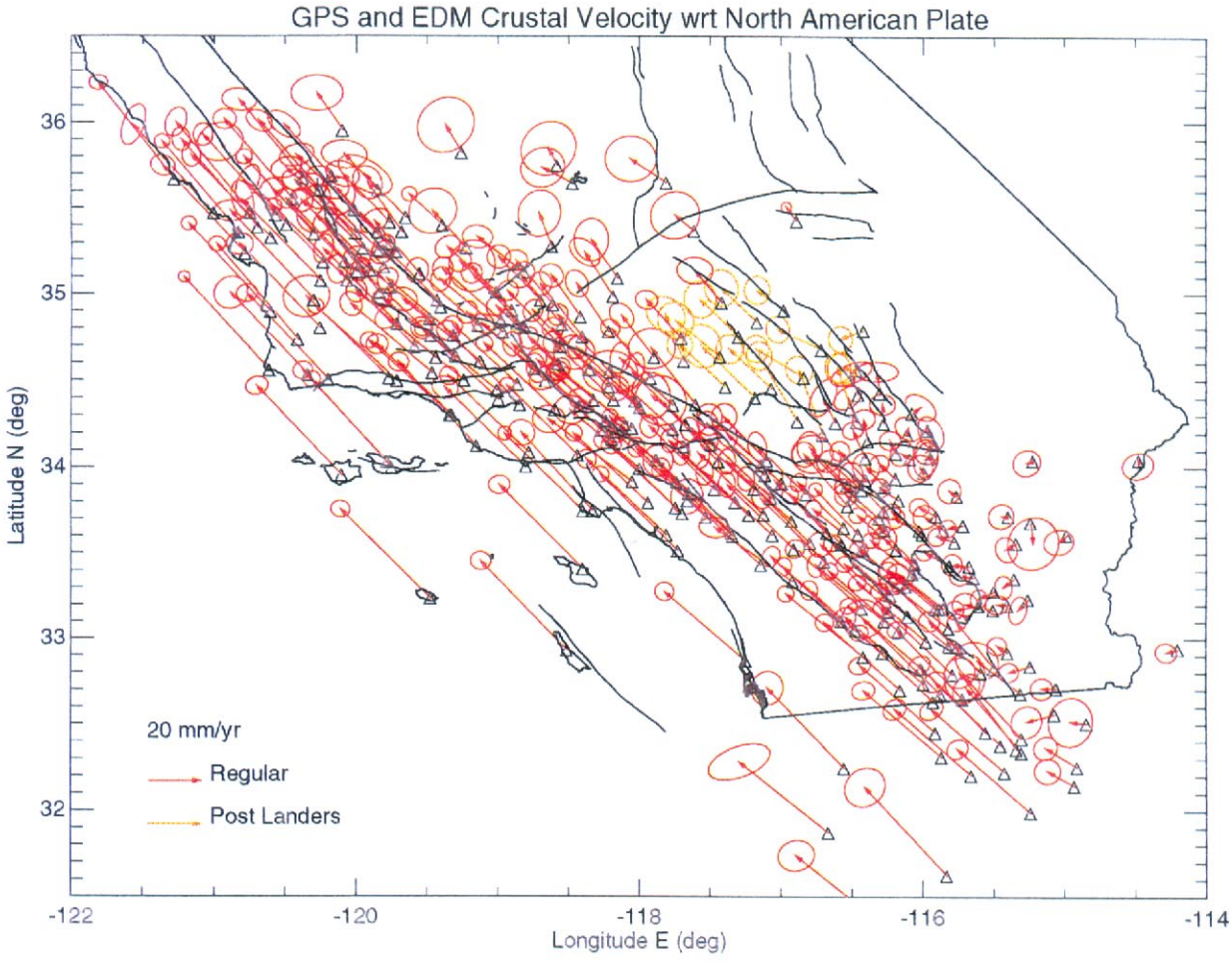

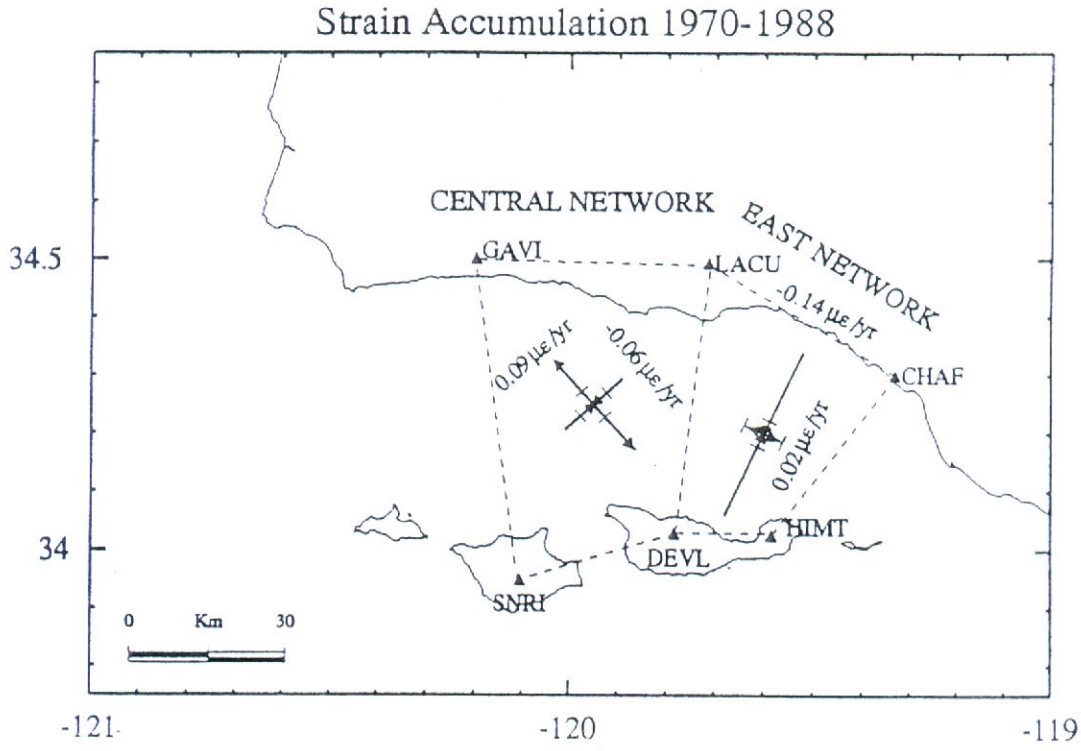

Figure 15 (top) Geodetic velocity field (1988-1996) determined using GPS. Velocity map provided by SCEC (Jackson et al., 1996). (bottom) Principal horizontal strain fields in the central and eastern Santa Barbara Channel (1970-1988) (Larsen et al., 1993).

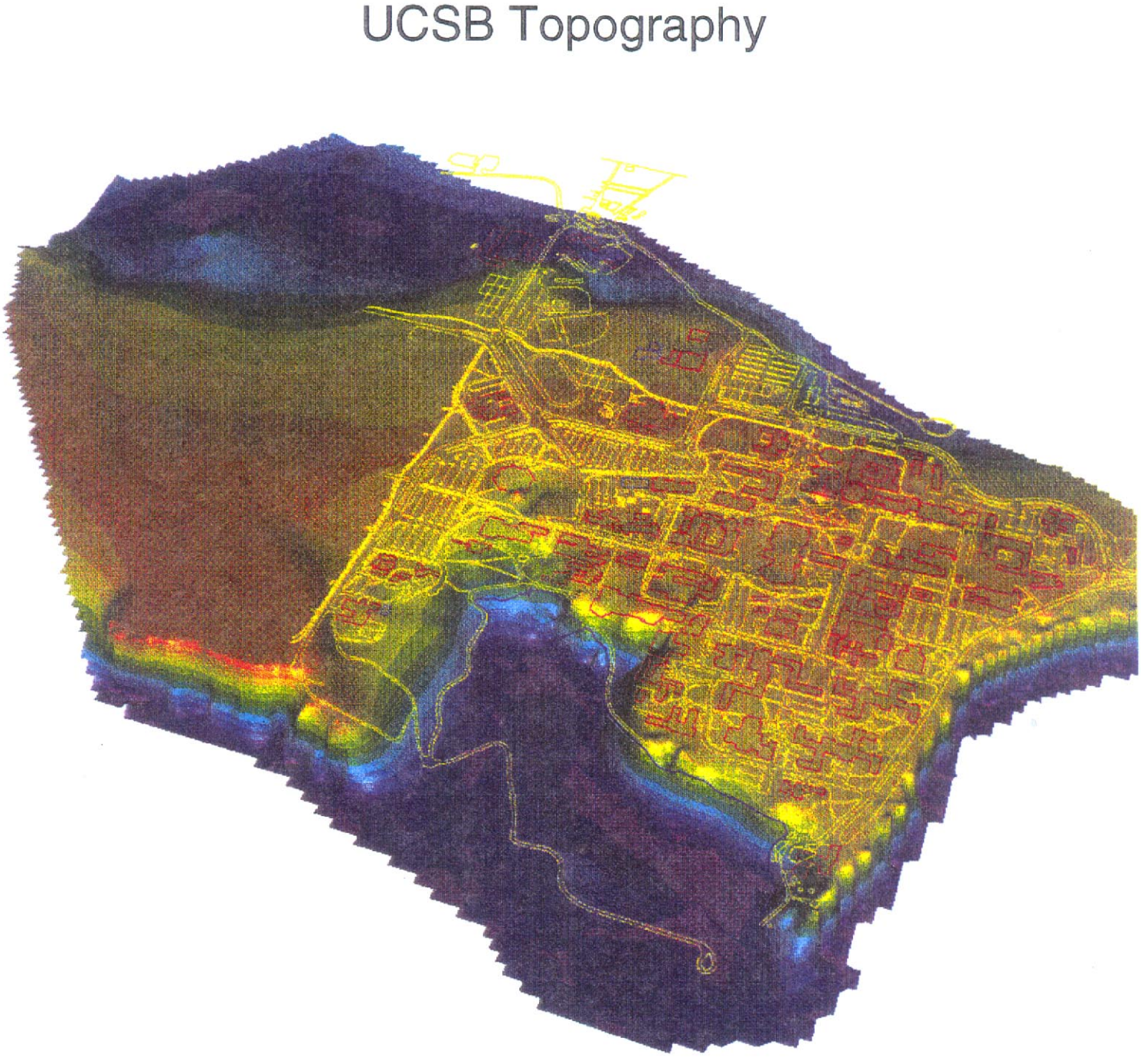

Figure 16. 3D perspective of the UCSB campus overlaid on topography. Figure provided courtesy of Jeff Wagoner (LLNL). Campus map data provided by Bill Hanna (UCSB).

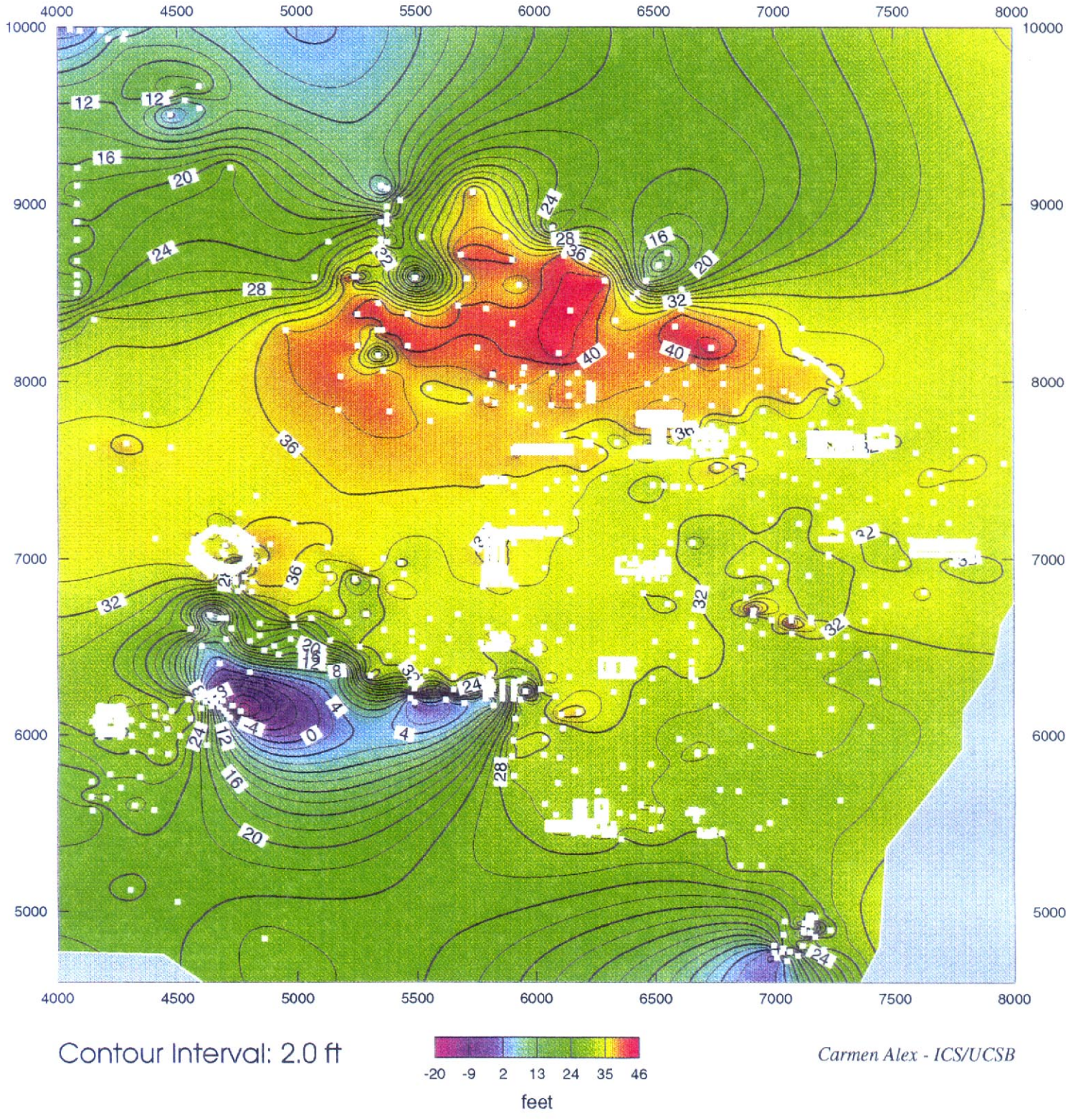

Figure 17. Structure contour map of the uplifted marine terrace (~47 ka) beneath the UCSB campus. Locations of boreholes are shown in white. Borehole data provided courtesy of Bill Hanna (UCSB).

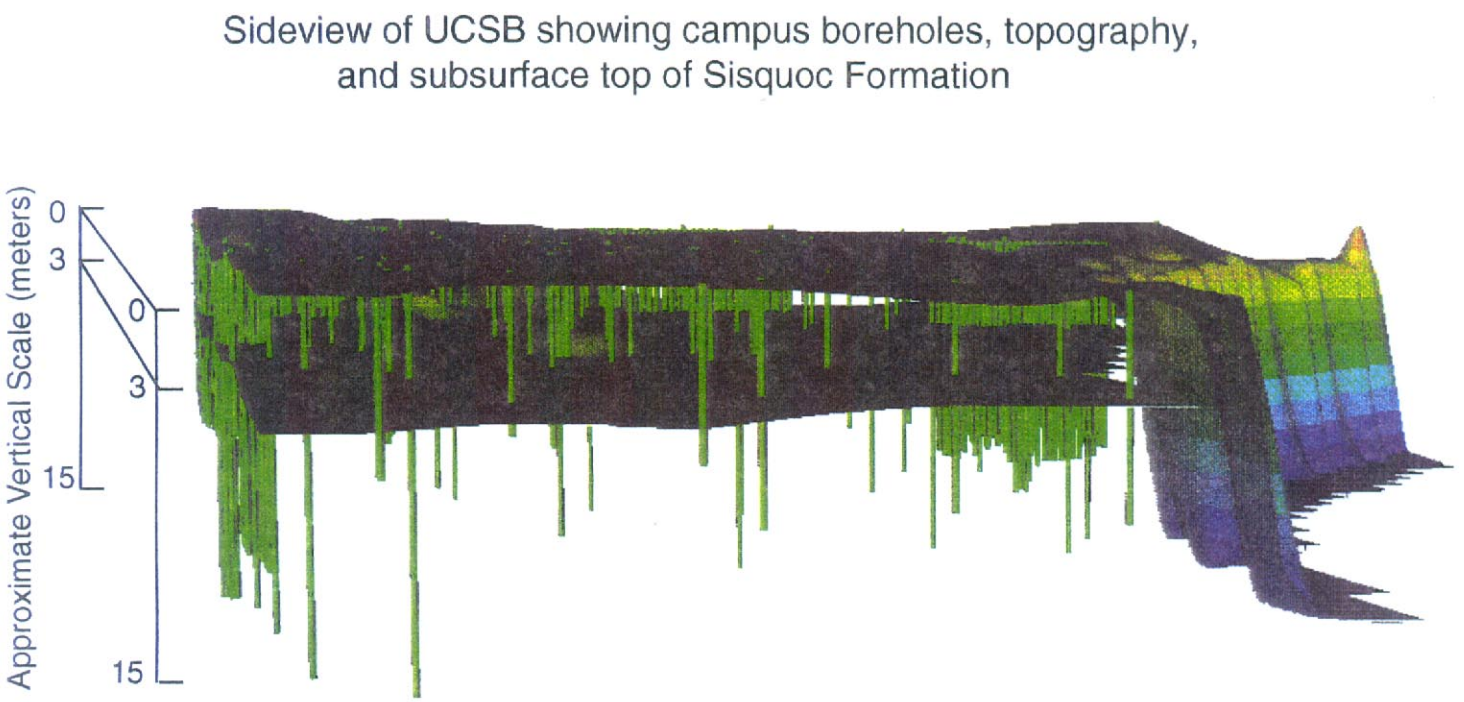

Figure 18. 3D perspective (sideview) of the UCSB campus showing surface topography, campus boreholes, and the top of the Sisquoc Formation structure contour suface. Figure courtesy of Jeff Wagoner (LLNL). Borehole data provided courtesy of Bill Hanna (UCSB).

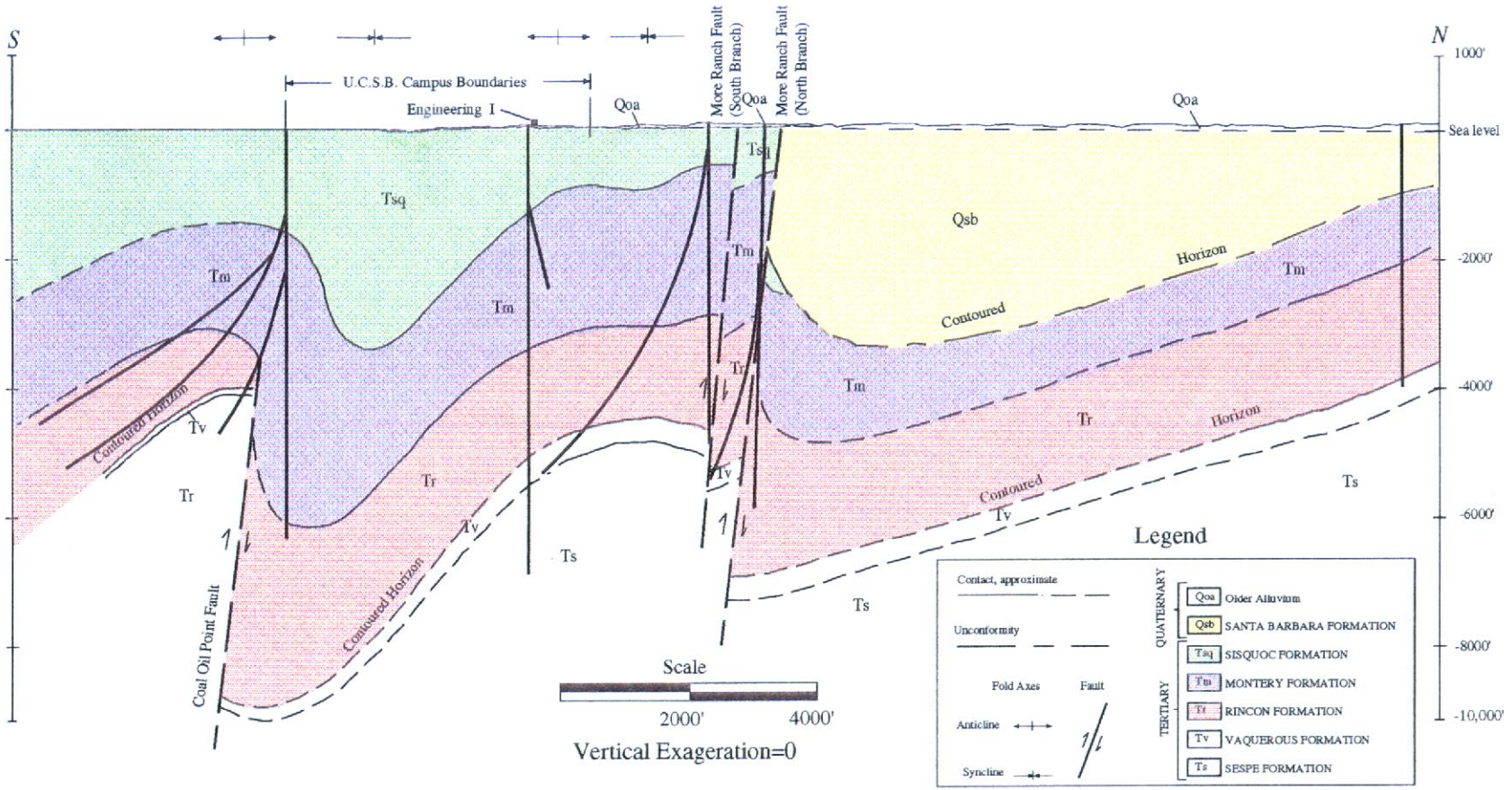

Figure 19. Vertical cross section (Olson, 1982) showing well control through the UCSB campus site.

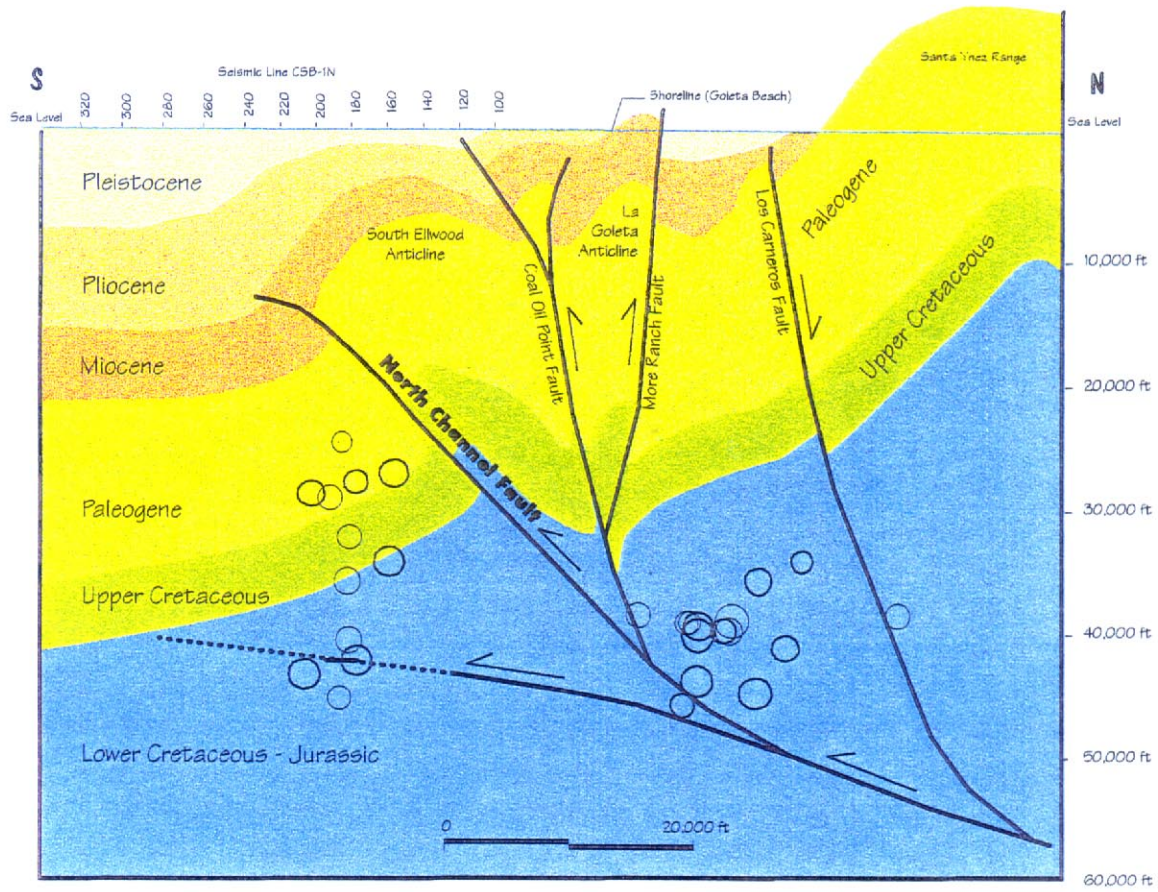

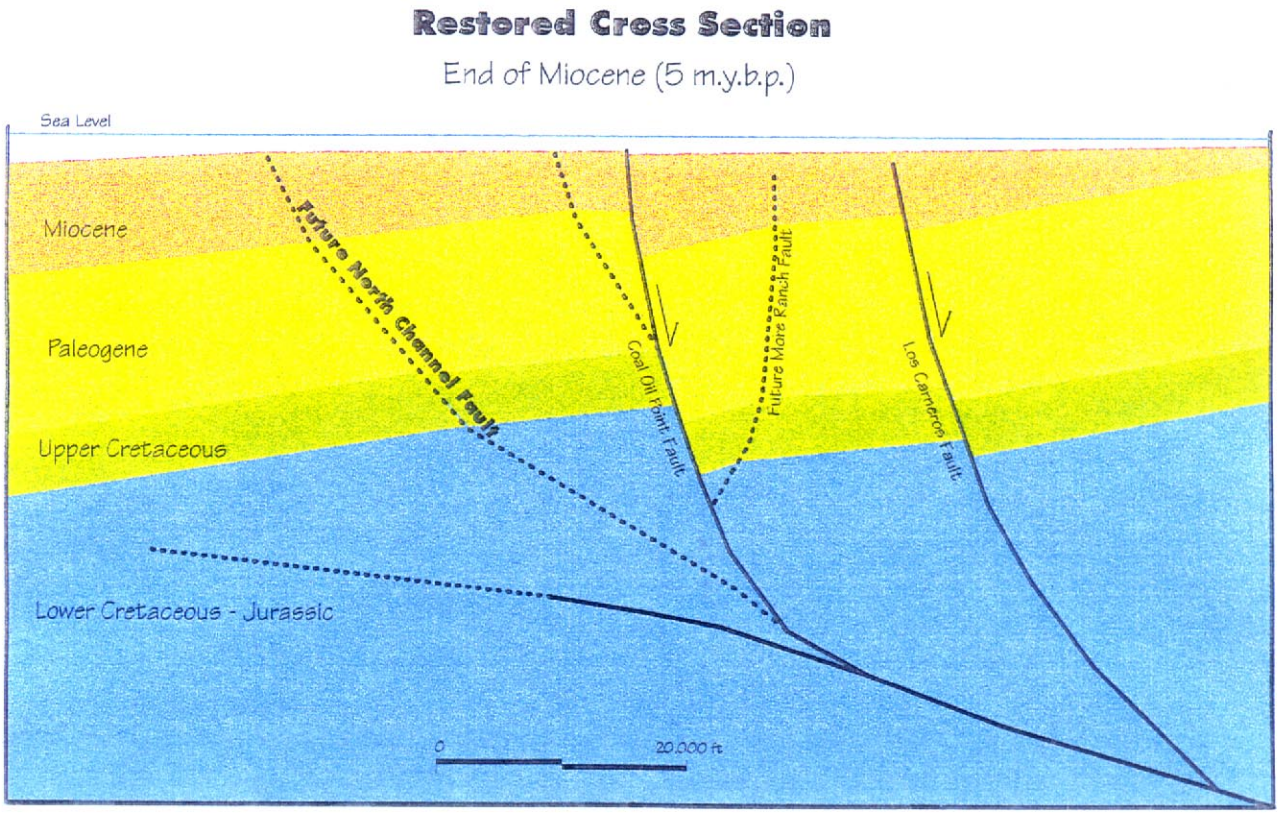

Figure 20. Vertical and restored cross sections (Hornafius et al., 1995) through the UCSB campus site.

Figure 21. (top) Trench excavated across More Ranch fault to evaluate slip rates

Figure 21. (bottom) UCSB students conducting shallow S-wave refraction studies next to Engineering I.

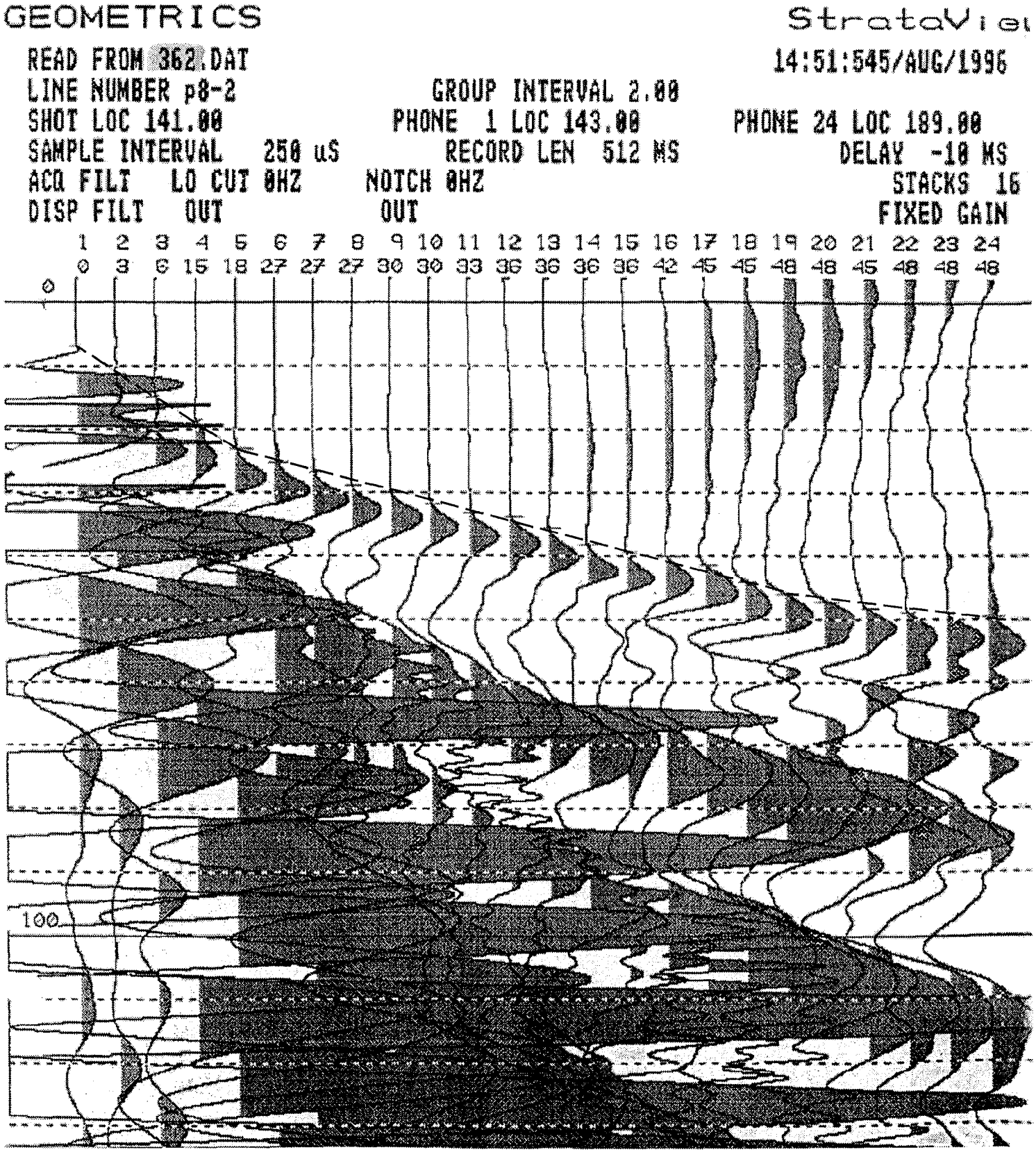

Figure 22. Example of 24-channel shallow P-wave refraction data recorded at UCSB. Three refracting horizons are clearly discernable from the first-arrival times: (1) a shallow layer about 5 m thick with velocity of 450 m/s; (2) an intermediate layer of about 1400 m/s that is about 15 m thick; and (3) a poorly resolved faster horizon at depth that may have velocities of 1800-2000 m/s.

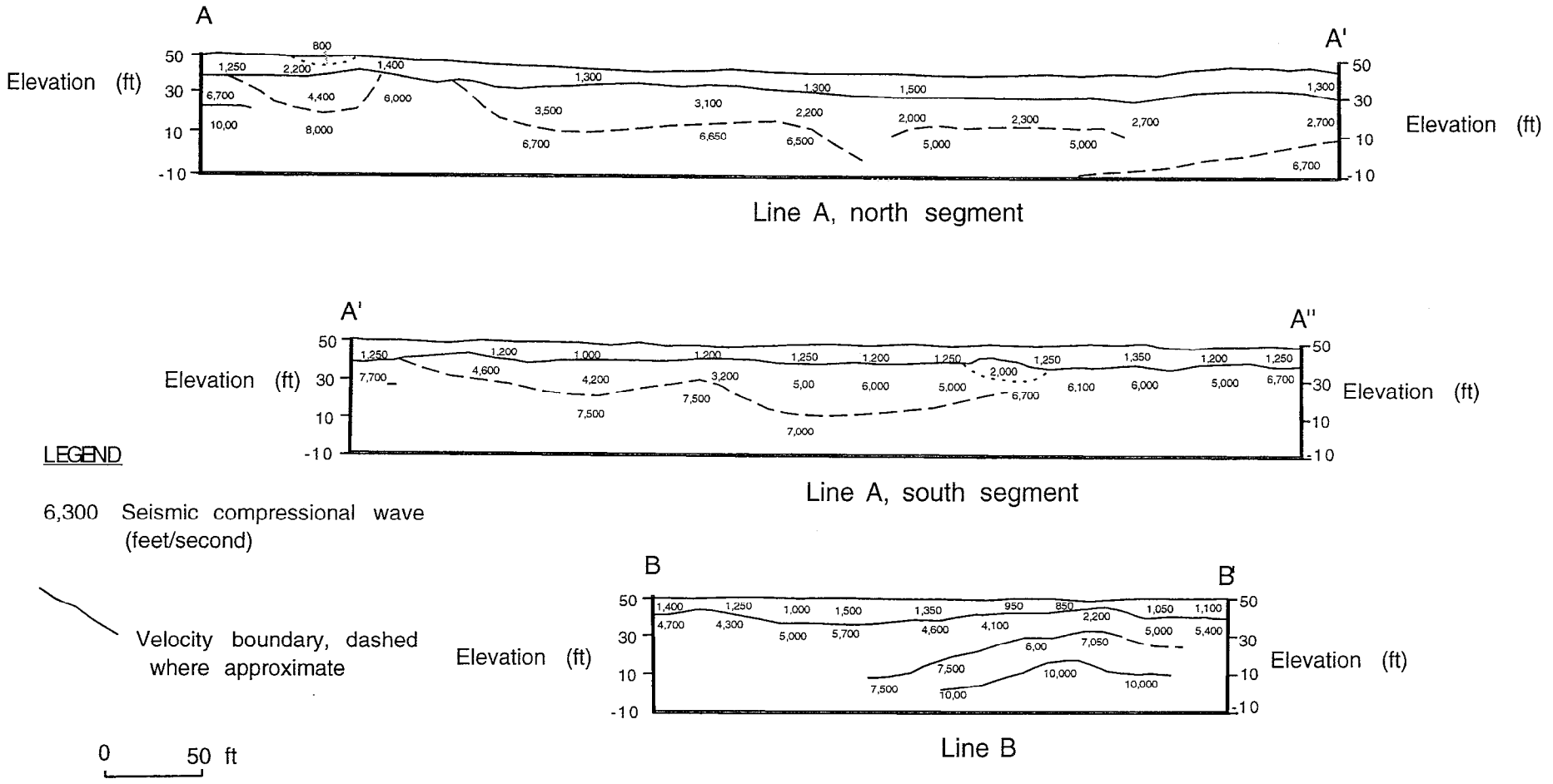

Figure 23. Simple 2D P-wave velocity model cross sections from shallow refraction studies near the UCSB Recreation Center.

Figure 24. (top) Cone-penetration test (CPT) truck in operation at UCSB adjacent to Woodhouse Laboratory.

Figure 24. (bottom) Drilling rig in operation at UCSB adjacent to Webb Hall. Two deep (~75 m) boreholes were made.

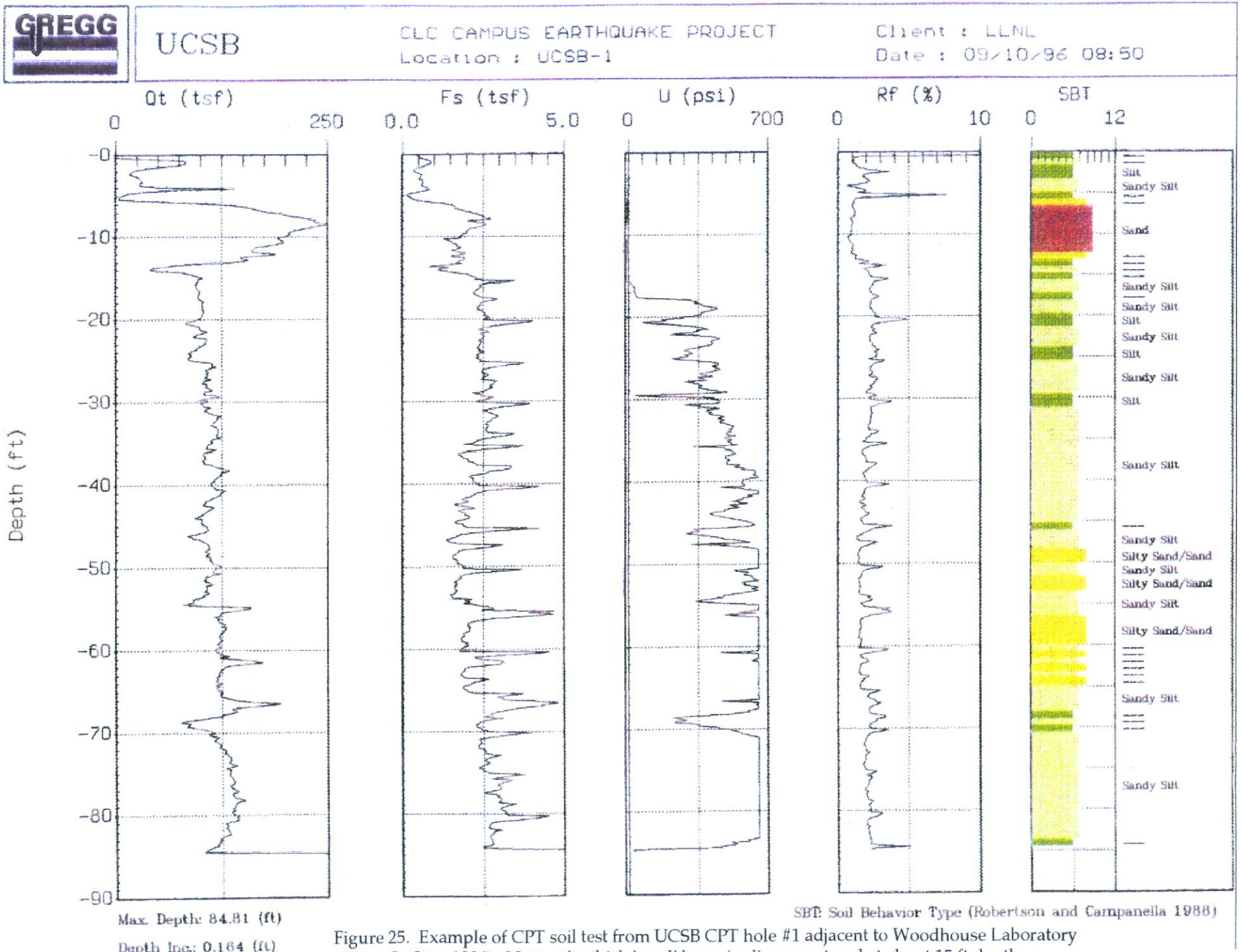

Figure 25. Example of CPT soil test from UCSB CPT hole #1 adjacent to Woodhouse Laboratory (Gregg In Situ, 1996). Notice the thick 'sand' layer (red) encountered at about 15 ft depth.

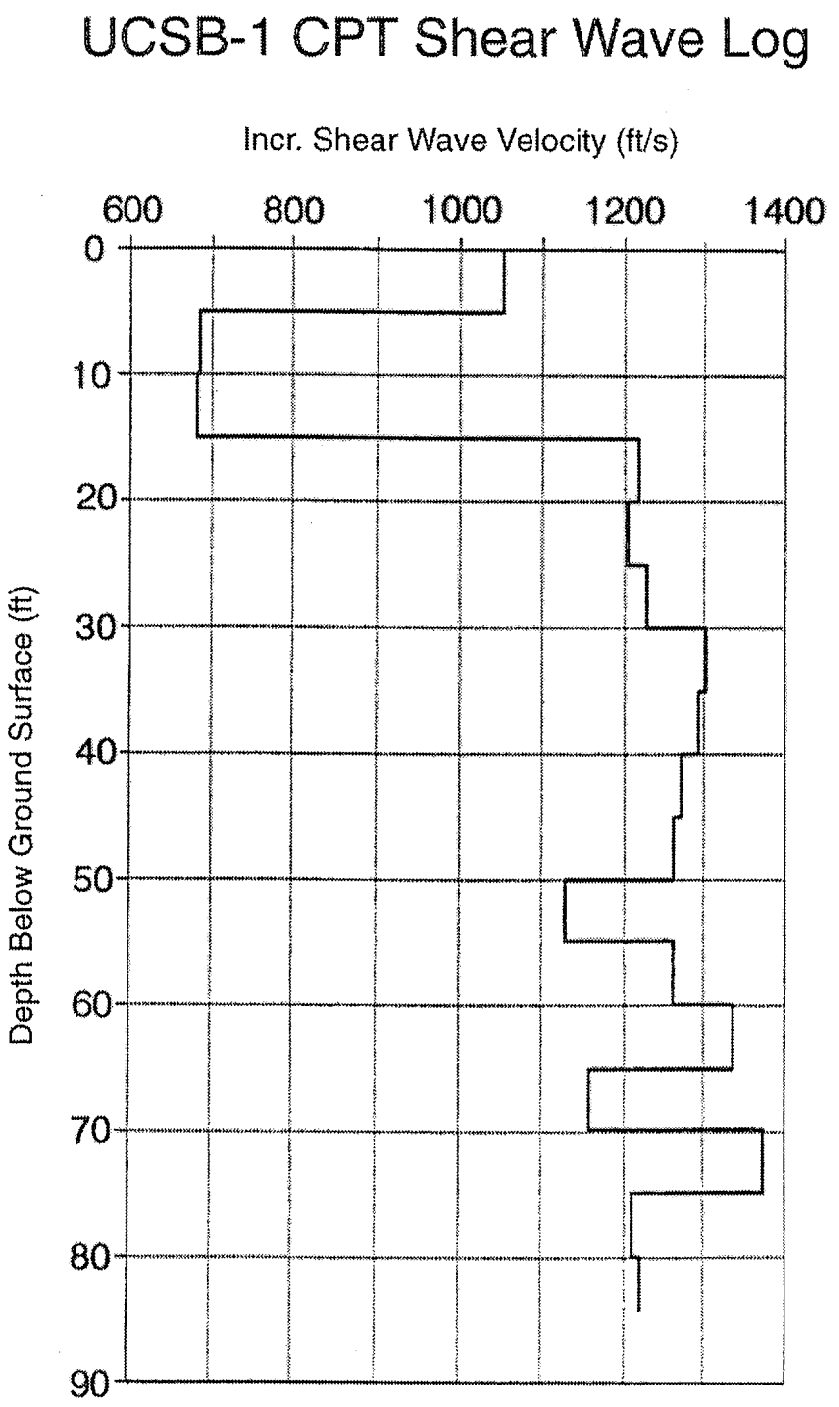

Figure 26. In situ shear-wave velocity measurements with depth in the UCSB CPT hole #1. The relatively low velocity sediments that overlie the raised marine terrace (at a depth of about 16 ft) make interpretation of shallow S-wave refraction data difficult to distinguish from the air-wave. Shear-wave velocities in the Sisquoc Formation based on these data range from 350 m/s to 410 m/s in the top 20 meters.

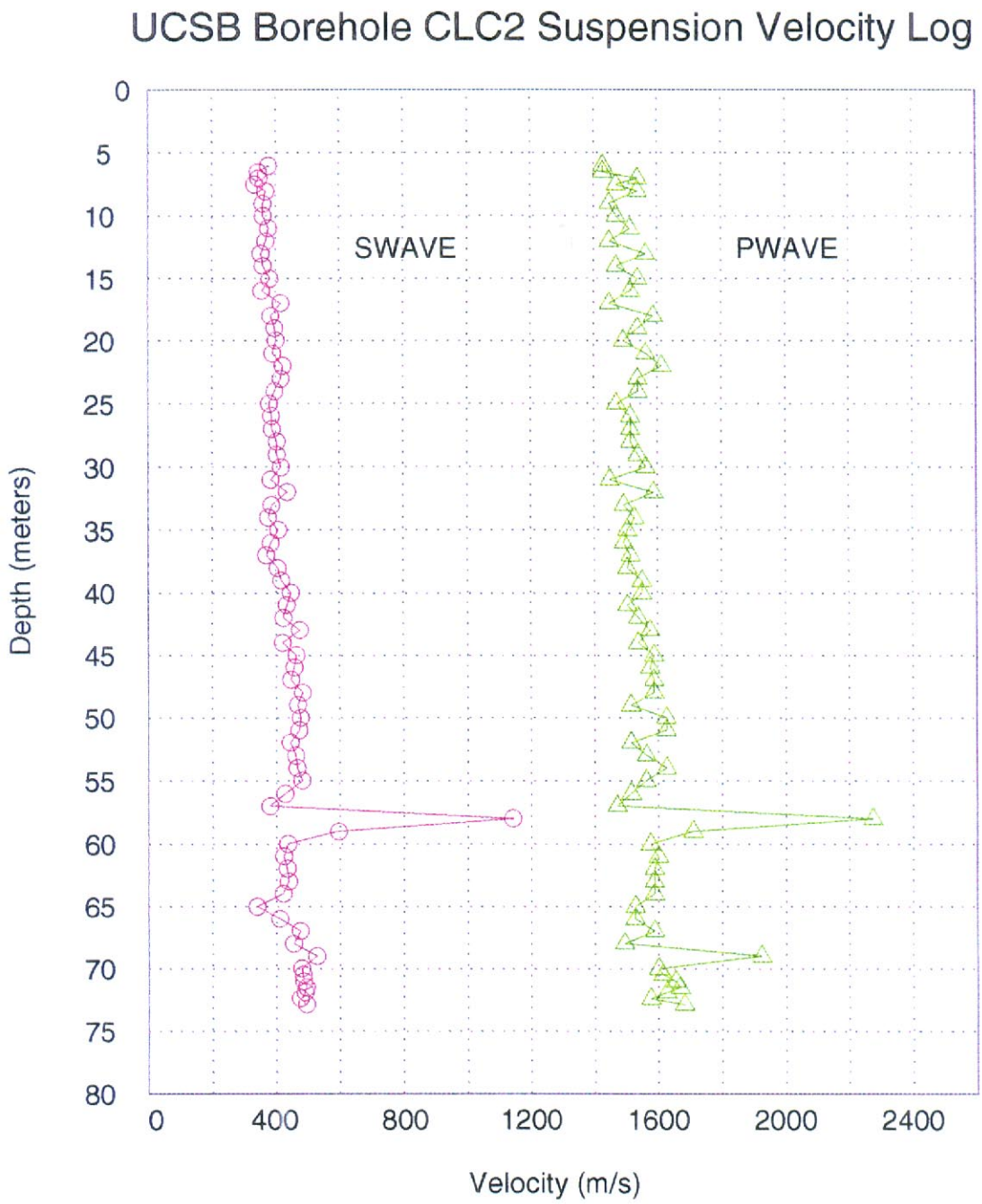

Figure 27. In situ P- and S-wave suspension velocity measurements in the UCSB deep drillhole #2. The data confirm that S-wave velocities within the Sisquoc Formation are typically quite low and only gradually increase from about 350 m/s at a depth of 6 m to about 500 m/s at about 75 m depth. The large spike in velocity at about 57 m depth is likely an usually thick chert lens.

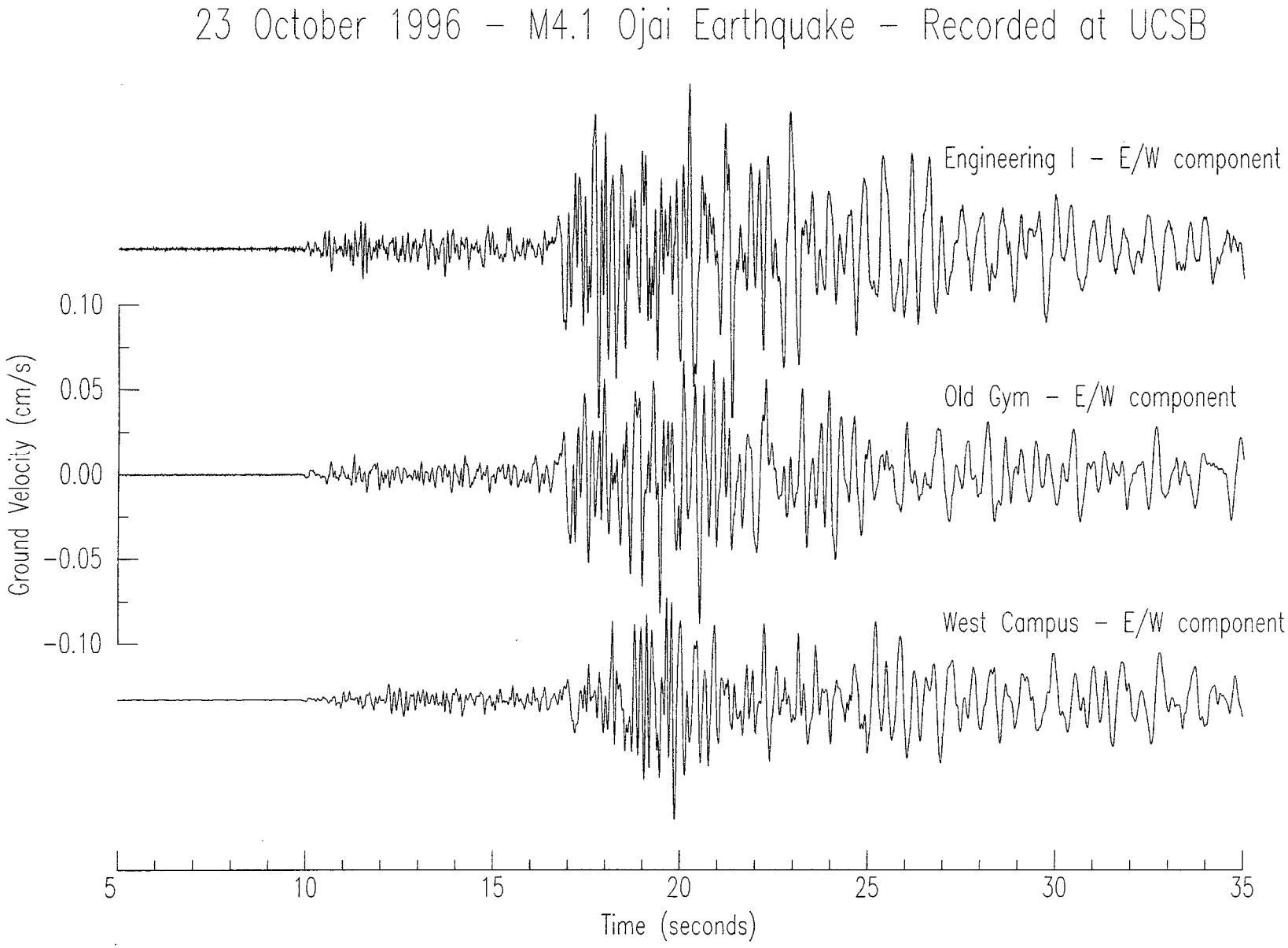

Figure 28. Seismograms of the 1996 M4.1 Ojai Valley earthquake at the three sites on the UCSB campus. Notice that the E-W component amplitudes are slightly higher at Engineering I (by about 30%), but that the spectral content of the waveforms is not significantly different.

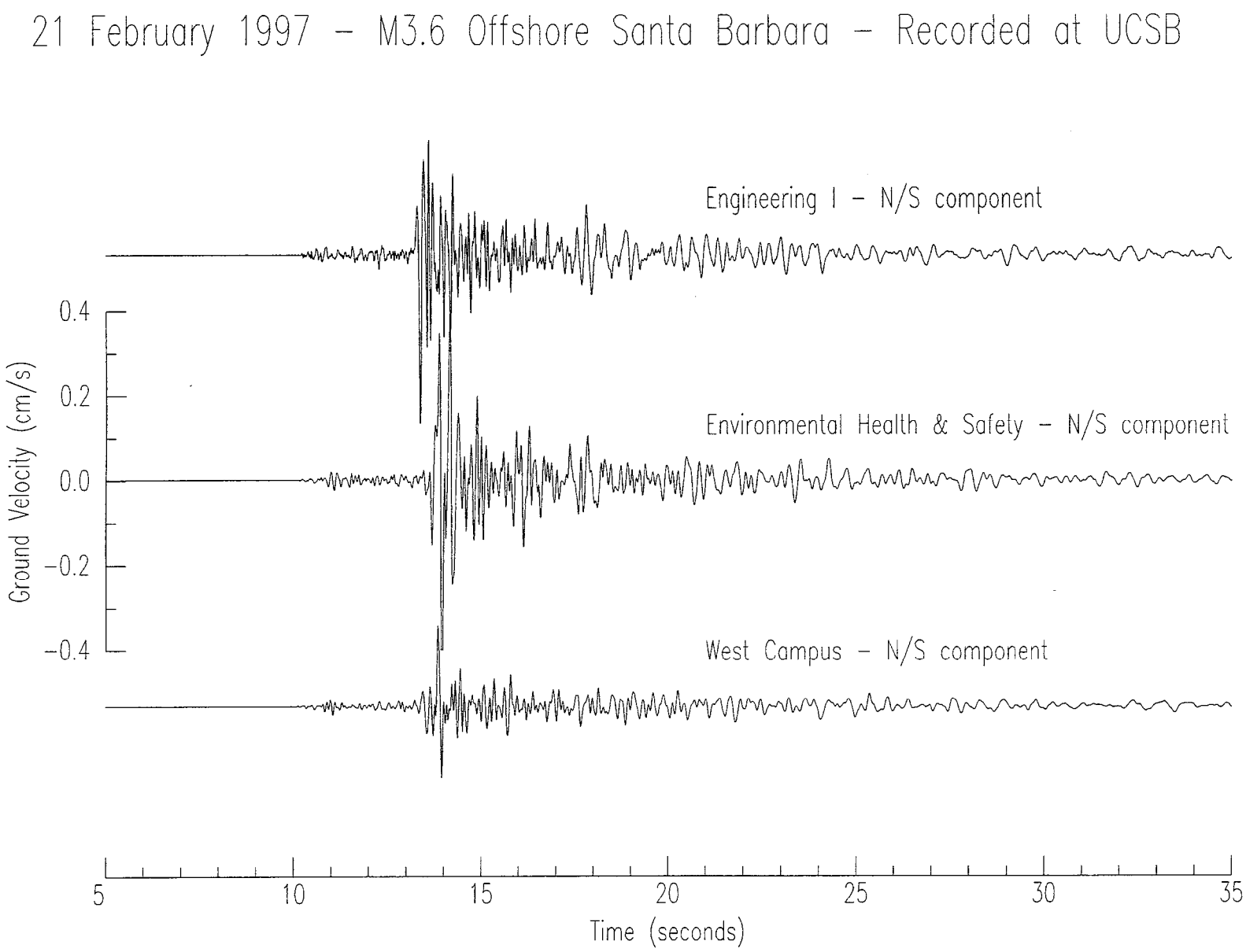

Figure 29. Seismic recordings of the 1997 M3.6 offshore Santa Barbara earthquake at three sites on the UCSB campus. Notice the high amplitude pulse on the N-S component at Environmental Health & Safety, which is located between the north and south branches of the More Ranch fault.

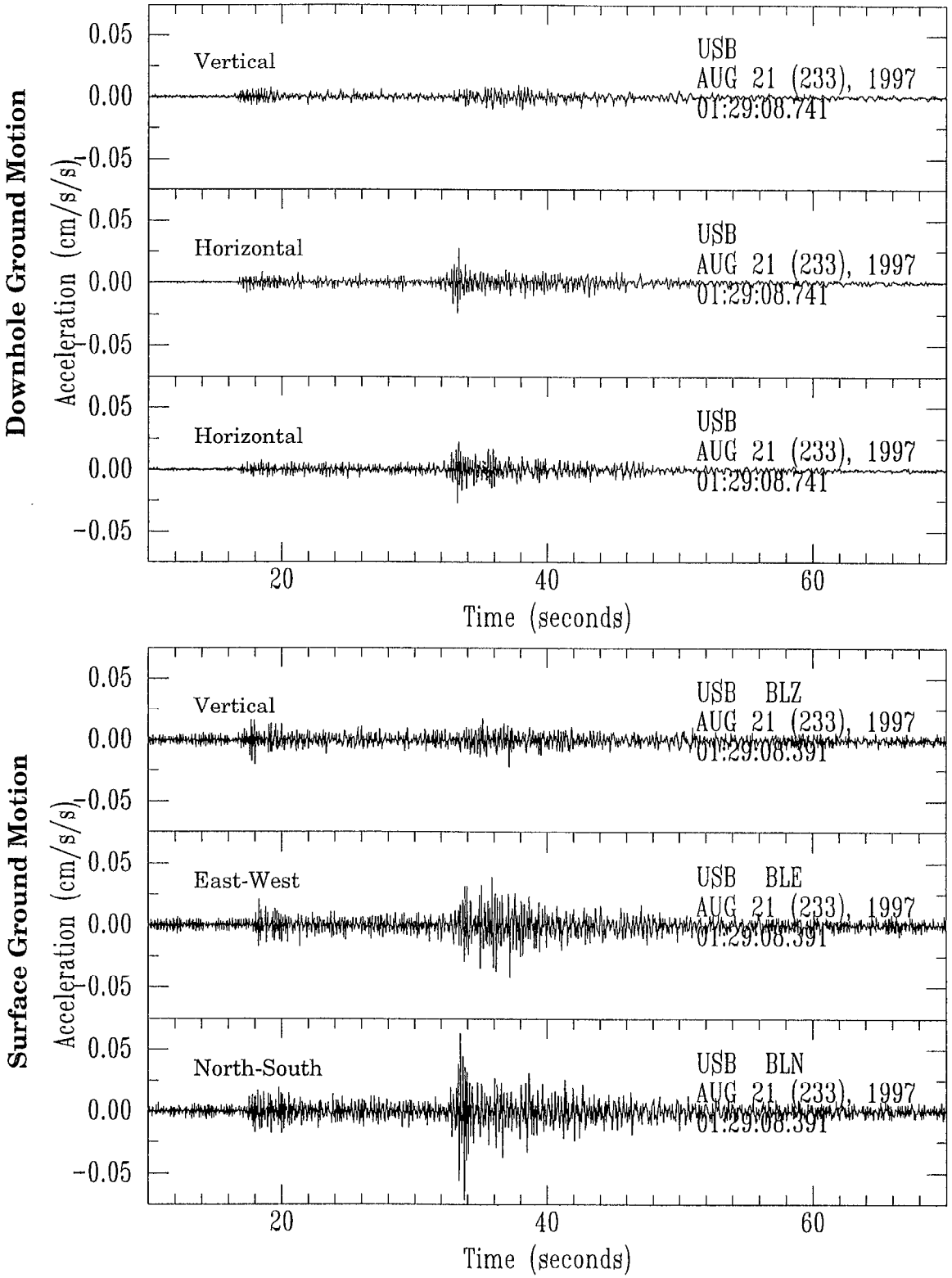

Figure 30. Micro-g level ground acceleration recorded at UCSB/CLC seismic station from a magnitude 3.3 Northrige aftershock. These downhole (top) and surface (bottom) accelerations with a sample rate of 20 sps were retrieved via the internet.

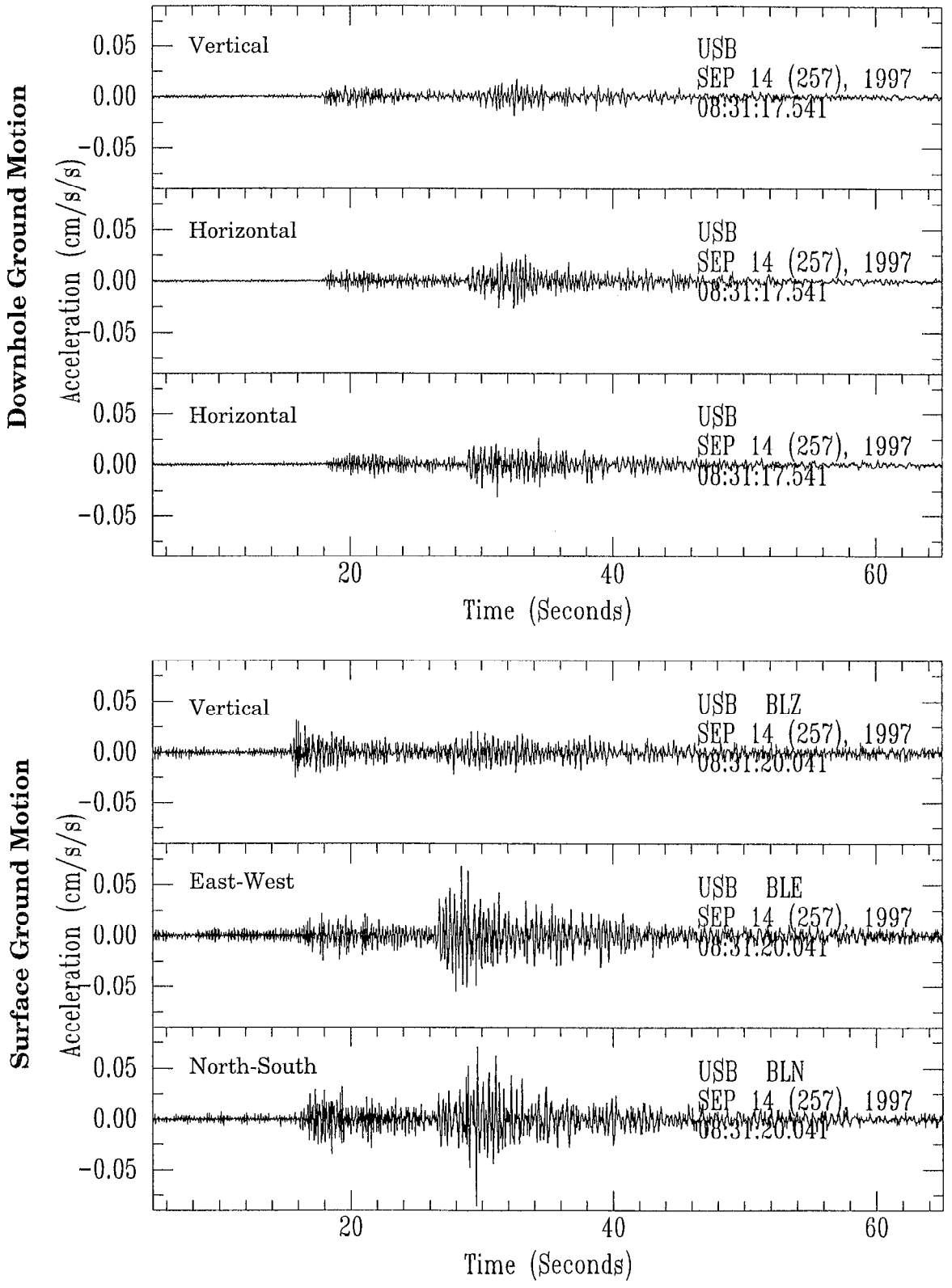

Figure 31. Micro-g level ground acceleration recorded at UCSB/CLC seismic station from a magnitude 3.2 earthquake near Santa Paula, CA. These downhole (top) and surface (bottom) accelerations with a sample rate of 20 sps were retrieved via the internet.

Technical Information Department • **Lawrence Livermore National Laboratory**
University of California • Livermore, California 94551